Tomas Bata University in Zlín
Centre of Polymer Systems

Doctoral thesis

Use of polymers in tissue engineering

Využití polymerů pro tkáňové inženýrství

Author: Ing. Leona Mahelová

Degree programme: Biomaterials and Biocomposites

Supervisor: prof. Ing. Petr Humpolíček, Ph.D.

Consultant: doc. Ing. Zdenka Víchová, Ph.D.

Reviewers: doc. Ing. Jana Sedlaříková, Ph.D.
Mgr. Zdenko Špitálský, Ph.D.

Zlín, September 2025

ACKNOWLEDGEMENT

First and foremost, I would like to express my deepest gratitude to my supervisor, prof. Ing. Petr Humpolíček, Ph.D. From my bachelor's studies to the completion of this dissertation, he supported and guided me throughout my academic journey with patience, thoughtful advice, and encouragement invaluable at every stage.

I am also grateful to my consultant doc. Ing. Zdenka Capáková, Ph.D. and all my colleagues for their help with my research and for making the office and lab environment supportive and fun.

I would also like to sincerely thank Dr. Sonia Kotowicz from the University of Silesia in Katowice, Poland, for her warm welcome and, most importantly, very beneficial stay for my research.

Finally, my heartfelt thanks go to my dear family, especially my parents, close friends, and my life partner, Ing. Danila Gorgol, whose love and unwavering support helped me persevere throughout this challenging journey.

This dissertation was supported by the Centre of Polymer Systems, Tomas Bata University in Zlín and the funding provided by Internal Grant Agency under the student projects IGA/CPS/2020/001, IGA/CPS/2021/001, IGA/CPS/2022/001, IGA/CPS/2023/001, and IGA/CPS/2024/007. Additional funding was provided by the Czech Science Foundation under the projects 19-16861S and 13-07425S. All financial support is acknowledged in the corresponding publications resulting from this research.

ABSTRACT

Medicine and pharmacy have experienced significant advances in recent years, yet there are still unmet goals, such as complete tissue and organ construction. The successful artificial construction of any tissue is based on the design of the appropriate biomaterial and the culture conditions, both of which should mimic the tissues' natural environment. This thesis focuses on understanding the material-cell-environment interactions and in particular looks at the impact of conductive polymers, scaffold design, and advanced culturing methods on the engineering of not only electrically sensitive tissues. Through a review of current research and experimental studies, the aim of this work is to improve the understanding of this complex system and potentially contribute to techniques for the artifical formation of cardiac tissue *de novo*.

Key words: *Tissue engineering, conductive polymers, tissue scaffold design, cytocompatibility, cell-material interaction.*

ABSTRAKT

Medicína a farmacie prožívá za poslední roky významné pokroky, existují však stále nedosažené cíle, jako je například kompletní konstrukce tkání a orgánů. Úspěšné vytvoření jakékoli tkáně je založeno na návrhu vhodného biomateriálu a kultivačních podmínek, přičemž obojí by mělo napodobovat přirozené prostředí tkáně. Tato práce se zaměřuje na pochopení interakcí mezi materiálem, buňkou a prostředím a zejména se zabývá vlivem vodivých polymerů, konstrukcí scaffoldů a pokročilých metod kultivace na inženýrství nejen elektricky citlivých tkání. Cílem této práce je prostřednictvím přehledu současného výzkumu a experimentálních studií přispět k porozumění tohoto složitého systému a potenciálně přispět k technikám umělé tvorby srdeční tkáně *de novo*.

Klíčová slova: *Tkáňové inženýrství, vodivé polymery, návrh tkáňového nosiče, cytokompatibilita, interakce buňka-materiál.*

TABLE OF CONTENT

1. INTRODUCTION

The standards and efficiency of medicine and pharmacy have been steadily increasing in recent years; however, some long-term challenges still remain, albeit in the distant future. The complete regeneration of any damaged tissue or organ within a living organism, or the acquisition of reliable results in drug testing on reconstituted tissues in a laboratory, eliminating the need for animal and clinical testing – these are the dreams that motivate researchers around the world to progress in the field of tissue engineering (TE).

Central to this progress in TE is the development of biomaterials that can mimic the complex macro and microenvironment of native tissues. When a biomaterial is designed and fabricated appropriately, it promotes cell adherence, growth, migration, specific stem cell differentiation and expected phenotype manifestation. Among the diverse range of biomaterials, polymers have emerged as versatile candidates for TE applications mainly due to their highly tunable properties and biocompatibility.

A subclass of polymers with intrinsic conductivity, called conductive polymers, has gained significant attention in TE strategies for their unique combination of facile synthesis and precise control over electron-based and ion-based conductivity. These properties are essential aspects for the engineering of functional electrosensitive tissues, such as nervous or cardiac tissues.

It is also important to consider that cell behavior is influenced not only by the carefully prepared biomaterial, but also by the environmental conditions during cultivation, which can amplify or suppress each other's effects. Thus, to obtain objective results from TE experiments, it is considered necessary to create dynamic culture conditions in a laboratory that will impose the same effects on the cells as in a living organism; for example, flowing media, mechanical stresses or electric fields.

In this thesis, the milestones of TE, the role and use of various polymers in TE, and the factors that need to be considered in the design and biocompatibility testing of tissue scaffolds are discussed. The aim of experimental part is to uncover and improve the understanding of how biomaterials and cultivation conditions influence cell behavior. Through a comprehensive review of the current state of the art, experimental studies and innovative approaches, this work aims to contribute to the development of TE techniques that hold promise for repairing damaged cardiac tissues and improving the quality of life of countless individuals affected by heart-related disorders.

2. TISSUE ENGINEERING

2.1 History and purpose

TE is a multidisciplinary field combining knowledge and principles of life sciences together with materials engineering to discover new biomaterials[1] and techniques for creating functional tissues. TE products have many different applications, here divided into 2 target types.

First, ***in vivo***[2] **applications** of TE products are aimed on the regeneration or replacement of damaged or diseased tissues in a living organism. This is one of the sectors of regenerative medicine. For this purpose, a biomaterial is prepared (mostly in a 3D porous form) that serves as a scaffold for cells. Such scaffold is then either directly implanted in a patient or is beforehand pre-cultured with the patient's cells in a laboratory and after that implanted.

The second approach to utilize TE products is in ***in vitro***[3] **applications**. Here, the main aim is to create functional tissues and organs or systems mimicking natural tissue/organ functions in a laboratory environment. Their use is very wide; for example, they serve as models for disease and drug research. Different drugs are applied to either healthy or specifically diseased tissues or systems (e.g., organs-on-chips) to find the drug effects and their metabolic transformations. This approach significantly reduces the number of experiments on animals.

In general, the main objective of TE is to save and improve the quality of lives. That is what drives TE research all around the world forward, even though it is very challenging and time consuming.

The very beginning of this race dates back to the early 20th century when Alexis Carrel, a French surgeon and later Nobel Laureate, demonstrated the feasibility of organ preservation outside of an organism when he successfully transplanted a segment of dog carotid artery after more than a week in cold storage. (Jay, 2000) Later he investigated the problem of prolonging the life of tissues isolated from an organism and developed techniques to keep pulsating fragments of a chick heart in a nutrient-rich solution for months. (Carrel, 1912)

---

[1] ***Biomaterial*** *is understood to mean any material intended to interact with biological systems in or on the surface of the human body.*

[2] ***In vivo*** *is a Latin term derived from the words in – in and vivus – alive. It is commonly used in life sciences to mean "in a living organism".*

[3] ***In vitro*** *is a Latin term derived from the words in – in and vitrum – glass. It is commonly used in life sciences to mean "in laboratory equipment" (including plastics).*

During the next few decades, a lot of progress has been made towards TE. Researchers investigated the process of tissue regeneration, pioneers of which were Goss and Grimes (1972, 1975) with their studies of the regeneration of rabbit ear holes. Other researchers developed scaffolds made of various natural and synthetic materials to support the growth and differentiation of cells. (e.g. Alexande et al., 1973; Oluwasanmi and Chvapil, 1976; Pruitt and Levine, 1984) Simultaneously at this time, other researchers improved cell culture techniques that allowed efficient and unlimited growth of cells *in vitro.* The first discovered cell line which divides an unlimited number of times under appropriate conditions in a laboratory was HeLa – naturally immortalized cells derived from cervix cancer of Henrietta Lacks. (Scherer et al., 1953) Another great step forward in this field was the creation of spontaneously immortalized mouse fibroblast cell line NIH/3T3 that is now one of the most utilized cell lines in the world. (Todaro and Green, 1963) Ultimately, many more cell lines were immortalized by an introduction of a viral gene affecting the cell cycle. (Graham et al., 1977; Henle and Henle, 1980)

Despite all these important discoveries, there is still debate among scientists about who is the "father" of TE? To my best knowledge, the term "tissue engineering" was first introduced in a published book by Y.C. Fung (1981). However, the fictional trophy actually bounces between 3 men who brought substantial success to the field of TE all at the turn of the 20th and 21st centuries: Robert Langer, Charles Vacanti, and Anthony Atala.

Robert Langer (Figure 2.1 A) is called a founder of regenerative medicine in the meaning as we know it today. He stands, for example, behind the creation of engineered blood vessels or skeletal muscle tissue. (Niklason and Langer, 1997; Niklason et al., 1999; Levenberg et al., 2005)

Charles Vacanti (Figure 2.1 B), in cooperation with his brother Joseph Vacanti, made TE famous by revealing a controversial photograph of the so-called "Vacanti mouse", which I introduce further in the subchapter 2.3. (Cao et al., 1997; Vacanti, 2006)

Anthony Atala (Figure 2.1 C) is the creator of the first 3D bioprinter. He and his team were also the first to successfully implant an engineered bladder tissue, also discussed in the subchapter 2.3. (Atala et al., 2006)

A  B  C 

*Figure 2.1 Fathers of TE: (A) Robert Samuel **Langer** Jr., ScD ("Robert Langer | Polaris Partners," n.d.), (B) Charles Alfred **Vacanti**, MD (Marcus, 2020), (C) Anthony **Atala**, MD ("Anthony Atala Quotes. QuotesGram," n.d.)*

2.2 Utilization of polymers

The first attempts to reconstruct damaged tissues were logically carried out by transplanting natural materials such as bone or skin from another organism, often resulting in limited success due to immune rejection and donor scarcity. With the advancement of medicine and material science, synthetic materials like metals, ceramics, and glass progressively became commonly used for medical implants and devices.

Metals, such as titanium and stainless steel, are popular in medicine and life science for their strength and durability. However, a metallic surface in its pristine form is not chemically and physically suitable for cell adherence. Metals are also too hard for most tissues and can undergo unwanted corrosion. Further, metal processing is often associated with cost and complexity and generates waste. All the aforementioned issues are being gradually overcome with the research of biodegradable iron-, magnesium-, or zinc-based scaffolds prepared by less-costly techniques such as additive manufacturing, foaming, or sintering. (Oriňaková et al., 2021; Petráková et al., 2024) Despite these advancements, the use of metals in TE remains largely restricted to applications involving hard tissues such as bone and dental structures, and only after appropriate surface modification to enhance their biocompatibility. (Li et al., 2023; Shu et al., n.d.) On the other hand, metals are increasingly used as an additive in biocomposites that may be applied to the TE of other tissues too. (Flora et al., 2023; Gorgol et al., 2024) The topic on metals as additives will be further discussed in the subchapter 3.2. Additives.

Ceramics, such as hydroxyapatite and tricalcium phosphate, have been used in TE for bone regeneration as they have similar chemical composition to natural bone and, in addition, can be fabricated into highly porous scaffolds with a structure similar to natural bone. However, they are very brittle, which makes them less suitable for load-bearing applications. Apart from bone and dental tissue, ceramics, as well as metals, are not useful for any other tissue. The use of ceramics is, therefore, very limited and researchers thus create various biocomposites to improve mechanical properties and bioactivity of ceramics. (Kim, 2001; Sagadevan et al., 2023)

Polymers overcoming all mentioned limitations were later developed. During the 20th century, more and more polymers were invented leading to considerable decrease in the use of metals and ceramics in all fields of interests, including medicine and life sciences research. Finally, polymers have become the largest family of materials used in TE. Why?

Polymers have one huge and important advantage over these traditional materials – the ability to easily and widely modify all the (chemical, physical, mechanical, and technological) properties they possess. This entails an enormous variability in their structures and shapes, as well as polarity, durability, flexibility, conductivity, manufacturability, and manipulability, also biocompatibility and biodegradability, and many others. Polymers and in particular polymer-based composites can develop combinations of properties that cannot be achieved using other materials, such as aforementioned metals or ceramics. Thus, polymers can be customized to the specific needs of an individual patient and his issues. In addition, polymers have relatively easy manufacturing and secondary processability with little material waste, plus they are usually reasonable priced.

Because polymers differ so greatly from each other, I have divided them into two groups for better organization: synthetic polymers, with a special attention to conductive polymers, and natural polymers.

2.2.1 Synthetic polymers

In medicine, as expected, polymers have been utilized for a wide range of devices and implants. One of the earliest examples, in the 1940s, was nylon. From a chemical point of view, it is **polyamide** 6.6 and it has been and still is used as surgical sutures. Before them, natural materials like silk, gut, and cotton were used; however, they were not that strong and durable.

Next polymer, which pushed for a modern application in medicine, was the creation of breast implants in 1962. They were made of **silicone** elastomer shell filled with polydimethylsiloxane silicone gel. (Cronin and Brauer, 1971; Perry and Frame, 2020; di Pompeo et al., 2022) Since then, breast implants have changed, but silicon is still an essential material and is also used in tracheal or gastrointestinal tubes. (Rahimi and Mashak, 2013)

Polyethylene, which is currently the most common thermoplastic in the world, is classified by its physical characteristics. In biomedical applications, the major role is played by ultra-high molecular weight polyethylene as a part of very durable joint replacements with a long service life. (Slouf et al., 2023)

Structurally similar to polyethylene is **polypropylene** which is widely used for wound dressings and sutures (Gogoi et al., 2014) or in the form of mesh for hernia repair (Wang et al., n.d.), and pelvic floor protrusions (Ostergard, 2012).

Polystyrene is used neither in medicine nor in TE; however, it is common material for the manufacturing of tissue culture flasks, which are widely used in biological laboratories.

In contrast, **poly(methyl methacrylate)** is very popular in medicine. Due to its excellent optical properties, it is used in contact and ocular lenses. (Wu and Liu, 2023) Moreover, bone cement for fixing joint prostheses is made specifically of this polymer. (Wang and Dunne, 2008) It is also used in facial fillers (Medeiros et al., 2014) and many other applications.

Polyurethane (PU) is also used in various implants, especially in the cardiovascular system, such as pacemakers and artificial heart valves. However, it has also become very attractive in the field of TE and regenerative medicine since PU can be fabricated in various products with wide range of properties, for example, it can be electrospun in nanofiber structure mimicking natural extracellular matrix. (Jaganathan et al., 2019) PU has been researched for engineering nervous, cartilaginous musculoskeletal, skin, and bone tissues. (Mi et al., 2017, 2018; Mani et al., 2019)

Polyesters have also found widespread use in medicine where I would divide them into 2 groups: 1) Non-biodegradable: poly(ethylene terephthalate), often used in sutures, artificial heart valves, vascular grafts, or catheters, (Çaykara et al., 2020) and 2) Biodegradable: poly(lactic acid) and poly(glycolic acid), which are used for bioresorbable sutures, bioresorbable scaffolds, and drug delivery systems. (Wu et al., 2021)

Polyvinylidene fluoride (PVDF) has garnered significant interest in the fields of medicine and TE due to its excellent piezoelectric behavior, which makes it suitable for applications such as sensors and actuators in biomedical devices. (Arsyad et al., 2023). Its copolymer with hexafluoropropylene (PVDF-HFP) creates more amorphous regions, enhancing processebility, flexibility and potentially improving the compatibility of the material with biological tissues. (Baji et al., 2021; Xia et al., 2017)

One of the newest polymers is heat-, chemical-, and mechanical-resistant **polyethers**. For example, polyetheretherketone is used in spinal implants (Schwendner et al., 2023) while polyethersulfone is used in separation membranes for hemodialysis (Zhang et al., n.d.)

There are many other polymers used in biomedical applications that have not been mentioned; for example, polysulfones, polyacetals, polycarbonates, bio-degradable polycaprolactone, or conductive polymers. The last in the list for its importance will be the subject of the next subchapter.

2.2.2 Conductive polymers

Recently, conductive polymers have come into the spotlight. They are specific in their electron-based and ionic-based conductivity and magnetic properties combined at the same time with low density and easy processability, unlike metals. Their importance was recognized in 2000 by the Nobel Prize award in chemistry to Alan Heeger, Alan MacDiarmid, and Hideki Shirakawa who, in the 1970s, created and characterized conductive polyacetylene. However, because of this awarding, previous investigations of conductive polymers have been overlooked. Already in early 1960s, Donald Weiss had been working on polypyrrole (PPy) while Rene Buvet and Marcel Jozefowicz on polyaniline (PANI). (Rasmussen, 2011) To date, PPy and PANI have been at the forefront of research on conductive polymers for the last decade. However, there are also other hitherto neglected conductive polymers and polyazulene (PAz) is one of them.

Chemical structure of conductive polymers (the most common representatives are shown in Figure 2.2) is specific by the conjugated π–bonds and binding sites for doping ions. They also can adopt various redox states and switch between them depending on environmental conditions. As a result, these polymers are preferably used in electrically sensitive applications, which are in biomedicine: scaffolds for cardiac and neural TE and biosensors.

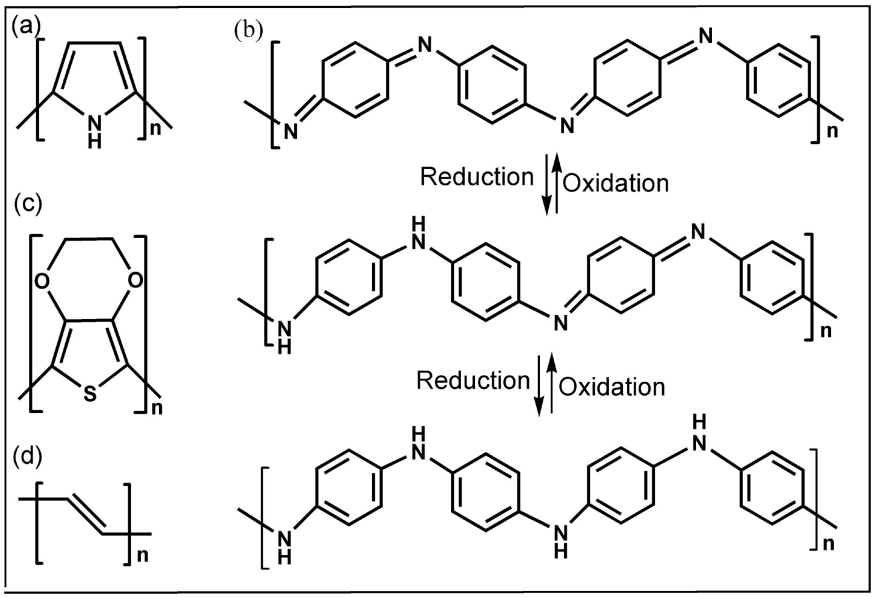

Figure 2.2 Chemical structures of conductive polymers: (a) PPy, (b) PANI at different redox states: top – pernigraniline base, middle – emeraldine base, bottom – leucoemeraldine base, (c) poly(3,4-ethyl-enedioxythiophene), (d) polyacetylene. (Gajendiran et al., 2017)

Polyaniline

PANI has been studied in TE for its conductivity enhancing cellular functions like adhesion and proliferation. As shown in Figure 2.2, PANI has garnered significant attention due to its unique redox states, which include leucoemeraldine, emeraldine, and pernigraniline. These states allow for versatile conductivity, with emeraldine base exhibiting lower conductivity compared to emeraldine salt. Under the best optimalized synthesis conditions and consequent full protonation (see Figure 2.3), PANI shows conductivity values of up to 1.29×10^3 S/cm. (Venkatesh and Vishista, 2018).

However, its cytotoxicity presents challenges, with studies showing that the oxidation state, molecular weight, and dopants significantly influence its toxicity. For example, the conductive emeraldine salt form of PANI exhibits considerable cytotoxicity in comparison to emeraldine base. (Beygisangchin et al., 2021a; Borah et al., 2022; Kašpárková et al., 2016)

Also, the conductivity of PANI can be influenced when placed in physiologically relevant environments, like cell culture media, by changes in pH and ionic concentrations that alter its redox states. PANI undergoes deprotonation, reducing its overall conductivity (Du et al., 2016) and thus impacting its functional applications in biomedical settings where consistent electrical properties are essential for cell signaling and growth.

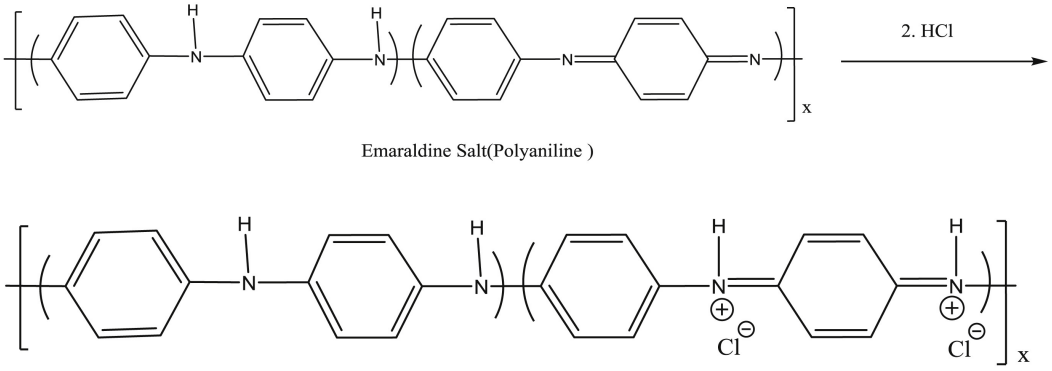

*Figure 2.3 Protonation of PANI emeraldine salt to fully protonated emeraldine hydrochloride salt, leading to higher conducti*vity. *(Venkatesh and Vishista, 2018)*

Polypyrrole

In comparison to PANI, PPy is especially promising due to its better stability. However, its biocompatibility still remains a question. On the one hand, there are studies confirming that PPy extracts do not induce acute and subacute toxicity, hemolysis, allergenicity, nor mutagenesis *in vivo* (Wang et al., 2004). On the other hand, some studies discuss the limits of PPy cytocompatibility with different cell lines. (Ateh et al., 2006) It has also been found to depend on whether it is a PPy salt or a PPy base because *in vitro* studies have shown differences in cytotoxicity and embryotoxicity. (Humpolicek et al., 2018a) It also depends on low molecular PPy products since they induce neurogenesis of embryonic stem cells. (Skopalova et al., 2021)

Most characteristics of conductive polymers, including biocompatibility and conductivity, can be regulated by the choice of synthesis method (chemical shown in Figure 2.4 or electrochemical), oxidizing agents, doping ions, concentration ratio of reactants, synthesis, and even post-synthesis manipulation and conditions. (Ferraz et al., 2012) For the synthesis of PPy, many different oxidizing agents may be used; for example:

- chlorides: **iron(III) chloride (FeCl3)** (Armes, 1987; Duchet et al., 1998; Ferraz et al., 2012; Upadhyay et al., 2014; Chen et al., 2019; Keša et al., 2021), cupric chloride (Sak-Bosnar et al., 1992),
- persulfates: **ammonium persulfate (APS)** (Mezhuev et al., 2015; Keša et al., 2021), sodium persulfate (Pich et al., 2006),
- peroxides: hydrogen peroxide (Vaitkuviene et al., 2014),
- phosphomolybdic acid (Razaq et al., 2009) and many others.

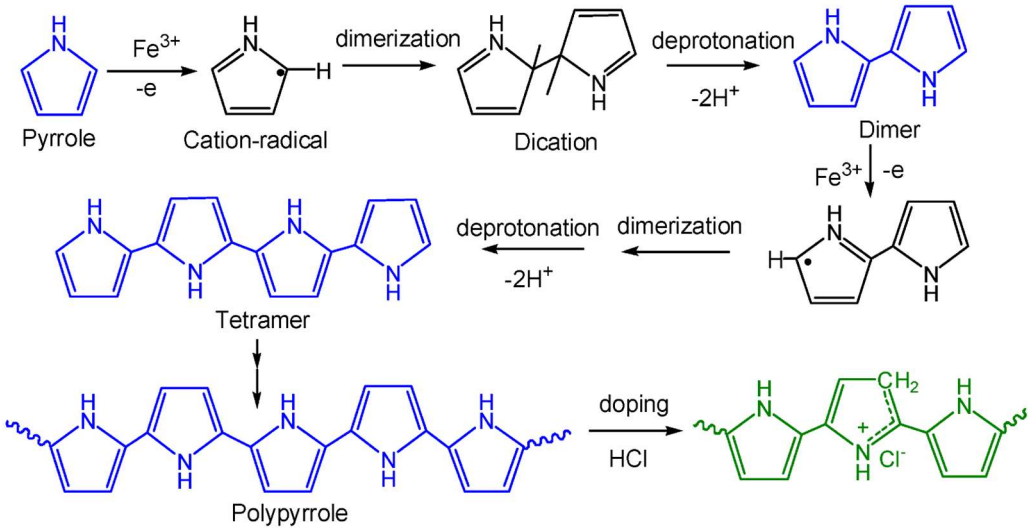

Figure 2.4 Chemical synthesis of PPy. (Chen et al., 2019)

Polyazulene

Azulene is a dark blue isomer of naphthalene, containing 5- and 7-membered combined rings, which can be oxidized to an azulenylium carbocation. This cation is more stable than azulene itself and has an electron-donating feature influencing electrochemical synthesis. (Neoh et al., 1988; Iwasaki et al., 1993; Latonen et al., 2009) It is not that often used but PAz can also be polymerized by a chemical reaction with brominated or jodinated azulen. (Neoh et al., 1988; Wang et al., 2003; Kaewchingduang et al., 2019) PAz polymerization also has been carried out by a direct chemical reaction of azulene with an oxidizing agent. (Grądzka et al., 2018)

In the synthesis of PAz, mostly 2 types of azulene monomer binding occur: 1,3 bonding and 1,5 bonding. The former leads to a planar configuration that forms a long conjugated chain favorable for π–electrons delocalization and high electric conductivity respectively. The second type of bonding, where the planar configuration is disrupted by steric crowding due to van der Waals radius of hydrogen atoms and the conductivity is thus reduced. To prevent this 1,5 bonding, an alkyl substituent can be introduced at 5- or 6-position. The bulkier the substituent, the fewer 1,5 bonds, the better the conductivity. For example, the conductivity of non-substituted PAz is 0.1 S/cm, while that of poly(5-isopropylazulene) is 7.3 S/cm. (Iwasaki et al., 1993) By other variants of substituent blocking, new types of bonding have been eventually created, such as 4,7 bonding *via* the larger cycle (Murai et al., 2012) or more recently carried out 2,6 bonding (Gao et al., 2019; Hou et al., 2022) and others (Zhuang, 2020). The most common types of azulene bonding in PAz are pictured in Figure 2.5.

Still, the conductivity of non-substituted PAz is a very questionable issue. However, it may be apparently increased by protonation, for example by oxygen exposure, the conductivity of non-substituted PAz enhances up to 0.6 S/cm. (Wang et al., 2003) This is given by various redox states PAz can take on (Latonen et al., 2009), as shown in Figure 2.5, similarly to polyaniline or PPy. These different redox states might also influence biocompatibility of PAz; however, to my knowledge, it has not been researched or at least published yet.

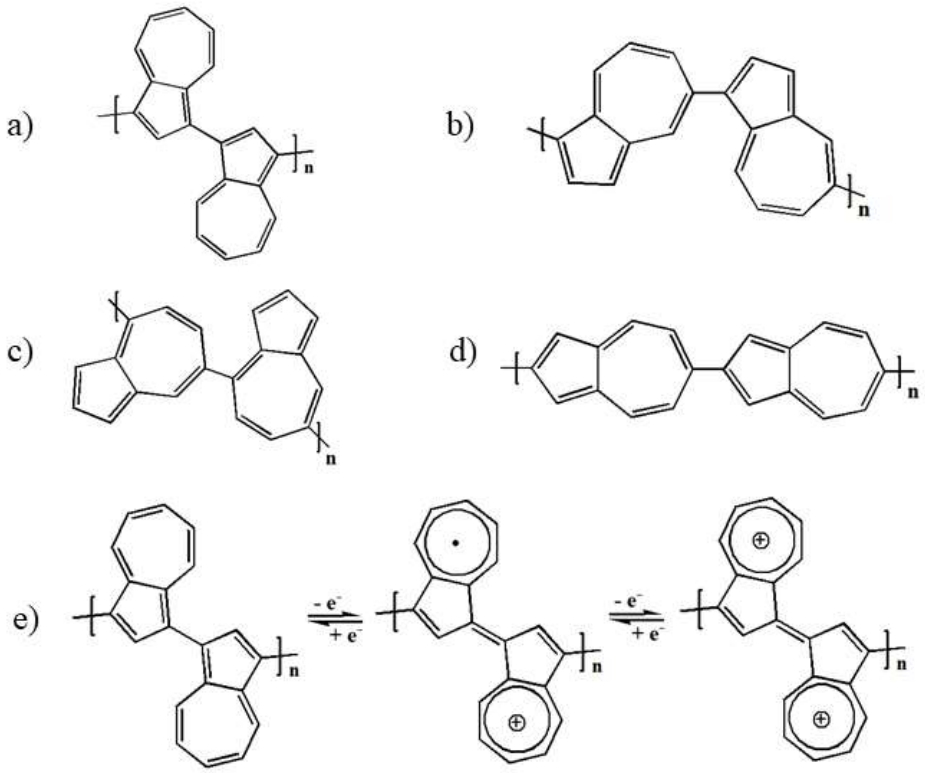

Figure 2.5 Bonding types of PAz: a) 1,3 bonding, b) 1,5 bonding, c) 4,7 bonding, d) 2,6 bonding. e) PAz redox reaction and distribution of charges in the monomer units: uncharged – polaron – dication. (Figure made by the author of this thesis).

Suggesting that conventional PAz should be called polyazulenylene or dehydropolyazulene, (Kihara et al., 1997) introduced a cationic polymerization method for "**true polyazulene**" (truePAz). As shown in Figure 2.6, the synthesis involved dissolving azulene in heated trifluoroacetic acid, followed by precipitation in methanol with triethylamine. The resulting brown powder contained 71% truePAz and 29% truePAz-acetate complex.

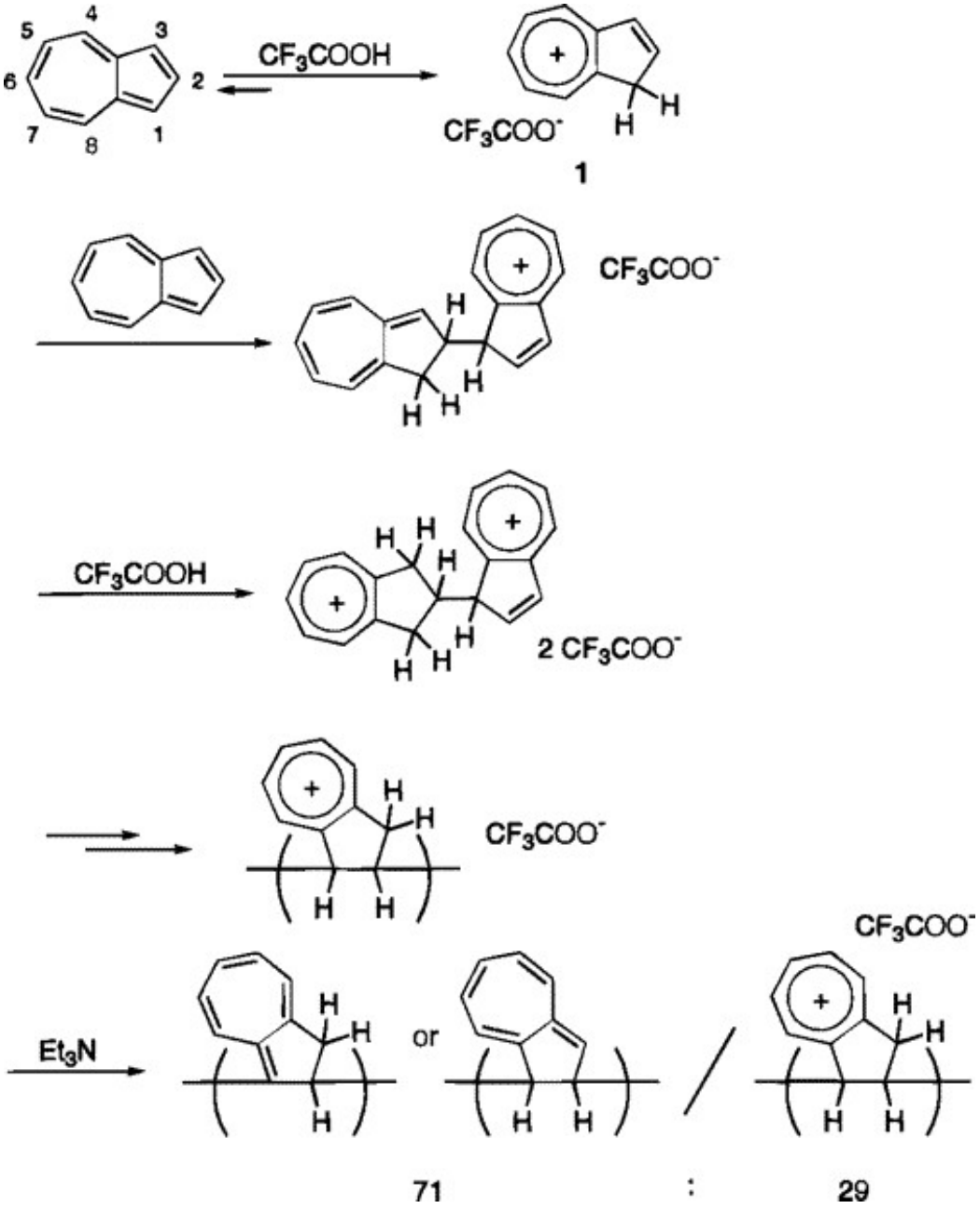

Figure 2.6 Scheme of the chemical synthesis of truePAz by cationic polymerization. (Kihara et al., 1997)

2.2.3 Natural polymers

Metals, ceramics, and most of the synthetic polymers have very limited biocompatibility and poor degradation properties. These issues can be overcome or at least supressed by replacing these materials with natural polymers, also called biopolymers (produced by a living organism). In general, we can divide them into 4 groups according to their structure:

- polynucleotides: e.g., deoxyribonucleic acid (DNA), ribonucleic acid,
- polypeptides (proteins): e.g., silk, wool, collagen, gelatin, albumin, fibrin, elastin,
- polysaccharides: e.g., cellulose, cotton, starch, alginate, chitosan, hyaluronic acid (HA),
- polyhydroxyalkanoates: e.g., poly(3-hydroxybutyrate), poly(4-hydroxybutyrate), poly(3-hydroxyvalerate), poly(3-hydroxyhexanoate), poly(3-hydroxyoctanoate).

Some of them are non-degradable such as silk or cellulose, which are used for semipermeable membranes in hemodialysis. Nevertheless, most of them are degradable. The degradability by natural processes plus the production from renewable resources sign a promising sustainable alternative to synthetic polymers. However, the importance of degradability can be also seen in regenerative medicine. Biodegradable biomaterials, such as sutures, coronary stents, and scaffolds for soft tissue, cartilage, or bone tissue regeneration, have been prepared. (Bose et al., 2018; Bonartsev et al., 2019; Wu et al., 2021)

Another specific approach to obtain a scaffold containing natural polymers is by decellularization of extracellular matrix (ECM) of a specific tissue. Decellularization removes cellular and antigenic components from tissues eliminating the possibility of evoking a negative immune response. (Keane et al., 2015) After the process, the ECM is left behind in a pristine form containing structural and signaling molecules, such as collagen, glycoproteins, or glycosaminoglycans. Decellularized ECM can be isolated from various tissue sources. The most common commercial ECM is Matrigel® that is derived from mouse tumors. (Kleinman and Martin, 2005) Decellularized ECM has served for many different applications, such as tissue regeneration, injectable or implantable carriers for therapeutics, *in vitro* tissue and organoid formation for disease modeling. (Badylak et al., 2011; Paduano et al., 2016; McCrary et al., 2020; Wu et al., 2021)

Natural rubber mainly contains biopolymer poly(isoprene) which is also applicable in TE since it is compatible with blood and has significant osteogenic and angiogenic supportive effects. (Furuya et al., 2017; Guerra et al., 2018) Its biocompatibility may however change after vulcanization depending on the type of crosslinking initiator. For example, X-rays and organic peroxides are more acceptable for medical applications than conventionally used sulfur.

2.3 What has been accomplished

In the past, there were many breakthroughs in the field of TE. The one that both popularized and discredited this line of research among common people in the late 1990s was the "Vacanti mouse", sometimes informally referred to as "Auriculosaurus". It was a mouse, or rather 10 mice, with human-ear-shaped cartilage implanted under the skin of their back (see Figure 2.7). This tissue in the form of a 3-year-old child's auricle was engineered from chondrocytes isolated from bovine articular cartilage seeded onto a nonwoven mesh of poly(glycolic acid) immersed in a 1 % solution of poly(lactic acid). After 12 weeks, analyses proved the feasibility of growing new tissue-engineered cartilage in the shape of a human ear. (Cao et al., 1997)

Figure 2.7 "Vacanti mouse" (Vacanti, 2006)

Next milestone in this field was crossed in 2006 by the first and successful implantation of an engineered tissue in a human being, or rather 7 beings at once (in ages from 4 to 19). This study was to help these people with end-stage bladder disease caused by myelomeningocele[4]. Cystoplasty, a surgery to enlarge the bladder, was based on an engineered bladder tissue (see Figure 2.8) from a scaffold made of collagen and poly(glycolic acid) seeded by urothelial and muscle cells derived from patient biopsy. After 7 weeks of cultivation, it was implanted either with or without an omental[5] wrap. Bladder tissue regeneration and its functionality showed excellent results. (Atala et al., 2006)

---

[4] ***Myelomeningocele*** *is a type of spina bifida. The nerves in the spinal cord that control the bladder did not form properly, patients therefore have problems with high-pressure or poorly compliant bladders.*

[5] ***Omentum*** *is adipose tissue covering and connecting the surface of intra-peritoneal organs. Its key functions are fat storage, immune regulation, and tissue regeneration. (Di Nicola, 2019)*

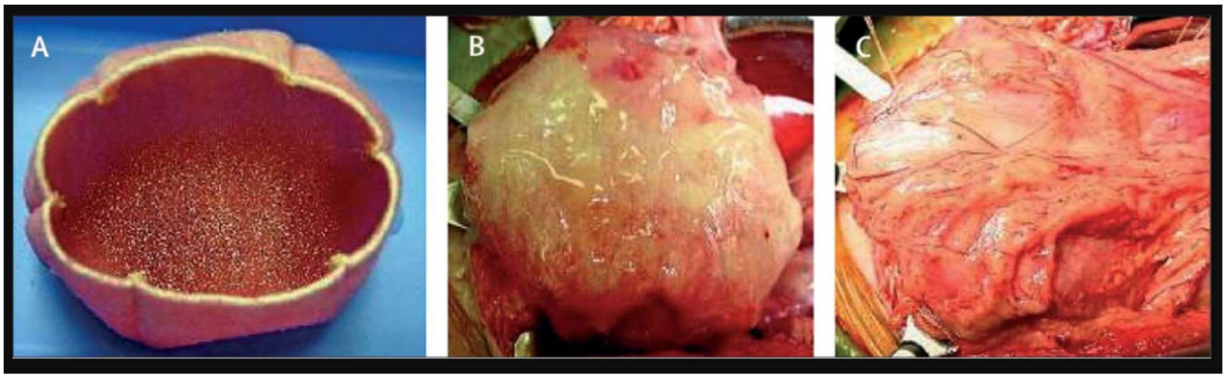

Figure 2.8 Atala´s engineered bladder tissue: (A) The scaffold with cells, (B) The scaffold anastamosed to native bladder, (C) The scaffold covered with fibrin glue and omentum. (Atala et al., 2006)

In recent days, the research of TE is rapidly advancing and it has gotten into relatively common applications in practice. For example, tissue-engineered **skin** is used to heal severe burns and chronic wounds. Some of the commercial scaffolds are biopolymeric Integra® (Ameloot et al., 2019) or MatriDerm® (Dickson et al., n.d.), decellularized human dermis AlloDerm™ (Ma et al., 2022), or synthetic NovoSorb BioTemporizing Matrix made of biodegradable polyurethane (Greenwood et al., 2016). The use of tissue engineered skin reduces the need for skin grafts; however, there still are some deficiencies, such as the absence of sweat glands that are crucial for thermo-regulation of patients with large surface area burns. (Boyce and Lalley, 2018)

However, the engineering of **neural tissue** is much more challenging, both in terms of regenerating peripheral nerves and central nervous system. In the case of an injury, such as deep burn or spinal cord damage, the environment in the injured site is disrupted, scar tissue forms, and that inhibits and limits the axonal regeneration. (Pourkhodadad et al., 2023) For this purpose, scaffolds are produced preferably in the form of uniaxial oriented fibers mimicking natural ECM of neural tissue. (Jin et al., 2022; Puhl et al., 2023) Scaffold material may vary from biopolymers like chitosan to synthetic polymers like polyurethane as well as their combinations. (Cheng et al., 2023; Pourkhodadad et al., 2023) Nevertheless, conductive polymers such as PPy or polyaniline have their special role here. It has been proven that conductive scaffold in a combination with electrical stimuli establishes an electrical environment that serves as a cell-instructive cue, accelerates nerve regeneration and achieves better recovery. (Huang et al., 2012)

Another tissue, where conductive polymers bring significant advantages, is the **cardiac tissue**. Cardiomyocytes are responsible for converting electrical impulses into mechanical work – contraction and relaxation. For the heart to beat properly, the cells must synchronize with each other. Various biomaterials and especially conductive polymers have been tested to both regenerate the damaged tissue and restore the flow of cardiac impulses. Some of the recent studies have shown that, for example, polyethersulfone/polyaniline electrospun aligned nanofibrous scaffolds significantly promote cardiomyogenesis due to uniaxial conduct of external electrical stimulation by the present polyaniline. (Mohammadi Amirabad et al., 2017) As another example, PPy added into chitosan hydrogel enables synchronization of contraction between two physically separated beating cardiomyocyte clusters *in vitro* shown in Figure 2.9. Further, this study observed an improvement in electrical-impulse propagation after *in vivo* intra-myocardial injection of the PPy/chitosan hydrogel into scar tissue. (Cui et al., 2018)

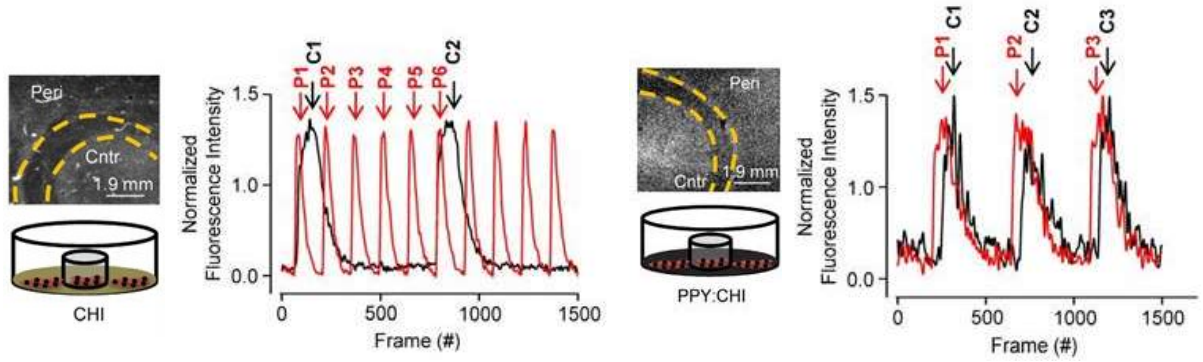

Figure 2.9 Effect of PPy on electrical-impulse propagation and synchronization: Neonatal cardiomyocytes were cultured on chitosan-coated (left) and PPy/chitosan-coated (right) dishes for 5 days with a glass ring separating the cells into peripheral (P) and central (C) populations. Spontaneous calcium transients were observed via Fluo-4-AM signal with representative fluorescence intensity graphed. (Cui et al., 2018)

Of course, there are many other groundbreaking studies in the field of TE research, with most of them based on the use of polymers. Therefore, only some of the most interesting papers (in general and for the author's research) are presented in this chapter. Further, this thesis focuses on the design and construction of a functional biomaterial, ideally with an added value of bioactivity. It then addresses in vitro biological testing, especially the pitfalls of traditional culturing and evaluation.

3. POLYMERIC SCAFFOLD DESIGN

When creating a potential biomaterial, the site of the intended application must first be considered. This is due to the vast differences in properties and functions across various tissues. Therefore, the successful assembly of scaffolds or biocomposites depends on understanding their interactions with cells and good biomimicry of the target tissue. Achieving suitable results thus relies on the design and fabrication of biomaterials with cell-specific properties.

The proces of scaffold designing is schemed in Figure 3.1 and discussed deeper further in this chapter. The first question that comes to mind when designing scaffolds is usually the choice of **matrix** – the bulk material or a combination of materials that provide mechanical support and a 3D framework for cells. Some matrices, usually the ones based on biopolymers such as HA or collagen, have considerably suitable mechanical and biological properties and can be used as they are. However, the use of bioactive materials is commonly limited for their inssufient strucutral stability. On the other hand, most polymers with desired mechanical properties lack bioactivity.

Therefore, various **additives** can be incorporated into the polymer matrix to modify different properties, including mechanical stability/degradation, bioactivity, as well as conductivity or stimuli responsiveness.

The next step is to process the matrix, with or without additives, into a scaffold with a suitable **architecture**. This is an essential part of scaffold engineering, creating a 3D shape that makes the scaffold habitable for cells and can also generate specific cell-instructive signals.

Last but not least, the **surface** of the designed and prepared scaffold is the site that directly interacts with cells and thus strongly affects the scaffold's success. Several approaches to surface modification are used, for example, coating, which changes the surface properties, improving its cell adhesion and overall bioactivity.

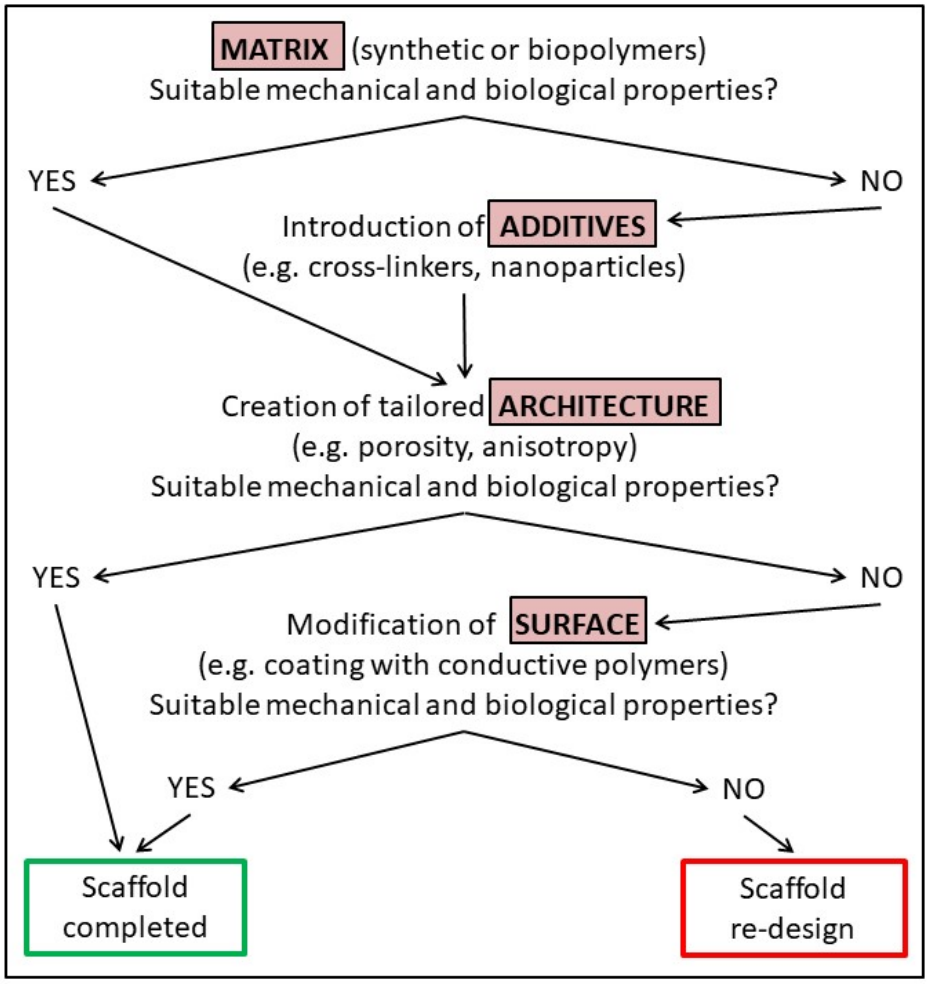

Figure 3.1 Simplified scheme of the main steps required for successful design of bioactive polymer scaffolds. (Figure made by the author of this thesis).

3.1 Matrix

The range of applicable polymers is extensive, as described in the earlier section 2.2 Utilization of polymers. Above all, the material must not be toxic, which means that it must not contain, produce, or release any substances that would damage the viability or function of cells, tissues, organs, or the organism as a whole.

Secondly, the **mechanical properties** of the biomaterial must be adapted to the intended tissue to be reconstructed. As already mentioned, biomimicry is the mainstay of TE. For example, a soft hydrogel cannot serve as a scaffold for hard tissue such as bone, and conversely, soft tissue responds to overly hard implants by insulating by forming fibrous capsules. (Maity and Sarkar, 2017) Moreover, even small variations in mechanical properties can have far-reaching effects on cells. For example, this topic was nicely presented in a study based on

elastomeric micropillars, shown in Figure 3.2, with different heights and consequently rigidity. Human mesenchymal stem cells cultured on short rigid micropillars had high focal adhesion with highly organized actin filaments and preferred osteogenesis (see Figure 3.2 d). In contrast, cells on soft micropillars showed a rounded morphology with disorganized actin filaments and low focal adhesion, and adipogenesis was favored (see Figure 3.2 f). (Fu et al., 2010)

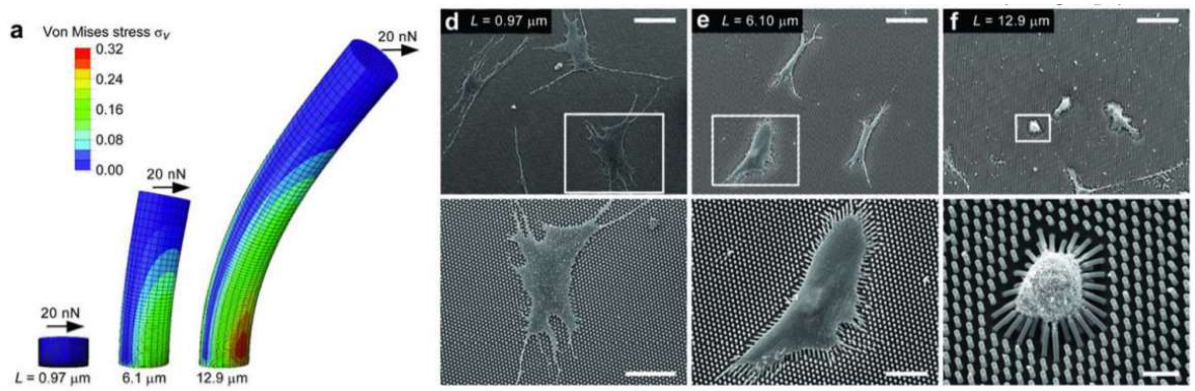

Figure 3.2 Example of the impact of mechanical properties on cytocompatibility: (a) The elastomeric micropillars with different heights in response to horizontal traction force. (d–f): Human mesenchymal stem cells cultivated on the microposts from the shortest to the highest. SEM scale: (top) 100 μm, (bottom from left to right) 50 μm, 30 μm, 10 μm. (Fu et al., 2010)

Polymers have a great advantage over metals and ceramics in this area because their mechanical properties such as strength, flexibility or durability can be regulated significantly and yet relatively easily. For example, PU is a polymer whose mechanical properties can vary across the board depending on the method of preparation and manufacture.

For example, scaffolds based on HA demonstrate mechanical characteristics suitable for various tissue types, as they can be engineered to possess shear moduli comparable to that of native tissues, such as brain and nerve tissues (100–1000 Pa), making them ideal for neural tissue engineering. (Nimmo et al., 2011) The elasticity and mechanical strength of HA scaffolds can be finely tuned through chemical modifications and cross-linking techniques to develop hydrogels that mimic ECM and support cell adhesion, proliferation, and differentiation. (Gorgol et al., 2024; Nimmo et al., 2011; Rezaeeyazdi et al., 2018; Vítková et al., 2022)

A special place in this field is occupied by liquid crystal-based polymers, which are unique due to the strong dependence of their physical properties on temperature, electric or magnetic fields, and molecular or surface interactions. (Adamow et al., 2020) They have been used, for example, in retinal and neural prosthetic implants. (Chauhan et al., 2019) Another polymer worth mentioning is PVDF, which is unique in its piezoelectric activity, making it particularly interesting for applications in cardiovascular and neural TE. (Adadi et al., 2020; Kitsara et al., 2022; Li et al., 2019; Lins et al., 2017)

Last but not least, the base material must be selected according to its **degradability** by natural processes in the biological environment. Depending on the application, it is desirable for some biomaterials to be stable for as long as possible, while others are expected to be degraded by the organism in a short time. In most cases, however, the scaffold must have good mechanical properties for a certain period of time; for example, until the cells migrate within the scaffold and form a complete confluence, and only then begin to gradually disintegrate. To achieve these two conflicting goals, non-biodegradable synthetic and biodegradable natural polymers are combined into copolymer or a composite. These materials can then be used for sutures, coronary stents, or scaffolds for soft tissue, cartilage, and bone regeneration. (Bose et al., 2018; Bonartsev et al., 2019; Wu et al., 2021)

3.2 Additives

After selecting the base material for a tissue scaffold, it is necessary to think about additives to improve the material properties. Most of the required modifications can be divided into three groups according to the desired change:

1) the modification of mechanical properties, biodegradability, or processability;

2) the enhancement of biocompatibility and bioactivity;

3) the creation of smart material.

Regarding the first point, the research by Kade et al., 2022 may serve as an interesting example. They explored the incorporation of carbonyl iron particles (CIPs) into PVDF and produced by melt electrowriting, resulting in scaffolds that maintained a consistent structure while achieving significant porosity.

Beyond that, the range of additives and their effects is as extensive as the range of polymers and their properties. The choice is rather narrowed down by the essential condition of non-toxicity. In order to increase the cytocompatibility

and biodegradability of the generated material, the choice is then even more limited, mainly to biopolymers and other biomolecules. However, **bioactivity** is currently the most challenging topic. A biomaterial that actively positively affects biological systems is usually quite complex and target-specific. They are usually based on drugs, therapeutics or signalling molecules usually bound to time- or stimulus-release carriers. (Mandoli et al., 2010; Pajvani et al., 2003; Wu et al., 2020; Zhang et al., 2008; Zhang and Zhang, 2002) Bioactivity can also exert negative effects on selected biological systems, specifically antimicrobial, antifungal, or antiviral effects. Metal oxide particles are commonly used for this purpose. (Padmavathy and Vijayaraghavan, 2008; Sawai and Yoshikawa, 2004)

So-called **smart scaffolds** are made of biomaterial that significantly and reversibly changes its properties or functionality in response to a small change in environmental conditions (such as pH, temperature, electric or magnetic field). Such sudden and repeated changes are common in *in vivo* tissues. Therefore, research on smart materials has grown in the last few years with the aim of approaching the mimicry of natural tissues. There are various ways how to create smart scaffolds. Most of them are based on the dispersion of active fillers (especially in nanoscale) in a neutral polymeric matrix. For example, magnetically-active particles, such as iron-oxide-based nanoparticles, lead to a magnetorheological effect, which implies a highly non-linear mechanical response of a material to the presence of an external magnetic field. (Bardajee and Hooshyar, 2014; Cvek et al., 2020; Tanasa et al., 2020; Vítková et al., 2022)

3.3 Architecture

The next step in scaffold engineering is to design the appropriate size, shape, and structure into which the prepared material will be processed. The main requirement for a 3D construct in TE is **porosity**. Pores must be interconnected to allow the migration of cells in the inner parts of a scaffold as well as the flow of the culture medium for nutrient supply and waste outflow. (Mukasheva et al., 2024) Not only the shape but also the size of pores is important, scientists have not yet fully agreed on their dimensions though. This is because of the complexity of the subject. Natural tissues *in vivo* are hierarchically structured, and cells are thus exposed to different environmental organizations, according to which they react differently. Therefore, scaffolds with graded porosity have been studied and have the ability to better mimic *in vivo*. (Loh and Choong, 2013; Murphy and O'Brien, 2010; Olaru et al., 2023; Xu et al., 2015)

The hierarchical architecture is linked not only to the pores but also to the substrate to which the cells are attached and are therefore even more sensitive to it. Since ECM and *in vivo* tissues are mostly anisotropic, material **anisotropy** thus plays a crucial role in TE. To create anisotropic scaffolds, two different processing technologies are mainly used. (Smith and Mele, 2021)

The first technology is electrospinning. This allows the production of micro- to nanometer filaments with certain adaptability in diameter, porosity, and alignment. Uniaxially oriented nanofibers produced in this way have been found to induce morphological changes in many cell types, including cytoskeletal remodeling, nuclear elongation, and even axon extrusion from neuronal stem cells. (Yin et al., 2010) It has been also demonstrated that not only structural but also mechanical anisotropy that increases with fiber alignment has an impact on cytocompatibility. (Fee et al., 2016)

The second technology is additive manufacturing, of which 3D printing is the most popular. It has a huge advantage in an incomparable offer of geometric creativity, allowing the preparation of very complex components that can also be patient-specific. Nowadays, bioprinting has become especially trendy and has already proven its usefulness. For example, a study from Jin et al. in 2022 showed a bioprinted linearly ordered collagen scaffold with incorporated human spinal cord neural progenitor cells and human spinal cord astrocytes that during *in vivo* experiments formed a spinal cord-like structure containing mature neurons and glial cells, as shown in Figure 3.3. (Jin et al., 2022)

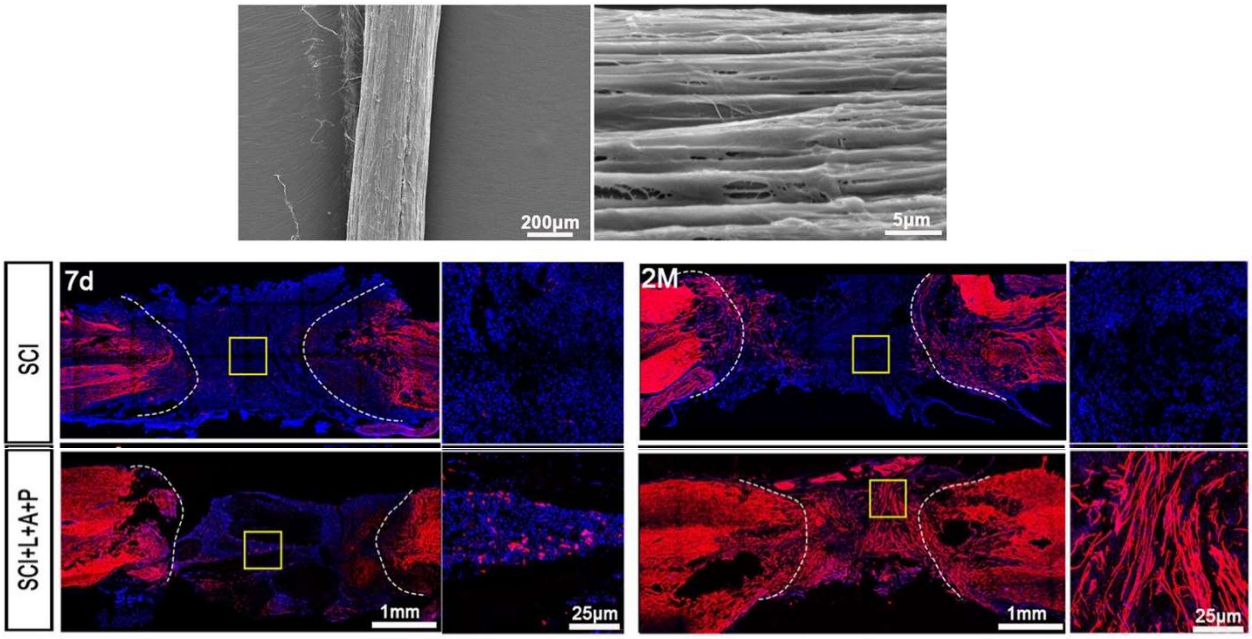

Figure 3.3 Example of the impact of anisotropic structure on cytocompatibility: (top) The bioprinted linearly ordered collagen scaffold implanted in a spinal cord injury in rats; (bottom) Tuj-1 immunostaining of the injury in SCI – control group without any implantation and SCI+L+A+P – tested group with a bioprinted scaffold at 7 days and 2 months post-injury. (Jin et al., 2022)

3.4 Surface

The interaction of any biomaterial with cells (or tissues, biological fluids or the immune system) always starts at the surface of the scaffold. Therefore, not only the architecture of the bulk scaffold but also its surface **topography** is an important clue that influences cell behavior. A study based on 2,176 polymeric chips, each with different topographic features, has made a significant contribution to understanding this issue of surface-cell interaction. (Unadkat et al., 2011) Although this study focused on osteogenic differentiation, many other studies have shown that most cell types change their morphology and behavior in response to topographic features. (Kulkarni et al., 2017; Nikkhah et al., 2012; Wrzecionko et al., 2017) Furthermore, anisotropic topographical features, such as microabraded uniaxial channels, can be used to obtain the *in vivo* phenotype of cardiomyocytes (aligned actin filaments, parallel arrangement of sarcomeres, and elongated nuclei) in an *in vitro* environment. (Bursac N. et al., 2002)

Deeper control of cellular behavior can be further achieved by using hierarchical topography mimicking the natural ECM, thereby promoting cellular responses that are critical for tissue regeneration and repair. (Kadlečková et al.,

2022; Pandey et al., 2023; Yang et al., 2014; Zheng et al., 2020) The interplay between micro-scale and nano-scale features leads to human mesenchymal stem cell (TCD) differentiation through cell mechanotransduction modulated by the integrin-activated focal adhesion kinase (FAK) (see Figure 3.4). (Teo et al., 2013)

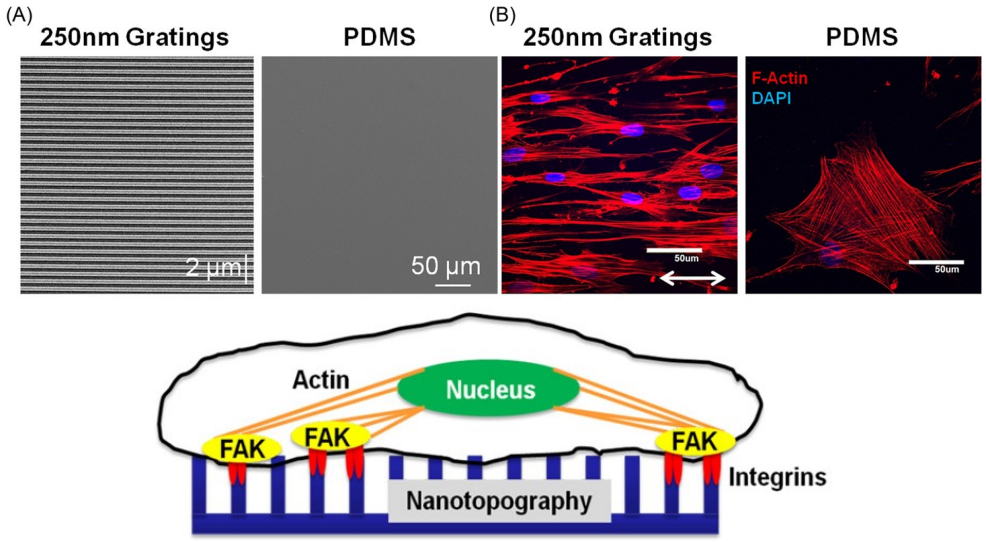

Figure 3.4 Example of the impact of topography on cytocompatibility: (A) SEM of 250 nm gratings and unpatterned substrates, (B) human hMSC on these substrates for F-actin (red) and DAPI (blue), (bottom) a scheme of nanotopography-induced hMSC differentiation modulated by the FAK. (Teo et al., 2013)

Moreover, the interaction of cells with surfaces is influenced by many other material properties, such as **chemical** composition or **physical** properties, both controlling the ability to adsorb adhesive proteins a thus regulates cellular response. To enhance cell adsorption and proliferation onto polymeric substrates, their surfaces can be modified by the formation of new functional groups and/or by increasing free surface energy. These can be done by many techniques, for example, by corona electric discharges, UV radiation, or chemical treatment.

There are also possibilities in modifications that increase the **biological** activity of surfaces. This is achieved by adsorption or chemical binding of bioactive molecules to the polymer surface to stimulate a specific cellular response. For example, the adhesion of ECM components supports the initial adhesion and growth of cells, which subsequently produce their own ECM and thus colonize the surfaces more easily. (Tallawi et al., 2015; Van Vlierberghe et al., 2011; Wu et al., 2020)

In regard to bioactivity, physical and chemical properties, and topography, all of these influencing factors can be modified all at once by surface coating. In addition, if the surface is coated with conductive polymers, another important cell-instructive cue occurs – **conductivity**. Biological tissues typically exhibit conductivity values in the range of 10^{-4} to 10^{-2} S/cm influenced by factors like electrolyte concentration, temperature, and extracellular matrix properties. (Hirata et al., 2010; Lee et al., 2022) Compared to that, conductive polymers have a broad range of conductivities from 10^{-10} to 10^{5} S/cm (see Figure 3.5) due to the various types having different properties, including conductivity, also strongly influenced by the synthesis process and conditions, redox transitions, doping, and treatment of the coatings after synthesis. (Grancarić et al., 2018)

Another significant advantage of coatings made of conductive polymers is their simple and rapid synthesis. Coating of the scaffold can be performed by *in situ* chemical oxidative synthesis, casting of/dipping in polymer solution, or electrochemical deposition (for which the scaffold must be conductive). Effects of PANI, PPy, and PAz on cytocompatibility are discussed in the chapters: 2.2.2 Conductive polymers, 2.3 What has been accomplished, and 4.1.2 Electrical field.

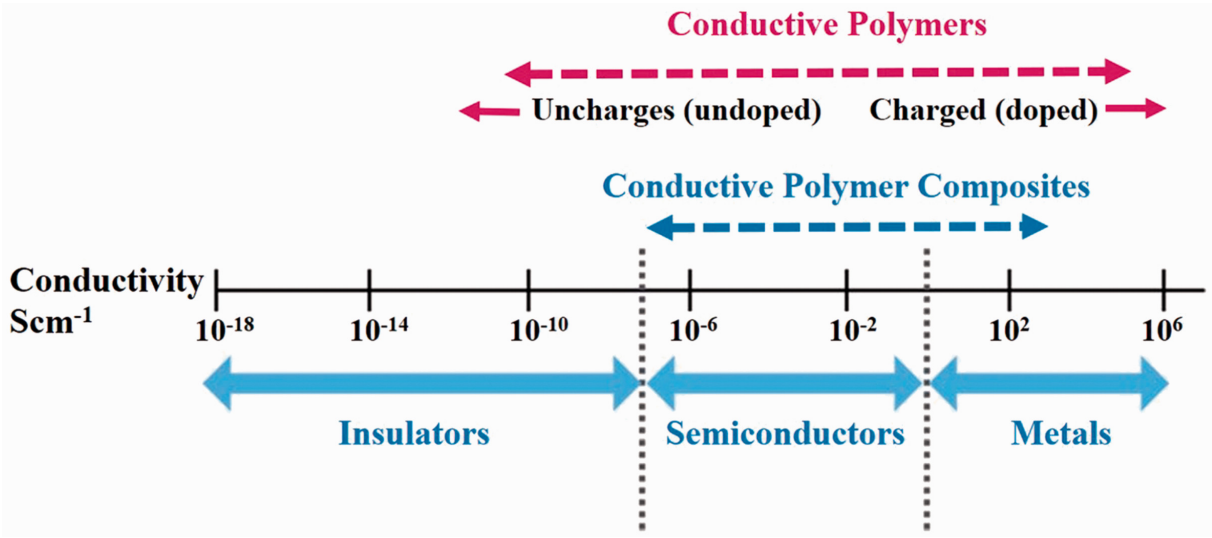

Figure 3.5 Scheme of the conductivity range of conductive polymers in compaison to other materials. (Grancarić et al., 2018)

4. BIOLOGICAL TESTING

4.1 Static versus dynamic cultivation conditions

Many studies have observed the impact of various properties of biomaterials and biocomposites on cellular behavior; however, the devastating majority of *in vitro* investigations have been carried on under static cultivation conditions. The traditional culturing of cells in tissue culture dishes (TCDs) statically placed in an incubator is a well-known, well-understood, and yet antiquated approach that comes with several drawbacks.

Disadvantages of static cultivation are, for example:

1) restrained diffusive transport of nutrients to the cells, especially to cells attached in the core of a biomaterial scaffold,

2) neglecting the importance and influence of mechanical and electrical stimuli on cell behavior, especially stem cells, and finally

3) the difference from the real *in vivo* environment.

Bioreactors are designed to mimic the dynamic stimuli of the natural *in vivo* tissue environment that static cultivation lacks. One of the first commonly used dynamic systems was a simple flask with an inner spinner (Figure 4.1 a) generating turbulent fluid flow providing a well-mixed culture medium around cells. It has been utilized for the expansion of cell aggregates, including embryonic stem cells and induced pluripotent stem cells. (Gupta et al., 2016; Krawetz et al., 2010) On the other hand, turbulent flow increases stress in cells, causing various issues in TE, such as the formation of an outer fibrous capsule in cartilage tissue construction.

Therefore, bioreactors with low fluidic stress on the cells have been developed. One of the most widely used is a rotating wall vessel (Figure 4.1 b) configured as a cylindrical or annular space with a silicone membrane providing gas exchange with the incubator environment. (Baker and Goodwin, 1997; Hammond and Hammond, 2001) Other bioreactors also used in TE are based on perfusion, which is suitable for culturing in 3D porous structures, or the pulsatile flow simulating cardiovascular conditions. (Chen and Hu, 2006)

All the listed bioreactors apply only one specific stimulus to the cells – hydrodynamic shear stress of the flowing medium. However, there are also other types of bioreactors applying other external stimuli, such as tensile/compressive and electrical stresses. For example, a bioreactor from Ebers, Spain (Figure

4.1 c) combines all of these stimuli, which are also fully controllable and adjustable. Another advantage is the possibility to apply cyclic loads, both mechanical and electrical. On the other hand, this complexity goes hand in hand with complicated setups, higher failure rates, and high costs. Hence, only a few studies/papers using this bioreactor have been published. (Deniz et al., 2020; Janvier et al., 2020)

a) 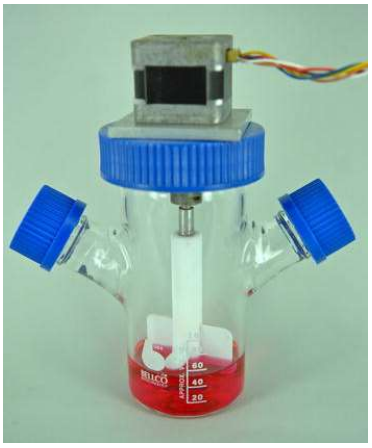 b)  c) 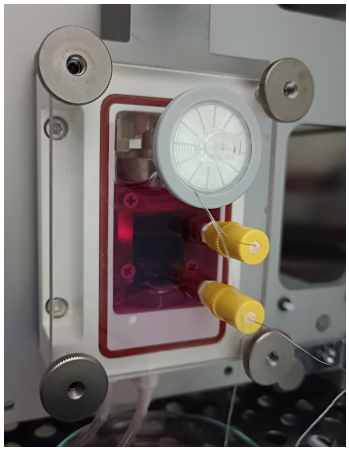

Figure 4.1 Examples of bioreactors: a) The spinner flask (Gupta et al., 2016)*, b) The rotating wall vessel (figure made by the author of this thesis), c) The multi-stimuli bioreactor (figure made by the author of this thesis).*

4.1.1 Mechanical forces

Cell function is greatly influenced by mechanical stimuli, which have various forms. The basic mechanical stimuli acting on cells even during static cultivation are based on the hydrostatic pressure of the culture medium, the stiffness of the environment of either the ECM or the biomaterial, and also intercellular tugging has its effect. In bioreactors, hydrodynamic pressure and shear stress are added due to constant flowing of medium over the surface of the structure and into the porous space of scaffolds. However, the most important and recently most studied is the specific mechanical loading (cyclic mechanical stretching or compression) that acts in the bioreactor.

Mechanical stimuli are a matter of fact in the natural tissue environment and indeed play a pivotal role in the normal function of tissues and organs. Mechanical stimuli are directly sensed by mechanosensitive compartments of cells and act as an active force for regulating cell physiology and directing cellular behavior. For example, mechanical stretch induces F-actin formation in cytoskeletons (see Figure 4.2) and vascular network formation, and influences the cell–cell interactions and endothelium–epithelium junctions. (Citi, 2019;

Joung et al., 2006; Le et al., 2016; Rodriguez-Boulan et al., 2005) However, inappropriate strain may cause issues in tissues as can be seen *in vivo*, such as chronic hypertension in blood vessels resulting in vascular endothelium dysfunction or chronic fast and shallow breathing that destructs the lung epithelium. (MacNee, 2006; Peng et al., 2019)

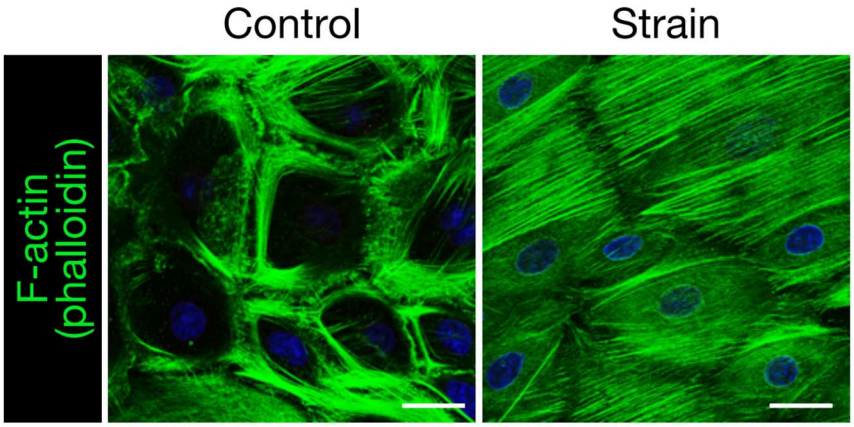

Figure 4.2 Example of the impact of mechanical stimulus on cell morphology: Actin formation in cytoskeletons of human primary epidermal keratinocytes stained by phalloidin dye (green color) shows increased F-actin stress fibers after 3 h of cyclic tensile strain. Scale bars, 25 µm. (Le et al., 2016)

The first description of changes in cellular activities as a response to mechanical forces was done by Wolff in 1892, who found differences in bone structures according to the magnitude of their load (Wolff, 1892). Since then, the roles of various physical cues during embryogenesis and development as well as in many pathological conditions have been studied, as there is evidence that mechanical stimuli substantially affect proliferation, morphogenesis, and migration of cells, including the differentiation of multi-potent stem cells. (Chen and Hu, 2006; Le et al., 2016; Lee et al., 2005; Nikkhah et al., 2012; Nokhbatolfoghahaei et al., 2020; Rosenfeld et al., 2016)

The effect of different types of mechanical stimuli on cells may vary, just as the effect of the same mechanical stimuli on different cell lines may vary. The cellular response to mechanical stress is based on the origin of the cell in vivo. For example, endothelial cells lining blood vessels are undergoing 2D circumferential stretch due to pulsatile blood pressure, whereas alveolar epithelial cells of the lung or cardiac myocytes are experiencing 3D stretch due to respiration and heartbeat. (Man et al., 2022)

4.1.2 Electrical field

In the case of many tissues, and especially of the electrosensitive ones – neural or cardiac tissue, the action of an external electrical stimulus is substantially impactful. It was found in 1964 by Bassett et al. that the direct electrical stimuli induce osteogenic differentiation and bone formation in adult dogs. (Bassett et al., 1964) Since then, it has been published that the electrical field can affect cell growth, migration, and some of the new studies have proved the impact of the applied electric current on the differentiation of multi-potent cells, especially neurogenesis and cardiomyogenesis. (He et al., 2019; Nazari et al., 2020; Shrestha et al., 2019; Yan et al., 2020) The positive impact of electrical stimulation on axonal regeneration of crushed facial nerve in *in vivo* experiments can be seen in Figure 4.3. (Jang et al., 2018)

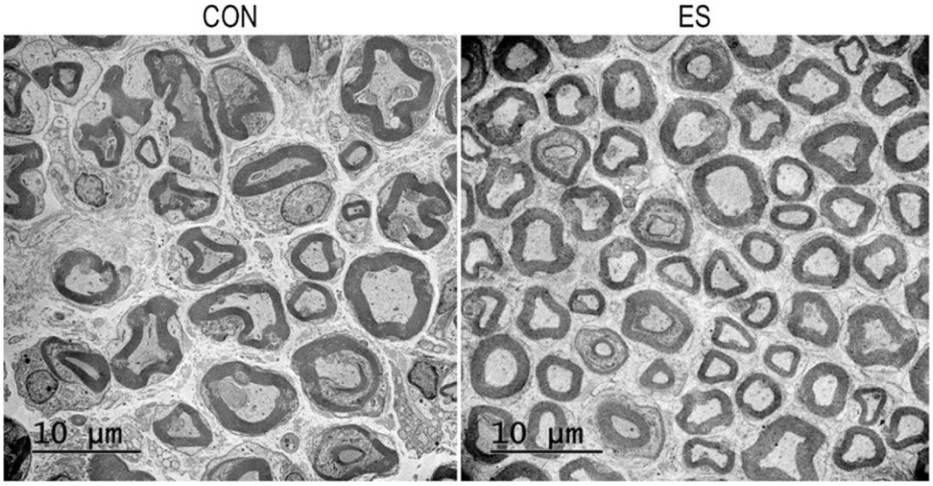

Figure 4.3 Example of the impact of electrical stimulus on nerve regeneration: At 4 weeks after nerve crush in rat facial parts, counts of regenerated axons were higher in the group exposed to electrical stimulation for 3 weeks (right) than the control group without electrical stimulation (left). The thickness of the myelin sheath was not significantly different. (Jang et al., 2018)

Impact of the external stimuli on cells can be further enhanced or directed by conductive biomaterial substrates. Organic conductive polymers, which are nowadays popular, have been determined to affect cell activities, help cells communicate with each other, and to a certain extant control multi-potent stem cell differentiation. (Gajendiran et al., 2017)

The combination of electrical stimulation and a conductive scaffold has been already utilized few times in the field of TE, especially for cardiac or peripheral nerve injuries treatment. For example, chitosan/PPy scaffold in combination with electrical stimuli increased neurotrophin secretion in olfactory ensheathing

cells, which further enhanced nerve regeneration. (Qi et al., 2013) The acceleration of axonal regeneration and neural recovery due to electrical stimulus on chitosan/PPy scaffold was proved as well in *in vivo* experiments on rats. (Huang et al., 2012) Regarding cardiac TE, it has been found that polyethersulfone/polyaniline scaffolds with aligned nanofibers drove the cells more efficiently to cardiomyocytes under electrical stimulation than that multidirectional electrical stimulation produced by randomly oriented scaffolds. (Mohammadi Amirabad et al., 2017)

4.1.3 Magnetical field

Magnetical external stimuli can significantly influence cell morphology and behavior through mechanisms, such as changes in membrane integrity, intracellular biochemical pathways, and enhanced cell signaling. For example, exposure to static magnetic fields has been shown to affect cell membrane fluidity by inducing rotations in phospholipid layers, which subsequently alters ion channel activities and promotes differentiation pathways in cells such as osteoblasts. (Yang et al., 2018). Additionally, when subjected to alternating magnetic fields, cells experience stretching and deformation, leading to the activation of mechanosensitive ion channels that can trigger calcium influx and initiate apoptotic signaling pathways. (Wong et al., 2018)

Furthermore, the use of magnetic nanoparticles in conjunction with external magnetic fields enhances internal cellular processes by facilitating the uptake of therapeutic agents and amplifying mechanical stress on cell membranes. For instance, Figure 4.4 showes the silk fibroin-based scaffold combined with poly(2-hydroxyethyl methacrylate) and embedded with magnetite nanoparticles and seeded with mouse embryonic preosteoblasts. When exposed to a low static magnetic field (120 mT), cells more proliferated with more organized orientation and actin filament alignment and also osteogenic differentiation was significantly enhanced. (Tanasa et al., 2020)

Additionally, the alignment and migration of cells in *de novo*[6] engineered tissues can be directed by magnetic forces, resulting in improved tissue organization and functionality, as demonstrated in vascular tissue constructs subjected to longitudinal stretching mediated by magnetic forces. (Du et al., 2017) Overall, these magnetic manipulations provide a dynamic approach for controlling cellular behavior in various TE and therapeutic applications.

[6] ***De novo*** *is a Latin term derived from the words de – from and novo – new. It is commonly used in life sciences to mean "anew" or "from the beginning".*

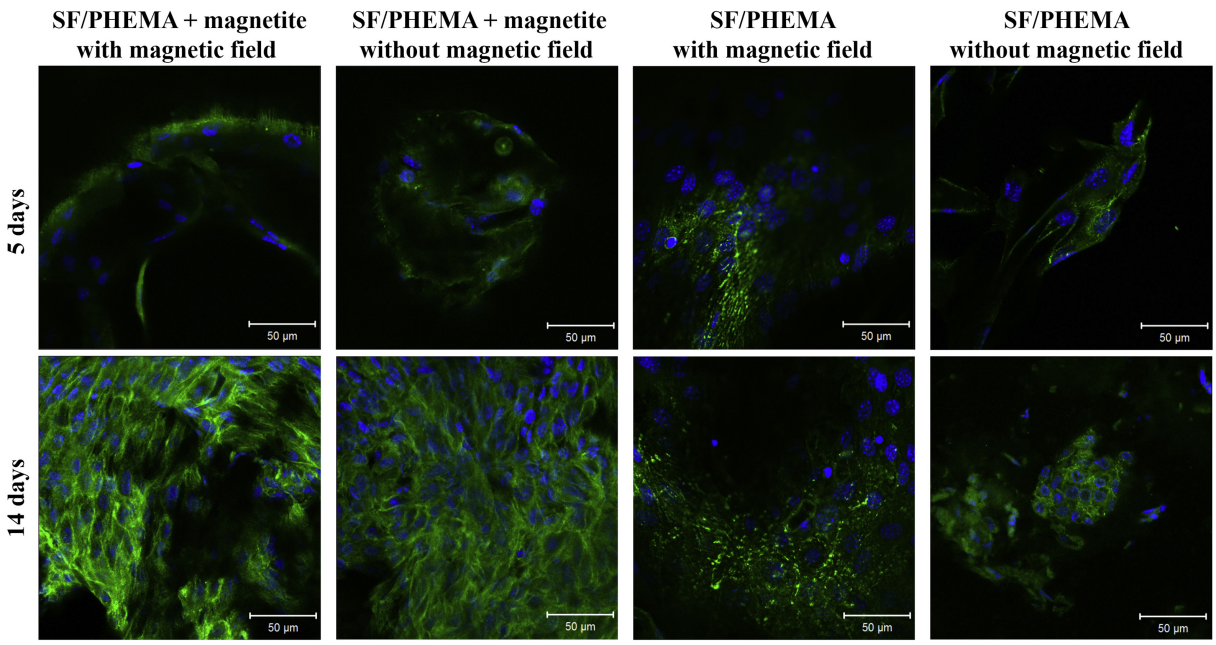

Figure 4.4 Example of the impact of magnetical stimulus in the combination with magnetical nanoparticals in the scaffolds on 3T3-E1 preosteoblasts morphology (actin filaments – green, nuclei – blue). The comparison of 5 and 14 days culture inside the scaffolds with and without magnetite under the exposure or absence of a 120 mT magnetic field. (Tanasa et al., 2020)

4.2 Cell image analysis

There are various ways to assess and evaluate the impact of a tested biomaterial or cultivation conditions or other factors of interest on cell viability and behavior. Variations of two basic principles are commonly used.

First, cell viability is usually evaluated by either flow cytometry or spectrophotometric measurement of staining substances bound or produced only by living/dead cells, such as the MTT assay or the neutral red uptake assay. The main advantage of these tests is that they can be used for a high number of tested factors, while the disadvantage lies in the specific limits of the use of each assay; for example, inappropriate coloration, the presence of proteins, or volatility in solvents of a tested material.

Secondly, cells and various cell components are commonly visualized by either fluorescence microscopy. It allows the morphology of the cells to be observed and the internal structures of the cells to be imaged using fluorescent dyes. The limitation of this method then lies in the evaluation that relies mostly on researcher's eyes and knowledge.

However, what if cells cannot be quantified by standard approaches? Is it possible to require cell counts from microphotographs (without manual counting)? Is there a way to quantify not only the number of cells but also their morphology? Yes, the combination of quantification and qualification of different cell features is possible by **image analysis**. Software tools, such as open-access CellProfiler (Carpenter et al., 2006), can determine the count, size, shape, and texture of cells or separately cytoplasms, nuclei, or other organelles (see Figure 4.5). Image analyses can also indicate cell cycle phase or the level and localization of proteins and phosphoproteins. Further, it can evaluate cell migration in the scratch assay or yeast growth patches in yeast colonies. Another important advantage is processing, evaluating, and comparing arbitrary amounts of data and cell images.

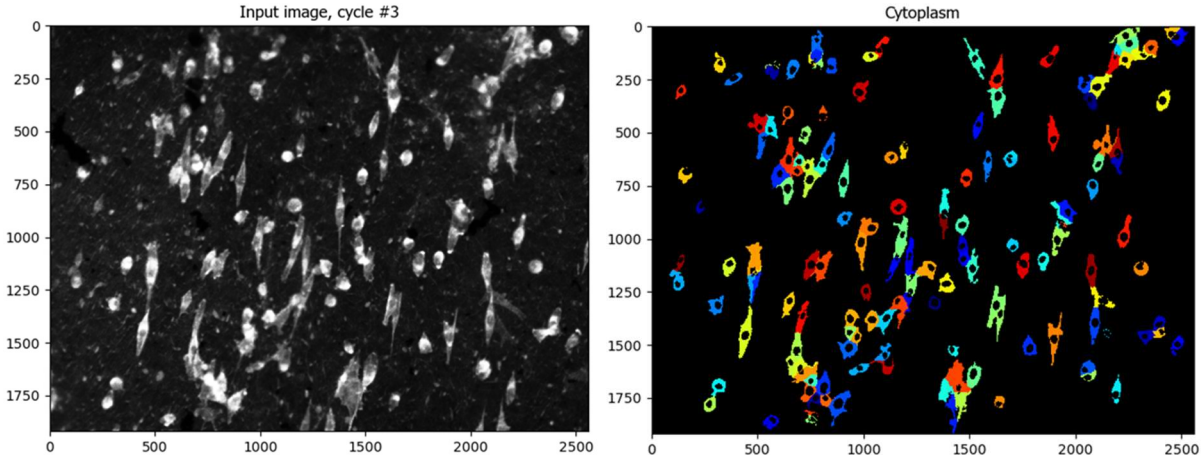

Figure 4.5 Example of the cell image analysis: On the left – fluorescence microphotograph of NIH/3T3 mouse fibroblasts grown on a tested material. On the right – the process of the image analysis focused on the cytoplasm size and shape. (Figure made by the author of this thesis).

5. OBJECTIVES OF THE THESIS

The main objective was to advance our understanding of how to coordinate the key components, such as biomaterial design, external stimuli, and selected cell lines, in order to achieve harmonious integration leading to the *de novo* formation of functional tissue, much like orchestrating individual instruments to create a cohesive and beautiful symphony.

To achieve this objective:

- Various thin films and scaffolds with potentially bioactive properties were designed and fabricated.
- Material properties of such films and scaffolds were characterized to reveal their compliance with requirements.
- Cytocompatibility and bioactivity of such films and scaffolds were determined using advanced *in vitro* biological evaluation to confirm the performance quality.

6. EXPERIMENTAL PART

6.1 Preparation of thin films

In the field of TE, conductive polymers have been very well known as highly promising materials, particularly for applications involving electrosensitive tissues, such as cardiac and neural systems. Their unique ability to conduct electrical signals makes them ideal for supporting the function and regeneration of cardiomyocytes, which rely heavily on synchronized electrical activity. Additionally, conductive polymers have shown potential in enhancing wound healing in skin tissue by promoting cell migration and proliferation under electrical stimulation.

During my research of conductive polymers, I focused on **PANI**, **PPy**, and **PAz**, each offering distinct advantages. PANI is known for its controllable conductivity and redox states, while PPy boasts more stabile electroactivity in biological environment. In contrast, PAz introduces a unique nonbenzenoid backbone that may open new avenues for functional design, but its practical advantages in TE remain unknown.

Conductive polymers were predominantly synthesized *via* **chemical oxidative polymerization**. With the aim of their application in TE, emphasis was placed not only on producing polymer powders, but especially on the fabrication of thin films. In the case of PAz, however, the results obtained through conventional chemical synthesis were questionable. Therefore, alternative approaches were employed: **electrochemical synthesis** of polyazulene and chemical synthesis of so-called '**true polyazulene**'.

Due to the high novelty of the research of PAz, the preparation procedure and results are not included in the dissertation. However, the committee will have access to the manuscript that has been submitted to a peer-reviewed journal.

The key material property investigated was the specific conductivity, determined using the four-point van der Pauw method. Furthermore, surface free energy by contact angle was analyzed, as it significantly influences cell and protein adhesion at the material interface. These and additional characterization techniques were conducted in collaboration with colleagues from the Centre of Polymer Systems and the Faculty of Technology, Tomas Bata University in Zlín.

6.2 Preparation of scaffolds

Another part of the research was the preparation and subsequent modification of various polymeric substrates in order to create a biocompatible scaffold with multiple cell-instructive cues. The choice of materials of interest must be in accordance with the intended application. For heart TE, thus, the scaffold must possess significant elasticity since cardiomyocytes are responsible for the contraction of the heart. Cohesion and rift resistance were also important properties necessary for reliability under further handling and stress.

The primary substrate I focused on was medical-grade **PU** electrospun into nanofibrous mats. After process and post-process optimization, scaffold with stable cytocompatibility was obtained. However, the product of electrospinning had randomly oriented fibers. To better mimic *in vivo* environments such as extracellular matrix or myocardium structure and thus provide cells with cues, **anisotropy** needed to be involved in the substrates. Therefore, the PU mats were modified to align their fibers in one direction. Whether the anisotropy was not only structural, but also mechanical, was determined by tensile testing.

Another material I investigated as a suitable alternative for the preparation of tissue scaffolds for electrosensitive tissues was **PVDF** and its copolymers. This material is particularly interesting due to its piezoelectric properties and, as demonstrated this work, its good cytocompatibility. With the use of a new electrospinning device, it was possible to fabricate anisotropic nanofibrous scaffolds directly during the spinning process, rather than through post-processing, as was the case with polyurethane.

The main functions of cardiomyocytes are induction, propagation, and reaction to electrical impulses. Thus, scaffold **conductivity**, which facilitates cell-to-cell communication, serves as a strong cellular cue possibly promoting stem cell cardiomyogenesis. For this purpose, conductive polymers were applied to substrate surfaces by *in situ* polymerization.

Characterization of the physicochemical properties of the prepared scaffolds was carried out in cooperation with my colleagues from the Center for Polymer Systems and the Faculty of Technology of Tomas Bata University in Zlín.

However, even the most sophisticated scaffold design is useless when cells do not adhere to the scaffold. This occurs for many reasons; for example, unsuitable functional groups on the surface and associated too low or too high free surface energy. These limitations in **cytocompatibility** were overridden by coating the scaffold's surface with serum albumin and bovine gelatin.

6.3 Cytocompatibility testing

The research was followed by a series of cytocompatibility tests, utilizing unipotent cells – mouse embryonic **fibroblast** cell line NIH/3T3, human **keratinocyte** cell line HaCaT, and totipotent cells – mouse embryonic **stem** cell line ES R1, including their formation of embryonic bodies that differentiated towards cardiomyocytes.

A series of standard experiments was implemented to determine the overall cytocompatibility of the prepared thin films and scaffolds. In addition to these biomaterials, the author cooperated with other colleagues and characterized the biological properties of **other scaffolds** with a potential for employment in TE of electrosensitive tissues: porous scaffolds made of CIPs, hyaluronan-based hydrogel scaffolds containing CIPs, and Pebax scaffolds.

Another essential component of my study was the **dynamic cell cultivation**. The cultivation of cells with various external stimuli is intended to mimic *in vivo* physiological conditions. Using three different bioreactors, as well as self made electrodes, I devoted myself to explore the use of electromagnetical filed, hydrodynamic shear stress, and tensile strain as such external stimuli to cells.

During my research activity, I encountered several approaches to evaluate cell viability, such as MTT, ATP, and Red uptake assays, and the use of UV-VIS. For cell morphology visualization, optical microscope, fluorescence inverted microscope, and confocal laser microscope were used. For the observation of cellular migration, a scratch assay was used.

Cell image analysis is an advanced evaluation technique that allowed to quatify viable cells which could not be quantified by other standard approaches. Moreover, it was used it to qualify cell morphology more accurately. Cell image analysis was performed in the open-access CellProfiler software.

7. SELECTED PROCESSING METHODS

7.1 Synthesis of conductive polymers

7.1.1 Polyaniline

PANI powder was synthesized *via* chemical oxidative polymerization. A 0.2 M aqueous solution of aniline hydrochloride (Penta, Czech Republic) was mixed with a 0.25 M aqueous solution APS (Sigma-Aldrich, USA) at room temperature. After 24 h, the resulting green precipitate was vacuum filtered, thoroughly washed with 0.2 M hydrochloric acid (HCl, Penta, Czech Republic) and methanol (Penta, Czech Republic), and then air-dried.

PANI films were formed directly on TCDs, or indium tin oxide (ITO) glass, or pre-fabricated scaffolds by *in situ* polymerization that was carried out under the same conditions as the synthesis of PANI powder, except for earlier termination of the polymerization reaction, specifically after 1 h.

7.1.2 Polypyrrole

PPy powder was synthesized *via* chemical oxidative polymerization. A 0.2 M aqueous solution of pyrrole (Sigma-Aldrich, USA) was mixed with a 0.25 M aqueous solution of either APS or anhydrous $FeCl_3$ (IPL, Czech Republic) at room temperature for 24 h. The resulting black precipitate was vacuum filtered, thoroughly washed with 0.2 M HCl and methanol, and then air-dried.

PPy films were formed directly on TCDs, or ITO glass, or pre-fabricated scaffolds by *in situ* polymerization that was carried out under the same conditions as the synthesis of PPy powder except for earlier termination of the polymerization reaction, specifically after 60 s.

7.2 Preparation of scaffolds

7.2.1 Electrospinning of polyurethane

PU Desmopan 385 S (Covestro AG, Germany) was electrospun into nanofibrous mats using the electrospinning device Nanospider (Elmarco, Czechia). The PU solution was extruded into 32 jets into a 75 kV electric field to the planar collector with a moving film. Four deposited layers were collected, and the produced PU mats were then rinsed in ultrapure water for at least 7 days (changed every 2-3 days) to wash out residual monomers and additives. The alignment of fibers in one direction was introduced by hand stretching of the PU mats above a 150 °C heat source with subsequent securing to a microscope cover glass that served as a holder with a united surface area (22×22) mm^2.

7.2.2 Electrospinning of polyvinylidene fluoride

PVDF with various molecular weights (Sigma-Aldrich, USA) or PVDF-HFP with various molecular weights (Sigma-Aldrich, USA) was dissolved in dimethylformamide (Sigma-Aldrich, USA) at 60 °C while stirring for at least 1 h to create a 10 wt. % solution. Electrospinning was then done on the device built by colleagues at the Faculty of Technology, Tomas Bata University in Zlin. The solutions were extruded from 1 jet into a 14–40 kV electric field to either a planar or a cylindrical collector. The higher the speed of cylinder rotation, the more aligned the fibres.

7.2.3 Surface coating

Coating with conductive polymers, especially PPy, was done by *in situ* polymerization as already described above. Coating with biopolymers was done by rinsing the scaffold into solutions of serum albumin and bovine gelatin (Sigma-Aldrich, USA), separately or combined, for 20 min.

7.3 Material characterization

7.3.1 Specific conductivity

The electric conductivity of conductive films deposited on TCDs or ITO glass substrates was determined by the four-point van der Pauw method. A system consisting of Keithley 6517B electrometer, Keithley 2410 source meter, and Keithley 7002 switch (Keithley Instruments, USA) was used at room temperature.

7.3.2 Free surface energy

Measurements of contact angles on conductive films on the surface of TCDs were done by a Theta Optical Tensiometer (Biolin Scientific, Finland) with demineralized water, ethylene glycol, and diiodomethane (all from Sigma-Aldrich, USA). Contact angles were measured at 10 µL droplets after (10 ± 2) s at room temperature with consequent ten times repetitions. The surface free energy was calculated using the "acid-base" method.

7.3.3 Tensile properties

Tensile properties of PU mats were measured on MT350-5CT (Testometric, UK). The samples were cut in a rectangle shape with a length of 40 mm, width of 10 mm, and thickness of 0.015 mm. The elongation was carried out with a speed of 100 mm/min. and at the room temperature.

7.4 Cell lines

7.4.1 Mouse embryonic fibroblast cell line

Mouse embryonic fibroblast cell line NIH/3T3 (ATCC CRL-1658 NIH/3T3, USA and ECACC 93061524, England) was cultivated in Dulbecco's modified eagle's medium (BioSera, France) + sodium hydrogen carbonate (Penta, Czech Republic) + calf serum (to 10 vol. %) (BioSera, France) + 100 μg/mL antibiotics penicillin/streptomycin (to 1 vol. %) (BioSera, France).

7.4.2 Human keratinocyte cell line

Human keratinocyte cell line HaCaT (Boukamp et al., 1988) was cultivated in RPMI medium 1640 with L-glutamin (Gibco™, USA) + sodium hydrogen carbonate + fetal bovine serum (to 10 vol. %) (Gibco™, USA) + 100 μg/mL antibiotics penicillin/streptomycin (to 1 vol. %).

7.4.3 Mouse embryonic stem cell line

Mouse embryonic stem cell line ES R1 was cultivated in Dulbecco's modified eagle's medium (Gibco™, USA) + fetal calf serum (to 16.5 vol. %) + 100 μg/mL antibiotics penicillin/streptomycin (to 1 vol. %) + 100 mM of non-essential amino acids (Gibco™, USA) + 0.05 mM β-mercaptoethanol (Sigma-Aldrich, USA) + 5 ng/mL leukemia inhibitory factor (LIF) (Chemicon, USA).

7.4.4 Cell co-culturing

Mixed cell population was created by two approaches. First, fibroblasts and stem cells were seeded on gelatinized (0.1 % gelatin from bovine skin) surface at once at the concentrations of 5×10^4 fibroblasts/mL of complete culture medium and 4×10^3 stem cells/cm^2 of the surfaces area. Second, the fibroblasts (2×10^5 fibroblasts/mL of complete culture medium) were seeded first and after 24 h of cultivation, stem cells (8×10^3 stem cells/cm^2 of the surfaces area) were seeded on top of the fibroblasts. In both approaches, the stem cell line culture medium containg LIF was used. The cultivation was carried out for 4 days with medium changes every day.

7.5 Cultivation under static conditions

All cell lines cultivated under standard static conditions were maintained in a HERAcell 150i incubator (Thermo Scientific, USA) under standard culture conditions: 5% CO_2 atmosphere, a stable temperature of 37 °C, and consistent relative humidity.

7.5.1 Extraction and cytotoxicity

Extracts of various tested materials were prepared according to ISO 10993-12 standards. The extraction was carried out in closed containers at 37 ± 1 °C while stirring for 24 h. Subsequently, the extracts were separated from the samples by centrifugation at 1000 g for 15 min followed by filtration through a 0.22 μm Millex GV filter (Merck, Darmstadt, Germany). The parent extracts (100 %) were diluted in complete medium to obtain a series of dilutions. Within 24 h, all extracts were applied to precultivated fibroblasts in 96-well plates and in at least three repetitions for each dilution. After 24 h of exposure, the cytotoxicity testing was conducted according to the ISO 10 993-5.

7.5.2 Cell adhesion and proliferation

All tested materials were sterilized before coming in contact with cells. The method of sterilization was chosen in accordance to the material properties. For example, hydrogels were rinsed in ethanol for at least 1 h and then in ultrapure water for at least 3 days, while thin film layers of conductive polymers were briefly rinsed with ethanol and then sterilized by 30 min exposure to UV light.

Fibroblasts, keratinocytes, or stem cells were seeded onto the surface of the tested materials and references at various concentrations but mostly regularly at 1×10^5 cells/mL of complete culture medium. For stem cells, all tested substrates, including references, were coated with 0.1 % gelatin from bovine skin (Sigma-Aldrich, USA) in ultrapure water. The samples with cell suspension were then incubated for at least 4 days with medium changes every 2 days.

7.5.3 Cell migration

To evaluate the migratory capacity of cells, the scratch assay was carried out. In this method, a uniform straight scratch was manually introduced into a confluent monolayer of cells using a sterile pippet tip. After removal of loose cellular debris and application of fresh medium, the migration of cells into the wound area is monitored and documented using optical microscopy at defined time intervals, ussualy every 1 h for 8 h period (during the day) and then the next morning (at 24 h since the scratch was done). The wound coverage was then evaluated by image analysis software.

7.5.4 Cell differentitation

Differentiation of embryonic stem cells ES R1 was initiated *via* embryoid body formation using a microwell culture plate AggreWell™800 and anti-adherence rinsing solution (StemCell Technologies, USA). The cells were

cultured within microwells containing approximately 400 cells each and with the complete medium lacking LIF. After five days, the resulting embroyd bodies were individually transferred to the surface of tested materials or reference, all precoated with gelatin and further maintained for 11 days in serum-free DMEM-F12 medium supplemented with 100 μg/mL antibiotics penicillin/streptomycin (to 1 vol. %) and an insulin–transferrin–selenium (ITS) mix (to 1 vol. %) (Thermo Fisher, USA). The medium was refreshed every 2 days throughout the cultivation period.

7.6 Cultivation under dynamic conditions

Dynamic cultivation builds on standard static conditions by introducing external stimuli while keeping the same controlled environment within the incubator (37 °C, 5% CO_2, high humidity).

7.6.1 Electrical and magnetical external stimuli

Direct current stimulation was introduced to cells through selfmade electrodes to investigate how electric fields influence cellular behavior, particularly in the context of conductive polymeric substrate. Cells were exposed to either constant or pulsed direct current electrical stimulation, with varying exposure/pause intervals and voltage levels ranging from tens of volts lasting minutes to tens of millivolts lasting for hours.

Magnetic fields, particularly when coupled with magnetic nanoparticles like CIPs, can be utilized to remotely control cell behavior and scaffold properties. This non-invasive approach was applied to cells using a permanent magnet to generate a stable magnetic field.

7.6.2 Mechanical external stimuli

One of the mechanical stimuli that was applied to cells and investigated was hydrodynamic shear stress. To apply this stimulus, the Rotary cell culture system (Synthecon, Inc., USA) and the Ibidi pump system (Ibidi, Germany) were used. For the former, cells were pre-adhered to a substrate that was then attached to a sel-made holder and placed in to the Rotary system. For the latter, the cells were seeded directly in to the testing chamber. Both systems allowed for the continuous circulation of culture medium over cell monolayers, creating controlled hydrodynamic shear stress conditions

7.6.3 Multiple external stimuli combined

The TC-3 bioreactor (Ebers Medical Technology, Spain) enables the application of multiple stimuli at ones: hydrodynamic shear stress from flowing media, tensile strain from stretching, and electrical pulses delivered by electrodes. Cell cultivation on electrospun PU mats was conducted with fibroblasts and embryonic stem cells at a concentration of 1×10^5 cells per mL of culture medium. The cells were allowed to proliferate under static conditions for 3 days before being transferred to the bioreactor. The system was set to apply cyclic stretching (1 mm at 1 mm/sec speed) for various time periods (e.g. 10 min of stretching followed by 50 min pause) together with electrical field or pulses (0.1 V) over a 3-day period. Due to repeated infections, gentamycin (20 μg/mL) was added to the medium to prevent contamination.

7.7 Cell viability evaluation

7.7.1 MTT assay

MTT assay is a colorimetric method based on 3-(4,5-dimethylthiazol-2-yl)-2,5-diphenyltetrazolium bromide (Duchefa Biochemie, Netherlands) which is reduced by mitochondrial enzymes of living cells to violet formazan. The absorbance of formazan dissolved in dimethylsulfoxide (Duchefa Biochemie, Netherlands) is then measured on the Infinite M200 Pro NanoQuant spectrophotometer (Tecan, Switzerland) at 570 nm with the reference wavelength 690 nm. The results are expressed as a relative reduction in cell viability compared to the reference cells.

7.7.2 ATP assay

An alternative approach to assess cell viability involves measuring intracellular adenosine triphosphate (ATP) levels. This technique relies on the luminescent reaction of firefly luciferase, which produces light in response to ATP in the presence of luciferin, Mg^{2+} ions, and oxygen. The intensity of the emitted light is directly proportional to the ATP concentration. In this study, the Cellular ATP Kit HTS (Invitrogen Corporation, USA) was employed to determine ATP content, and luminescence readings were obtained using an Infinite Lumi luminometer (Tecan, Switzerland).

7.7.3 Neutral red uptake assay

The Neutral red uptake assay is a method for evaluating cell viability based on the ability of viable cells to incorporate and bind the dye neutral red. This weak cationic dye accumulates in lysosomes of living cells, where it is retained by active transport and proton gradients. Damaged or non-viable cells lose this ability due to compromised membrane integrity and lysosomal function, leading to reduced dye uptake. Following incubation with the dye, excess is removed and the absorbed neutral red is subsequently extracted and quantified by measuring absorbance at 540 nm on Infinite M200 Pro NanoQuant.

7.7.4 UV-VIS

Another method employed for cell quantification in this work was UV-VIS spectrophotometry. After detachment from the surface of tested materials using trypsin, the harvested cells were resuspended in phosphate-buffered saline. The resulting cell suspension was then analyzed using the Implen NanoPhotometer® NP80 UV/Visible Spectrophotometer, which allows rapid and accurate absorbance measurements in microvolume samples.

7.8 Cell morphology visualization

7.8.1 Microscopy

For regular checks on cell behavior, a phase-contrast **optical** microscope (Olympus IX51, Japan) was employed. For a further determination of cellular morphology, the cells were fixed with 4% formaldehyde (Penta Chemicals, Czech Republic) in ultrapure water and permeabilized with 0.5% Triton X-100 (Sigma-Aldrich, USA) in phosphate-buffered saline. Fluorescent dyes ActinRed^{555} or ActinGreen^{488} (Life Technologies, USA) and Hoechst 33258 (Sigma-Aldrich, USA) were used for staining. ActinRed or ActinGreen binds to the proteins contained in the cytoskeleton of the cells and Hoechst penetrates the nuclei of the cells where it binds to the DNA. Then the stained cells were observed under a phase-contrast inverted **fluorescence** microscope (Olympus IX 81, Japan). In the case of 3D scaffolds, a **confocal** laser scanning microscope (Olympus FV3000, Japan) was used.

7.9 Image analysis

Cell image analysis is used to, among other things; more accurately quantify cells as well as qualify cell morphology. The image analyses were performed in the open-access CellProfiler software 4.0.7. (Carpenter et al., 2006)

For successful and more presice analysis, the fluorescent cell photographs were divided into separate images of nuclei and cytoskeletons, converted to grayscale, and slightly adjusted for higher contrast and less fluctuation in brightness, especialy those caused by substrate structural inequities.

Cell image analysis provides a variety of results, such as cell/cytoskeleton/ nucleus number, area, perimeter, major and minor axis length, eccentricity, orientation and much more. Therefore, only the most relevant features were always selected and discussed. Cellprofiler was also used to evaluate scratch test assays.

8. SUMMARY OF RESULTS

The primary motivation of this research was to deepen the understanding of how polymer-based conductive and electroactive biomaterials influence cell behavior, particularly in the context of the engineering of electrosensitive tissues.

As electrosensitive tissues rely on precise electrochemical signaling for its development, function and regeneration. The development of scaffolds that both mimic native tissue structure and support electrical conduction represents a promising strategy for their *in vitro* building and *in vivo* repair and replacement. (Guarino et al., 2016; Ning et al., 2018) In addition, the study and implementation of tailored dynamic culture conditions may induce specific cellular responses, especially in totipotent cells. (Hippler et al., 2019; Kamble et al., 2018; Mojena-Medina et al., 2020) If mimicking natural physiological conditions, this potentially leads to more precise cytocompatibility testing results corresponding to real *in vivo* cell behavior, particularly in a combination with advanced evaluation methods.

To address these challenges, the experimental work encompassed the synthesis and detailed characterization of conductive polymers, the fabrication of composite scaffolds with multiple cell-instructive cues, each followed by comprehensive cytocompatibility testing and evaluation, as described in 6. Experimental part.

8.1 Preparation of bioactive thin films and their impact on cells

Conductive polymers have been widely explored in TE due to their straightforward synthesis, favorable biocompatibility, and intrinsic conductivity (Jasenská et al., 2021), as was discussed in more detail in 2.2 Utilization of polymers. Compared to traditional conductive metallic materials, conductive polymers offer a distinct advantage: they can be engineered to replicate the mechanical properties of native biological tissues. This tunable flexibility enables them to conform more naturally to soft tissue environments, thereby improving integration and significantly minimizing the risk of triggering adverse immune responses. (Humpolicek et al., 2018b; Jeong et al., 2015)

Recently, the most commonly studied conductive polymers are PANI and PPy. To achieve reproducible and tunable conductivity at once with biological stability, various modifications to the polymers have been introduced, such as doping (Capáková et al., 2020; Hursán et al., 2022; Uda et al., 2021), colloid formation (Kim et al., 2018; Kucekova et al., 2014), or incorporation into different complex biocomposites (Ben Ayed et al., 2022; German et al., 2019).

The author of this thesis also researched, during her doctoral studies, several methods to enhance the overall performance of conductive polymers; for example, the stabilization of PANI colloids with chitosan, or the preparation of pickering emulsions based on PANI and nanocellulose. However, her main attention was paid to the preparation of polymer conductive coatings (see Figure 8.1) that can be synthesized directly on various surfaces by a method as easy, fast, and versatile as possible. The fulfillment of these conditions is necessary for the successful application in practice.

During the reaserch of PANI, it has been found it often exhibits higher toxicity and poor stability in physiological environments due to dedoping and subsequent loss of conductivity. (Beygisangchin et al., 2021b; Firda et al., 2021) In contrast, PPy generally shows superior cytocompatibility and bioactivity, while maintaining its electroactivity and conductivity when exposed to physiological conditions; for example, by contact with cell culture media, making it more suitable for biomedical use. (Firda and Jeon, 2022; Gh et al., 2017) As a result, PPy became the more favored option for my further studies.

While PANI and PPy are well-known polymers in biomedical research, PAz, on the other hand, is not at all. PAz presents a novel approach to material design *via* its nonbenzenoid structure, which imparts unique electronic and mechanical properties that differ from traditional conductive polymers. This study thus potentially opens new pathways for biocompatible electronic applications of PAz (see Figure 8.1).

The author supervised the master thesis on the topic of PAz biological properties and there comparison to PANI and PPY: Stuchlíková, S., 2023. *Polyazulen a jeho biologické vlastnosti.* Master thesis. Tomas Bata University in Zlín, Faculty of technology.

Figure 8.1 Concuctive polymer films: (left) PANI, (middle) PPy, (right) PAz films on TCDs all prepared by in situ chemical polymerization oxidized with APS. (Figure made by the author of this thesis).

8.1.1 Polypyrrole surface coating within a minute

The easy, fast, and versatile synthesis of PPy can be achieved by chemical oxidative polymerization, enabling the formation of both powder and thin film forms suitable for biomedical integration. While effective, utilizing this method for PPy coating often requires electrical input, uncommon solvents or stabilizers, long reaction times, and/or low temperatures. (Golgovici et al., 2020; Maráková et al., 2017; Thunberg et al., 2015)

Through a series of chemical *in situ* oxidative polymerizations of PPy under different settings and conditions, a method was developed that allows the synthesis of a uniform conductive layer of PPy in aqueous solution without any additives at room temperature, all done within a minute. The description of this PPy coating method alongside its characterization, application on PU fibrous scaffolds, and cytocompatibility testing was published by **Mahelová, L.**, Slobodian, P., Kocourková, K., Minařík, A., Moučka, R., Trchová, M., Martínková, M., Skopalová, K., Víchová, Z., Kašpárková, V., Humpolíček, P., 2024. *Method for in situ polypyrrole coating, and the example of its use for functionalization of polyurethane anisotropic electrospun mats.* Heliyon 10. https://doi.org/10.1016/j.heliyon.2024.e27883 **(Article I).**

The simplicity of this PPy thin layer synthesis method makes it well-suited for routine use or large-scale production. Scientific progress often depends not only on the publication of methods that can be reproduced by other researchers. The value of this article lies not only in the introduction of a novel procedure for the preparation of PPy films, which in itself represents a significant scientific contribution, but also in the clear documentation of the specific skills required for the successful fabrication of these films. In particular, it highlighted the

necessity of maintaining a very short polymerization time, which is critical for achieving reproducible results. Also, due to the reaction's rapid pace, precise control of polymerization time is crucial. As shown in Article I, prolonged reaction leads to the growth of PPy particles until they detach from the surface, compromising the coating continuity. Conversely, the earlier the polymerization procedure is terminated, which can be done by removing the reaction solution and rinsing the newly formed PPy with hydrochloric acid, the more uniform PPy coating layer is manufactured.

Additionally, PPy coatings synthesized within only 15 seconds demonstrated favorable conductivity levels, specifically in higher tens of S/cm. These are relatively good conductivity results since similar PPy products may occupy a range beginning at zero or approximately 10^{-10} S/cm, ending with less than 2×10^{3} S/cm. (Gh et al., 2017; Guimard et al., 2007; Mahmoodian et al., 2015; Navale et al., 2014; Pang et al., 2021; Sasso et al., 2011; Thunberg et al., 2015). To establish the conductivity of PPy thin layers, the four-point van der Pauw method was utilized as it is commonly used for measuring the resistivity of thin-shaped materials. (Kašpárková et al., 2017; Patois et al., 2010) However, the drawback of this method is that it is strongly dependent on the film thickness.

To measure the true thickness of PPy thin-layer coatings, the clear edge had to be created first. Figure 8.2 shows how this was achieved. A silicon mask was placed to the centre of a TCD and firmly clamped to its surface. Then, the *in situ* oxidative polymerization of PPy was carried out as usual. After the reaction termination, it was left to dry (still clamped), and only after that, the mask was removed, revealing the rectangular shape of the pristine TCD surface with clear edges, where the thickness of the PPy film was then determined by profilometry.

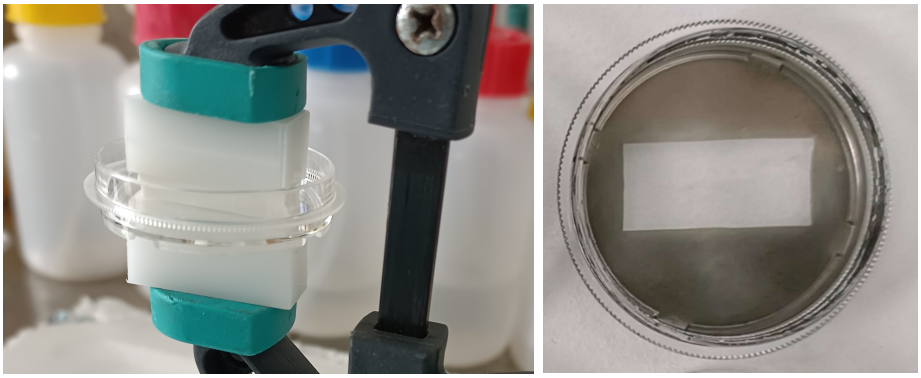

Figure 8.2 Creation of edges in PPy film: (left) the silicon mask placed and secured in the middle of a TCD, (right) the resulted PPy film after the mask removal. (Figure made by the author of this thesis).

The thickness of PPy films was different based on the length of reaction time and also the oxidizing agent used, APS or $FeCl_3$. In connection with this, also conductivity and surface roughness varied; however, it is not surprising, as it has been known since Chen et al., 1995 that the choice of oxidizing agent affects the properties of the resulting polymer. Despite some variations, both oxidizing agents led to coatings with limitations in cytocompatibility, largely attributed to unsuitable surface free energy. It was measured by contact angles that were slightly above the Berg limit of $\sigma = 65°$. (Berg et al., 1994; Vogler, 1998)

However, this issue can be and was effectively addressed through standard surface modification techniques used in cell culture, such as adhesion of proteins, such as albumin or gelatin, to the PPy film surface. This approach significantly enhanced the cytocompatibility of the film, in particular when the combination of albumin and gelatin was used. For more details on PPy synthesis and properties, see Article I.

8.1.2 Polyazulene holds great potential in tissue engineering

Polyazulene is particularly intriguing due to its unique nonbenzenoid structure, which imparts unconventional electronic properties along with potentially favorable mechanical and optoelectronic behavior; however, despite these promising characteristics, it has not yet been explored within the field of biomedicine, making it a novel and entirely untapped material in this context. An article addressing this issue was prepared and submitted for peer review. At the time of submitting this dissertation, the article had not been published yet. Therefore, the methodology and results are not presented here; however, the article will be available for inspection during the thesis defence: **Mahelová, L.,** Trchová, M., Kotowicz, S., Škoda, D., Kocourková, K., Víchová, Z., Vícha, J., Kašpárková, V., Humpolíček, P., 2025. *Is polyazulene cytocompatible? It depends.* (**Appendix I**) Beyond the scope of the paper, I can present the following results.

Research into PAz began with the same objective as for other conductive polymers – finding a synthesis method as easy, fast, and versatile as possible. Through a series of various synthesis set-ups and conditions, PAz powders were synthesized with chemical oxidative polymerization and characterized. FTIR and Raman spectroscopy revealed that the use of (ultra pure) water as a solvent resulted in a significantly higher amount of oxidized derivatives of azulene and

its oligomers, compromising the quality of the obtained product, in comparison to the results when ethanol solvent was used. Other solvents such as acetonitrile or dichloromethane were also tried and considered; however, ethanol was chosen as the best option since it is much less cytotoxic and does not compromise TCDs.

Another method of PAz synthesis is electrochemical polymerization. However, due to the lack of suitable equipment, it was not possible to perform this synthesis at the laboratories of the Centre of Polymer Systems. Therefore, the author attended an internship at the University of Silesia in Katowice, where the electrochemical synthesis of PAz was carried out. The most significant influence was observed with changing azulene concentration in a solution. The differences in the resulting PAZ films are notable to the naked eye in Figure 8.3.

Figure 8.3 Electrochemicaly prepared PAz: (left) the standard three-electrode cell with coiled Pt counter electrode, ITO glass working electrode, and Ag reference electrode; (right) films on ITO glass prepared from azulene concentrations 5×10^{-4}, 1×10^{-3}, and 5×10^{-3} mol/dm^3 respectively. (Figure made by the author of this thesis).

To further understand these differences see Figure 8.4 – a voltammetric plot of the oxidation of azulene at various concentrations and the subsequent formation of PAz. It is evident that at the lowest concentration, the cyclic voltammetric curves showed low, well-defined peaks, indicating slow, controlled film growth. As the concentration increased, the peak currents increased and the voltammograms broadened, indicating faster polymerization and thicker film formation. At the highest concentration, the curves were distorted by high capacitive currents, indicating rapid, less controlled deposition and possible electrode passivation. For more cyclic voltammetric plots with different variables, see Appendix I and its Supplementary Material.

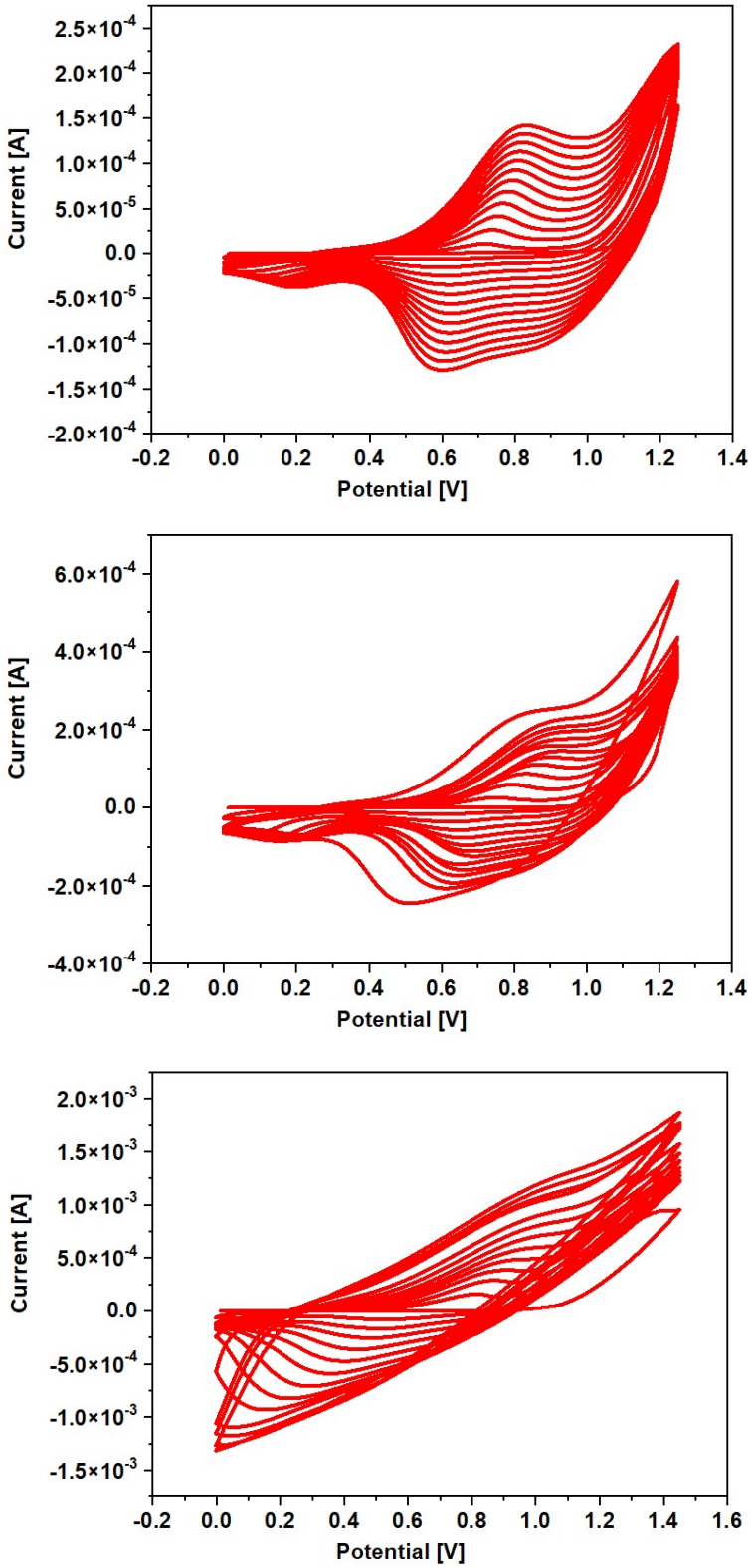

Figure 8.4 Electrochemicaly prepared PAz: Cyclic voltametry of azulene oxidation and electrochemical PAz polymerization on ITO glass in 13 cycles with 100 mV/s scan rate and different azulene concentrations: (up) 5×10^{-4} mol/dm^3, (middle) 1×10^{-3} mol/dm^3, (down) 5×10^{-3} mol/dm^3. (Figure made by the author of this thesis).

Electrochemical synthesis has proven effective for producing conductive PAz films; however, it also presents limitations – most notably, the requirement for conductive substrates such as platinum and other metals or ITO, FTO glasses, both of which are not suitable for TE applications since most tissues are soft tissues. However, a flexible alternative has emerged lately: ITO coated PET – transparent, conductive and flexible. (Krukiewicz et al., 2023; Nur Hidayah et al., 2024)

Regardless of the preparation method, synthesis and characterization are constrained by the high cost of the monomer azulene, largely due to its limited commercial availability. Nevertheless, further physico-chemical and biological evaluations are warranted as PAz represents an unexplored yet promising material.

8.2 Preparation of bioactive scaffolds and their impact on cells

8.2.1 Polyurethane scaffolds benefit from the introduced anisotropy

Since the main aim of this thesis is to prepare and characterize biomaterials in respect to electrosensitive TE, it was clear elastic materials would be searched for first. A set of various PU fibrous scaffolds were electrospun on Nanospider device in cooperation with colleagues at the Centre of polymer systems. Primary cytotoxicity testing showed differences between various PUs used and also revealed the importance of thorough wash out (constant shaking in ultrapure water for at least 10 days with water change every second day). The reason behind this lies in removal of remaining solvents that may be cytotoxic, salts that may impare pH of the environment, and other potentionally harmfull impurities.

All PU scaffolds were originally isotropic, featuring randomly oriented fibers. However, the anisotropy of biomaterials plays a critical role, as the ECM *in vivo* is typically anisotropic. (Hoque, 2017) This property is particularly important when aiming to replicate the native architecture of the myocardium. Cardiomyocytes cultured in anisotropic environments adopt their physiological phenotype – aligned actin filaments, organized sarcomeres, and elongated nuclei (Bursac N. et al., 2002) and their contractile function is closely tied to cell alignment and elongation. (Nikkhah et al., 2012) To introduce anisotropy into the PU scaffolds, a combination of heating and manual stretching was applied. Each PU sample responded differently to this treatment, some tore under stress,

while others exhibited well-aligned fibers. Ultimately, PU Desmopan 385 S was selected as the most suitable candidate due to its optimal balance of elasticity, anisotropic alignment, and cytocompatibility. Further details regarding the PU scaffold anisotropic structure and properties can be found in the **Article I**.

Topographical anisotropy of the stretched PU scaffold was confirmed by SEM and AFM; however, what about mechanical anisotropy? The introduction of structural anisotropy into the PU scaffold presumably also evokes mechanical anisotropy, which cells may sense and be affected by. To determine this, tensile testing was carried out. However, a few challenges arose in the process. First of all, cutting the PU scaffolds into a suitable and unite shape with clean edges was tried with several approaches: from laser cutting, over manual die cutting press, cutting with a heated scalpel, to regular cutting with scissors. None of these tactics worked perfectly; however, the use of scissors when handled diligently resulted in a sufficiently precise cut with minimum edge jams, which would act as a soft spot, causing a premature rupture. Another issue that complicated the tensile testing was the easy disruption of the PU scaffolds by the tensile device clamps and the constant slipping out of the clamps at the same time. This was overcome by taping the top and bottom edges with a regular tape. However, the taping had to be done carefully and precisely as well, because even small deviations were affecting the tensile testing results.

The tensile testing results are shown in Table 8.1 and Figure 8.5. Even though, there are indisputable deviations, the results showed mesurable differences. In comparison to the isotropic PU scaffold, anisotropic PU scaffold tested parallel to fibre orientation withstanded higher forces with elongation not significantly changed. On the other hand, the tensile test of anisotropic PU scaffold perpendicularly to fibre orientation led to notably higher elongation and lower stress build compared to isotropic PU scaffold. Therefore, the mechanical testing suggests mechanical anisotropy in the PU scaffolds with aligned fibres.

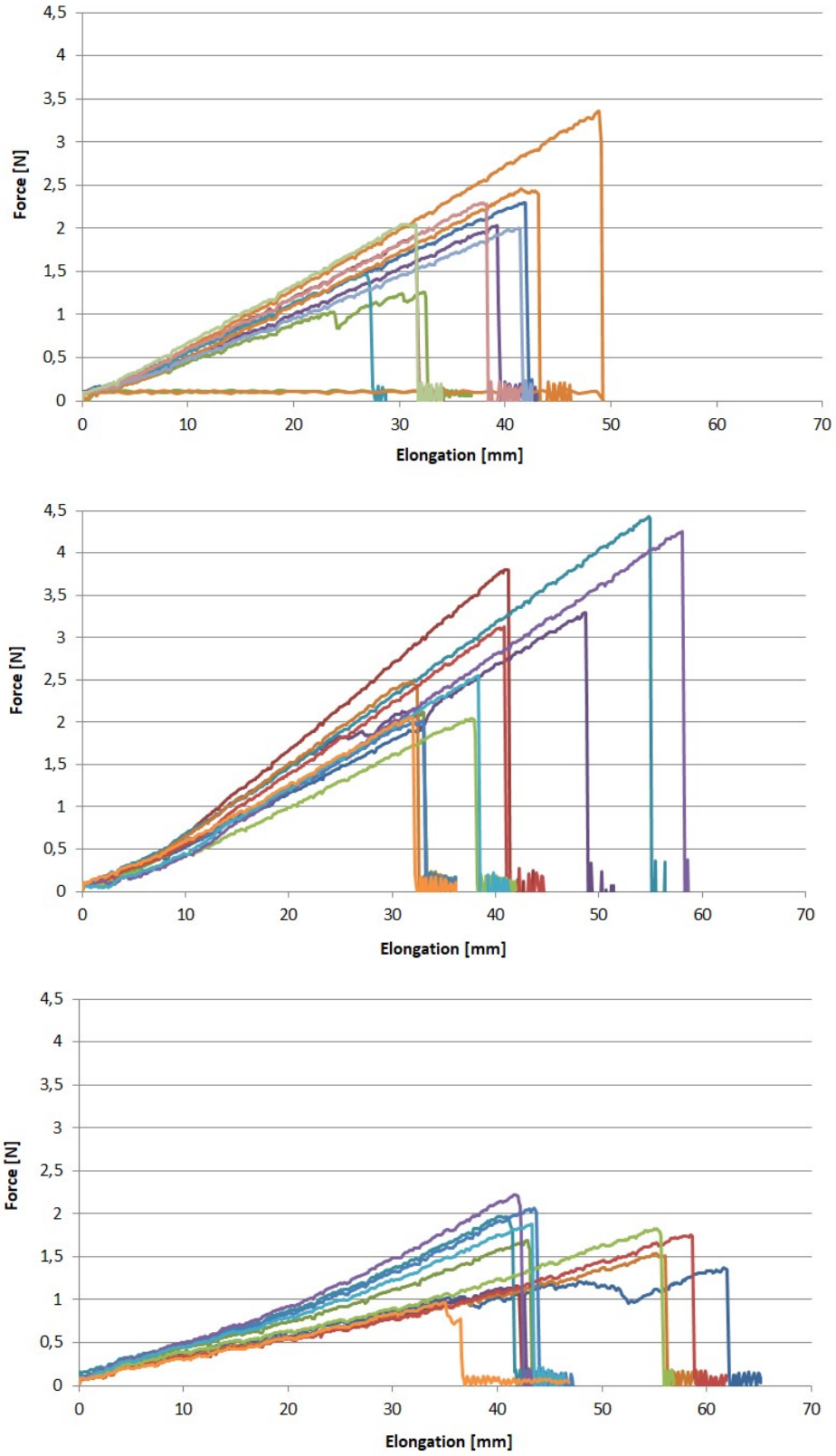

Figure 8.5 Graphs from tensile testings: (up) isotropic PU scaffold; (middle) anisotropic PU scaffold tested parallel to fibre orientation; (down) anisotropic PU scaffold tested perpendicular to fibre orientation. (Figure made by the author of this thesis).

Table 8.1 Results of tensile testing (stress, force nad strain peaks) of isotropic and anisotropic PU scaffolds (tested parallel or perpendicular to fibre orientation). The values given are the mean with the standard deviation of the mean. (Table made by the author of this thesis).

	Stress peak [N/mm²]	**Force peak [N]**	**Strain peak [%]**
Isotropic PU scaffold	14	2,1	92
	± 4	± 0,6	± 18
Anisotropic PU scaffold **Parallel** to fibre orientation	19	2,9	100
	± 7	± 0,9	± 30
Anisotropic PU scaffold **Perpendicular** to fibre orientation	11	1,6	120
	± 3	± 0,4	± 30

To introduce conductivity to PU scaffolds, both isotropic and anisotropic, were coated with PPy by chemical *in situ* oxidative polymerization. This synthesis method and resulted film properties were discussed in 8.1.1 Polypyrrole surface coating under a minute and Article 1. As already mentioned, the PPy thin film coatings in their pristine form are not quiet suitable for cells due to the uncomplying free surface energy. Thus, the PUPPy scaffolds were coated with the combination of albumin and gelatin, improving thus the scaffold surface cytocompatibility.

Figure 8.6 Quality of PPy coating on PU scaffolds: (left) pristine PU scaffold; (right) PU scaffold coated with PPy. (Figure made by the author of this thesis).

To summarize it, PU scaffolds possess several cell-instructive cues: 1) mechanical properties mimicking natural tissue properties, in particular elasticity of cardiac muscle tissue; 2) structural and mechanical anisotropy mimicking the structure of ECM and significantly affecting *in vitro* cell behaviour; 3) conductivity from PPy coating that helps cells to communicate with each other and is especially intriguing for TE of electrosensitive tissues; 4) bioactivity given from protein coating enhancing cell-surface interactions and thus giving cells cues to adhere.

The results of cytocompatibility testing of PU scffolds were published in Article 1. In short, fiber orientation alone significantly affected the morphology of mouse fibroblasts, both cytoskeletons and nuclei became elongated and aligned in the direction of the fibers. However, when coated with PPy and albumin and gelatin, anisotropic surface reduced its influence on fibroblasts, providing a more uniform surface. In contrast, mouse embryonic stem cells with LIF remained unaffected in terms of morphology or differentiation.

8.2.2 Polyvinylidene fluoride scaffolds challenges cell seeding efficiency

Recently, PVDF has attracted considerable attention in biomedical and TE applications owing to its strong piezoelectric properties. This capability makes PVDF attractive especially for applications in cardiac and neural TE. For example, research of Thakur et al., 2012 indicates that PVDF can support cell alignment and maturation, providing the electrical scaffolding necessary for the development of electrosensitive tissues.

In collaboration with colleagues from the Faculty of Technology at Tomas Bata University in Zlín, PVDF was electrospun using a custom-built university electrospinning device. As the setup is still under development, achieving successful electrospinning was initially challenging and lacked reproducibility. However, the apparatus has been gradually improved, and comparing to commercial devices, it now offers certain advantages, such as the ability to electrospin from a small volume of solution or the option to electrospin onto a rotating drum, enabling fiber alignment directly during the spinning process.

MTT assays confirmed that extracts from the electrospun PVDF scaffolds were entirely non-cytotoxic. Consequently, direct cell adhesion and proliferation on the PVDF surface were investigated. However, this was complicated by the fact that the PVDF scaffolds floated on the medium surface. To enable cell

seeding, it was necessary to keep the scaffolds submerged. This was achieved using various methods, such as weighing them down with sterile stainless-steel rings, pinning them to the bottom with a clipped pipette tip between the sample and the TDC lid, or electrospinning PVDF directly onto stiff black paper, which then served as a support during the entire experiment. However, sometimes the PVDF released itself compromising the cell viability as shown in Figure 8.13.

Several challenges also arose during microscopic observation of the cells. Firstly, after staining, samples had to be transferred to fresh wells to eliminate background cells attached to the original well bottom. Due to their soft and deformable nature, the scaffolds often lost shape during transfer, potentially damaging cells or causing them to detach. Secondly, the uneven and curved surface of the PVDF scaffold made cell imaging difficult without access to a confocal microscope. Lastly, under fluorescence microscopy, the same wavelength used to visualize the ActinRed-stained cytoskeletons revealed non-specific red fluorescence in parts of the scaffold, which interfered with accurate imaging.

Furthermore, the copolymer PVDF-HFP was also electrospun, as it introduces amorphous regions that enhance the processability and flexibility of the final product, potentially improving its cytocompatibility. (Baji et al., 2021; Xia et al., 2017)

Fibroblasts proliferated well on the PVDF-HFP sample, even outperforming the reference TCDs. As shown in Figure 8.7, cells on the reference displayed typical fibroblast morphology, whereas those on PVDF-HFP exhibited more condensed cytoskeletons, many cells have even round shapes, with an increased number of short filopodia creating stellate-patterned morphology.

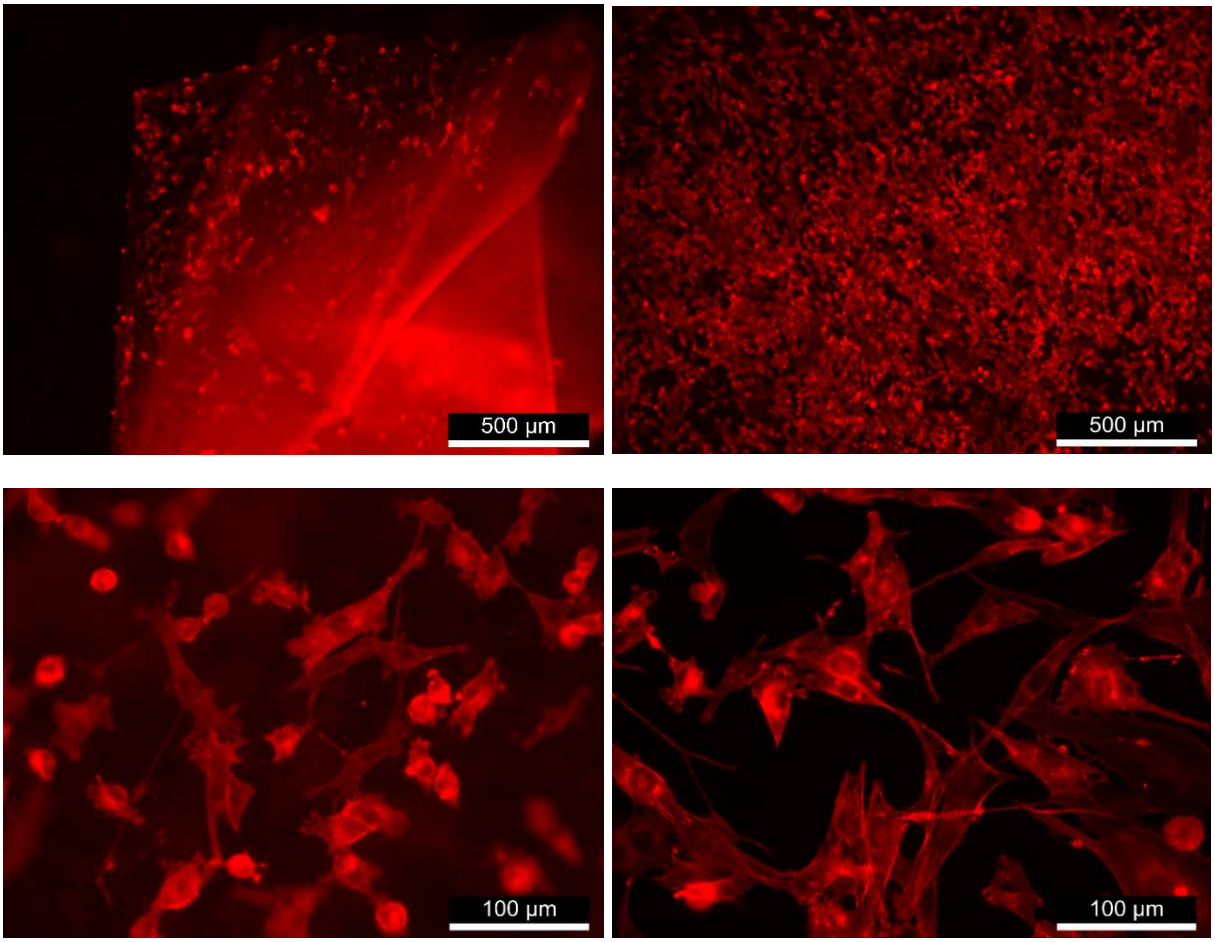

Figure 8.7 NIH/3T3 fibroblasts seeded on: (up left) PVDF scaffold, magnification: 40×; (up right) PVDF-HFP scaffold, magnification: 40×; (down left) PVDF-HFP scaffold, magnification: 200×; (down right) reference on TCDs, magnification: 200×. Red color – cytoskeletons. (Figure made by the author of this thesis).

8.2.3 Cytocompatibility testing as the final boss for scaffolds

In addition to primary research projects, the author of this thesis contributed to several collaborative studies on scaffold design. Although these scaffolds were not of her design, she played a key role in the cytocompatibility evaluation – an essential step in determining a scaffold's biological potential and readiness for further application. The following studies reflect some of the contributions.

RNDr. Radka Gorejová, PhD., from the Faculty of Science, Pavol Jozef Šafárik University in Košice, Slovakia, prepared porous biodegradable iron scaffolds (see Figure 8.8) by the impregnation of PU foam with a suspension of CIPs and gelatin, followed by thermal treatment in a tube furnace and subsequent sintering. For more details on the scaffold synthesis and corrosion behavior, see Gorejová et al., 2020.

The results of the NIH/3T3 fibroblast cultivation revealed that the cells were unable to adhere to the scaffold. In cases where some cells managed to attach or became entrapped within the internal spaces of the scaffold, their viability was significantly reduced in comparison to cells that adhered directly to the bottom of the TCD, as illustrated in Figure 8.8. Attempts to improve cell attachment by coating the scaffold with collagen or gelatin did not alter the outcome. Nevertheless, a positive finding was that fibroblasts cultured at the bottom of the TCDs in the presence of the scaffold survived and proliferated (when the cell culture medium was frequently replaced to prevent the accumulation of degraded scaffold fragments within the TCDs). This indicates that while the scaffold's current form does not support direct cell adhesion, it does not exert cytotoxic effects and, thus, this scaffold retains considerable potential and warrants further development and optimization for applications in TE.

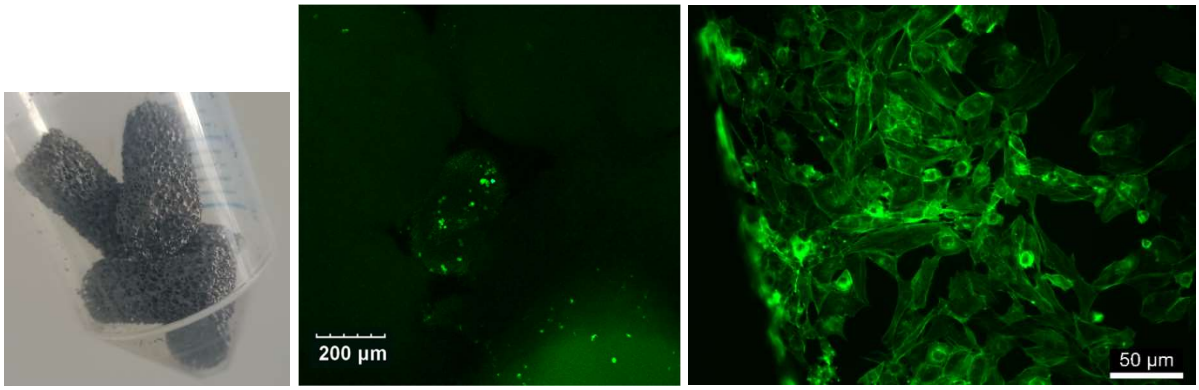

Figure 8.8 Cytocompatibility of the iron scaffolds: (left) the iron scaffolds; (middle) NIH/3T3 fibroblasts inside the scaffold, magnification: 25×; (right) on the bottom of TCDs containing the scaffold, magnification: 100×. Green color – cytoskeletons. (Figure made by the author of this thesis).

Ing. Lenka Vítková, Ph.D., from the Faculty of Technology, Tomas Bata University in Zlín, prepared hyaluronan-based hydrogels *via* dual cross-linking (see Figure 8.9). HA modified with adipic acid dihydrazide using coupling agents 1-ethyl-3-(3-dimethylaminopropyl)carbodiimide hydrochloride (EDC) or 4-(4,6-dimethoxy-1,3,5-triazin-2-yl)-4-methylmorpholinium chloride (DMTMM) was cross-linked *via* Schiff base formation with oxidized HA or dextran (DEX), followed by ionic cross-linking with Fe^{3+}. To enable magneto-responsive behavior, the hydrogels were filled with CIPs.

Cytocompatibility tests were performed on several series of the hydrogels with different formulations and degrees of oxidation. At first, some of the variants were excluded due to limited integrity, leading to disintegration upon the sterilization process (70 % ethanol for 1 h and ultra pure water for 48 h). The stability of some hydrogels was also impaired under cultivation conditions (cell culture media, 37 °C, 72 h at least), resulting in physical degradation.

Surprisingly, it was found out during the MTT assays with NIH/3T3 fibroblasts that unfiltered extracts had a significantly higher cytocompatibility in comparison to extracts filtered with a 0.22 μm Millex GV filter. One such case is shown in Figure 8.9. This phenomenon implies the possibility of successful fibroblast growth on the material surface in future proliferation testing.

After the strict selection and optimization of the hydrogels, the final MTT assay showed that all EDC-based hydrogels were cytotoxic at full concentration, likely due to residual side-products. Among DMTMM-derived formulations, only the hydrogel based on HA-OX with the degree of oxidation of 35 demonstrated non-toxic behavior across all tested concentrations. Other hydrogels exhibited partial cytotoxicity, likely due to the release of unreacted aldehyde groups or insufficient stabilization in the case of DEX-OX. These results were published in Vítková, L., Musilová, L., Achbergerová, E., Kolařík, R., Mrlík, M., Korpasová, K., **Mahelová, L.**, Capáková, Z., Mráček, A., 2022. *Formulation of Magneto-Responsive Hydrogels from Dually Cross-Linked Polysaccharides: Synthesis, Tuning and Evaluation of Rheological Properties.* Int. J. Mol. Sci. 23, 9633. https://doi.org/10.3390/ijms23179633

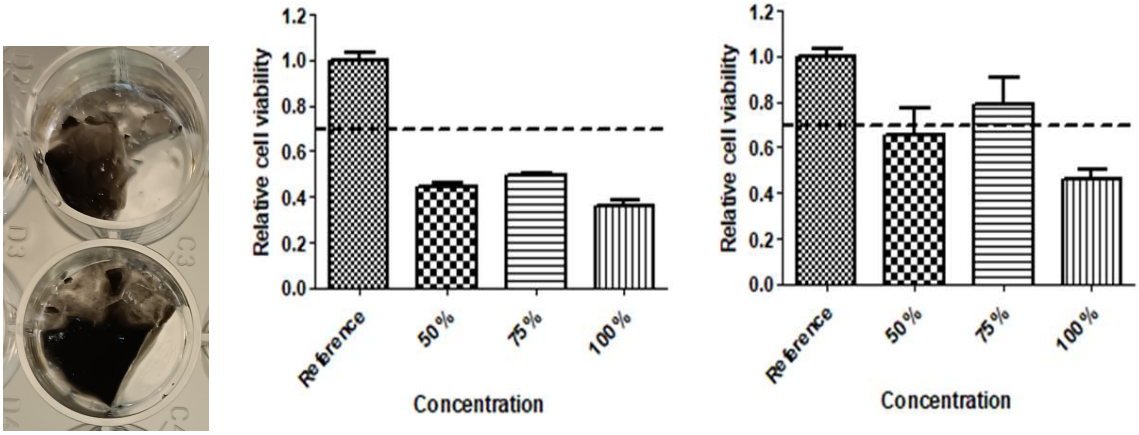

Figure 8.9 Cytocompatibility of the hyaluronan-based hydrogels: (left) the hydrogels; (middle) MTT assay results of filtered extract from DEX 20c CIP DMTMM hydrogel; (right) MTT assay results of unfiltered extract from DEX 20c CIP DMTMM hydrogel. (Figure made by the author of this thesis).

Ing. Danila Gorgol from the Centre of Polymer Systems, Tomas Bata University in Zlín, prepared magneto-responsive hydrogels based on HA of various molecular weights, cross-linked with the aid of EDC and N-hydroxysuccinimide (NHS), and filled with CIPs at various concentrations. Cytotoxicity assays confirmed all hydrogel extracts to be non-cytotoxic. Notably, hydrogels containing CIPs showed higher viability than their CIP-free counterparts, suggesting an additional supportive role of CIPs in cell interaction.

The formulation with 7 wt. % HA (377 kDa) and 30 wt.% CIPs demonstrated optimal rheological properties, like shear-thinning behavior and high yield stress, enabling extrusion-based 3D printing. The resulting scaffolds (see Figure 8.10) exhibited excellent shape fidelity, mechanical integrity, and magneto-responsiveness under an external magnetic field. NIH/3T3 fibroblasts seeded onto the scaffolds and cultured for 3 days (see Figure 8.10) exhibited fibroblast adhesion and spreading, with a significant number of cells directly on the scaffolds and slightly more cells on the bottom of TCDs but still in direct contact with the scaffolds, confirming their suitability for supporting cell growth. These results, published in Gorgol, D., Mrlík, M., Mikulka, F., Víchová, Z., **Mahelová, L.**, Ilčíková, M., Minařík, A., 2024. *Smart Biopolymer Scaffolds Based on Hyaluronic Acid and Carbonyl Iron Microparticles: 3D Printing, Magneto-Responsive, and Cytotoxicity Study*. ACS Appl. Bio Mater. 7, 7483–7493. https://doi.org/10.1021/acsabm.4c00567, indicate that HA-CIP scaffolds offer a promising platform for magneto-mechanically active TE biomaterials.

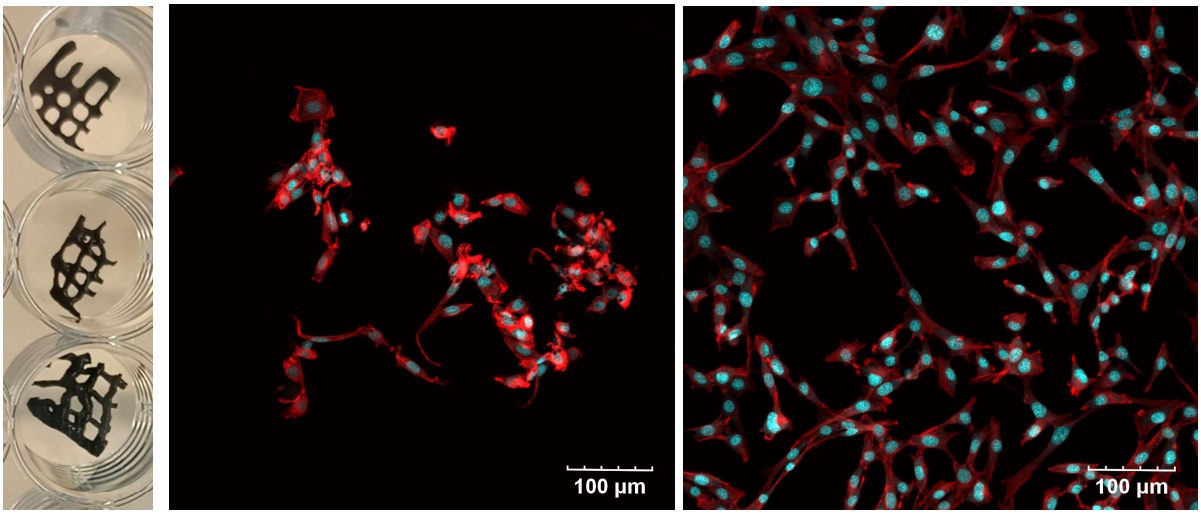

Figure 8.10 Cytocompatibility of the hyaluronan-based scaffolds: (left) the scaffolds; (middle) NIH/3T3 fibroblasts inside the scaffold; (right) NIH/3T3 fibroblasts on the bottom of TCDs containing the scaffold. Magnification: 50×, red color – cytoskeletons, blue color – nuclei. (Figure made by the author of this thesis).

Ing. Danila Gorgol from the Centre of Polymer Systems, Tomas Bata University in Zlín, prepared magneto-responsive hydrogels using EDC/NHS-mediated cross-linking of HA, but this time filled with CIPs modified with (3-aminopropyl)triethoxy silane, introducing amine groups on the surface of the particles. As in previous research, hydrogel scaffolds were 3D printed too.

Stem cells were seeded on gelatin-coated scaffolds. The reference cells and The MTT assay demonstrated that extracts of these hydrogels are non-cytotoxic across all concentrations, including the 100% extract, which caused a decrease in cell viability of less than 30%, still within cytocompatible limits according to ISO 10993. The 25% extract increased cell viability compared to the reference. Overall, the extracts resulted in good cell viability, despite being unfiltered, though the lack of filtration led to wider deviations.

To assess the scaffolds' impact on cell behavior, NIH/3T3 fibroblasts and ES R1 embryonic the cells under and around the scaffolds showed the same behaviour, proliferation, and morphology. Interestingly, stem cells adhered and proliferated more directly on the scaffolds than fibroblasts, despite being typically more sensitive (see Figure 8.11). These results have been processed into a manuscript that has not yet been submitted yet.

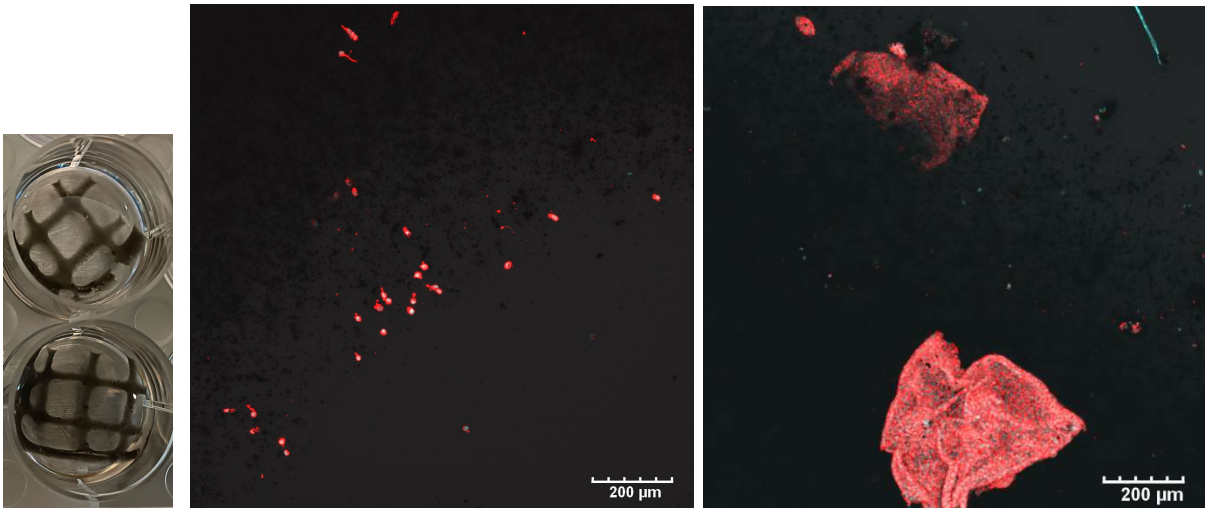

Figure 8.11 Cytocompatibility of the hyaluronan-based scaffolds: (left) the scaffolds; (middle) NIH/3T3 fibroblasts on the scaffold surface; (right) ES R1 embryonic stem cells on the scaffold surface. Magnification: 25×, red color – cytoskeletons. (Figure made by the author of this thesis).

Ing. Danila Gorgol from the Centre of Polymer Systems, Tomas Bata University in Zlín, prepared 3D printed scaffods made of Pebax. To evaluate the direct influence of these scaffolds on cellular behavior, *in vitro* adhesion and proliferation assays were performed using NIH/3T3 fibroblasts and ES R1 embryonic stem cells.

Interestingly, cell proliferation directly on the Pebax scaffold surface displayed a distinct pattern. Viable cells were consistently observed only in areas where the scaffold had been mechanically disrupted, such as cut edges created during sample division (see Figure 8.12). This suggests that cell adhesion occurred preferentially on rough or irregular surfaces.

In contrast, the majority of the scaffold's surface, composed of smooth, printed filaments, did not support effective cell attachment, likely due to insufficient surface roughness. As a result, cells were unable to anchor and subsequently settled at the bottom TCDs. Cell morphology of these cells appeared typical and healthy; however, a slightly reduced cell count was observed in the presence of the scaffold compared to the scaffold-free reference cells. This phenomenon was observed consistently across both tested cell lines asn shown in Figure 8.12. These results have been processed into a manuscript that has not yet been submitted yet.

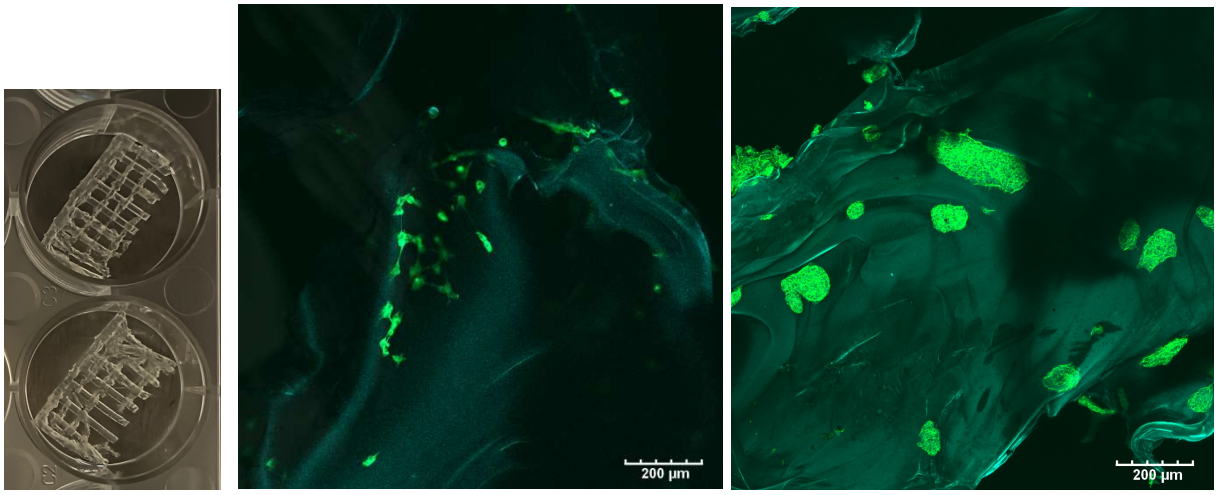

Figure 8.12 Cytocompatibility of the Pebax scaffolds: (left) the scaffolds; (middle) (middle) NIH/3T3 fibroblasts on the scaffold surface; (right) ES R1 embryonic stem cells on the scaffold surface. Magnification: 25×, green color – cytoskeletons. (Figure made by the author of this thesis).

8.3 Advanced cell cultivation and evaluation methods

The determination of cytocompatibility is a fundamental step in the development of any biomaterial intended for medical use. Cytocompatibility refers to the ability of a material to interact with cells in a manner that supports normal cellular function and does not cause adverse effects such as cytotoxicity, inflammation, or cell death.

Among the standard cultivation techniques that have been employed for the cytocompatibility testing of the presented substrates and scaffolds are:

- Indirect contact *via* extracts – This is one of the primary techniques often used to determine cytotoxic effects of released low molecular weight substances, by-products, and impurities.
- Direct contact with biomaterials – Cells are cultured directly on/within the material to evaluate its impact on cell adhesion, morphology, and viability. This provides insights into how cells interact physically with the material.

The testing is always carried out under standard cultivation conditions that are ensured in an incubator: 5% CO_2 atmosphere, a stable temperature of 37 °C, and consistent relative humidity. However, the cultivation methodology can be extensively adapted based on the characteristics of the tested material as well as the specific cellular responses under investigation and the intended biomedical application of the material.

8.3.1 Mixed populations behave different from single cell lines

It is usual to seed cells of one selected cell line, but for some purposes, an advanced technique of co-culturing, creating mixed cellular populations, can be utilized. This work's author used it on electrospun PU scaffolds prepared with either randomly oriented fibres (isotropic) or fibres oriented in one direction (anisotropic). As described in the chapter 8.2.1 and Article I, the anisotropy had a significant impact on the behaviour of NIH/3T3 fibroblasts. At the same time, ES R1 embryonic stem cells (cultured in medium with LIF) stayed unaffected.

The employment of mixed cell populations not only supports the structural complexity of engineered tissues but also instructs the differentiation and functional promotion of specific cell types through cellular cross-talk and nutrient sharing within a microenvironment. (Bian et al., 2011; Zhang et al., 2015) Furthermore, it has been revealed that incorporating fibroblasts alongside

cardiomyocytes is crucial for developing well-functioning cardiac tissues, as fibroblasts play an essential role in supporting cardiomyocyte viability and function. (Hookway et al., 2019; Tulloch et al., 2011)

Therefore, co-culturing of NIH/3T3 fibroblasts and ES R1 embryonic stem cells with LIF in media was applied to the PU scaffold in two different ways:

- Sequential mixed population – Fibroblasts seeded first and after 24 h, embryonic stem cells added, then co-cultured for 2 days.
- Simultaneous mixed population – Fibroblasts and embryonic stem cells seeded at once and co-cultured for 3 days.

Some of the results are shown in Figure 8.16. As expected, fibroblasts pre-cultured on the anisotropic PU scaffold created almost a monolayer of elongated cytoskeletons strictly oriented according to the orientation of fibres. Further, it can be noticed that stem cells seeded on the formed fibroblast monolayer formed clusters with round-like shapes as usual and of very various sizes. Controversially, stem cells seeded together with fibroblasts formed only big uniform clusters with the shape of an oval significantly oriented according to the orientation of fibres. In addition, fibroblasts seeded and grown together with stem cells resulted in even more prolonged and narrowed cytoskeletons.

These results suggest a synergistic effect where both material anisotropy and direct interaction with fibroblasts influence stem cell organization. This could be especially interesting when fibroblasts are co-cultured with stem cells or even embryoid bodies without the presence of LIF, potentially resulting in cell differentiation (without the use of signal molecules). The author will continue to address this topic in the bachelor's and master's theses she is currently supervising.

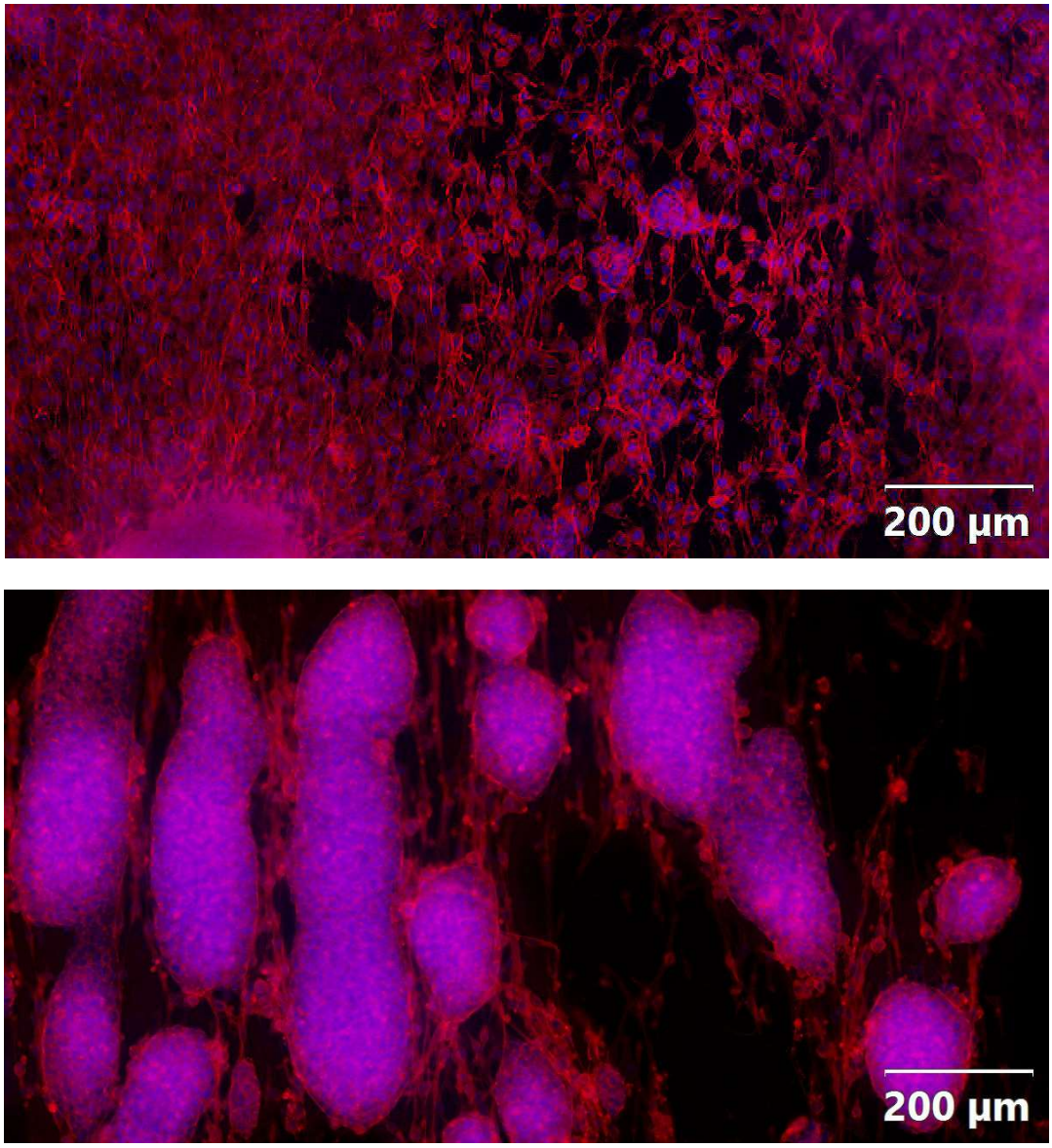

Figure 8.13 Mixed cell population of NIH/3T3 fibroblasts and ES R1 embryonic stem cells grown on anisotropic PU mats: (up) sequential mixed population; (down) simultaneous mixed population. Magnification: 100×, red color – cytoskeletons, blue color – nuclei. (Figure made by the author of this thesis).

8.3.2 Cultivation under dynamic conditions mimics *in vivo* environment

Standard static cell cultivation methods exhibit notable limitations, including restricted nutrient and oxygen diffusion, cultivation in unnatural two dimentions, and lack of various external stimuli. Advanced cultivation protocols, thus, including dynamic setups and systems like bioreactors applying electrical, magnetical, or mechanical stimuli, simulating *in vivo* physiological conditions. (Matějka et al., 2020; Ravichandran et al., 2010; Zuščíková et al., 2024)

Electrical external stimuli

According to the literature, electrical stimulation effectively modulates cell behavior, promoting proliferation, differentiation, and alignment across various cell types, with proven benefits for osteogenesis, neuroregeneration, and cardiomyocyte function. (Hernández et al., 2016; Tandon et al., 2009; Xia et al., 2024)

The research on electrical stimuli is important for TE of electrosensitive tissues, particularly in the context of the use of conductive polymeric substrates. To create an electrical field in cell culture at the Centre of Polymer Systems, the power source of direct current stimulation was combined with self self-prepared cultivation system of electrodes incorporated in TCDs. Cells were then exposed to either constant or pulsed direct current electrical stimulation, with varying exposure/pause intervals.

The results showed that the combination of conductive substrate and electrical stimuli of the appropriate setup causes cellular changes that are induced by neither of them separately. To summarize it, fibroblasts elongated protrusions and embryonic stem cells (with LIF in medium) formed a less condensed cluster with branched edges. The author supervised the master's thesis on this topic: Šandová, K., 2024. *Effect of electric field on cell behavior*. Bachelor thesis. Tomas Bata University in Zlín, Faculty of Technology.

Magnetical external stimuli

Static magnetic fields and magnetically responsive scaffolds have been shown to promote bone regeneration, cell proliferation, and osteogenic differentiation. (Bernhardt et al., 2011; Nishimura et al., 2015) Also, alternating magnetic fields can induce apoptosis in a dose-dependent manner, highlighting their potential in therapeutic strategies. (Wong et al., 2018)

The investigation of magnetic field effects on cells becomes particularly compelling when conducted in the presence of magnetic particles, such as CIPs. In this study, a permanent magnet was employed to generate a static magnetic field for cells cultured on a magneto-responsive smart scaffold composed of a hyaluronan-based hydrogel incorporating modified CIPs. The magnetic field produced was too stable and of insufficient intensity to induce any observable changes in the fibroblasts' behavior.

Mechanical external stimuli

Hydrodynamic shear stress is a key mechanical stimulus in bioreactor systems, significantly influencing cell morphology, signaling, proliferation, and differentiation by mimicking natural *in vivo* physiologically relevant conditions absent in static cultures. (Matějka et al., 2020; Raimondi et al., 2006) Appropriate shear levels enhance tissue engineering outcomes, while excessive stress may trigger apoptosis and metabolic disruption. (Han and Yuan, 2009; Velez-Suberbie et al., 2013)

The Synthecon rotary cell culture system and the Ibidi pump system are the two devices that were used to apply hydrodynamic shear stress to cells. For the former, cells were pre-adhered to a substrate, which was then attached to a self-made holder and placed into the dynamic chamber that rotated at a controlled rate. For the latter, the cells were seeded directly into the narrow testing chamber through which the cell culture media was pumped at a controlled rate. Both systems allowed for the continuous circulation of culture medium over cell monolayers, creating controlled hydrodynamic shear stress conditions that will be further studied by the author and her students.

Multiple external stimuli combined

When different stimuli act on cells simultaneously, a synergistic effect on cellular processes can occur. Moreover, such bioreactors provide the most faithful imitation of the in vivo dynamic environment. One such system is the Ebers TC-3 bioreactor, which allows the application of: hydrodynamic shear stress from the flowing medium, electric current supplied by electrodes, and also compressive strain by compression of the scaffold.

Zhang et al., 2024 demonstrated that cyclic stretching significantly affects cardiomyocyte function and can be used to classify cardiac cell physiology and disease. Therefore, the compression deformation of the bioreactor was replaced by tensile deformation with a custom 3D printed structure. It was designed and manufactured in collaboration with colleagues from the Faculty of Technology, Tomas Bata University in Zlín, so that it fits into a dynamic chamber (see Figure 8.14) and enables scaffold attachement and stretching.

The initiation of experiments in this bioreactor system was accompanied by a number of significant challenges. First, cells could not be directly seeded onto the scaffold inside the dynamic chamber for the lack of a support and therefore

had to be pre-cultivated in TCDs. The subsequent transfer of the cell-seeded scaffolds from the TCDs into the dynamic chamber (and vice versa) proved to be both technically demanding and time-consuming due to the delicate and soft structure of the scaffolds. The exposure of cells to air outside the medium and incubator during this process posed a serious risk to their viability. Additionally, several factors further delayed the assembly and filling of the system, such as the precise and careful connection of electrodes directly to the sample, which required a combination of fine motor skills, speed, and patience all at once. With progressive optimization of the protocol and practice, the time cells spent outside the optimal conditions was successfully minimized. Nevertheless, other complications occurred, such as medium leakage at various chamber sites, which, if not regularly checked and prevented, could leave the scaffold completely dry. Most notably, recurring contamination was observed despite rigorous sterilization and aseptic handling. This issue was partially mitigated by supplementing the culture medium with gentamicin (20 µg/mL).

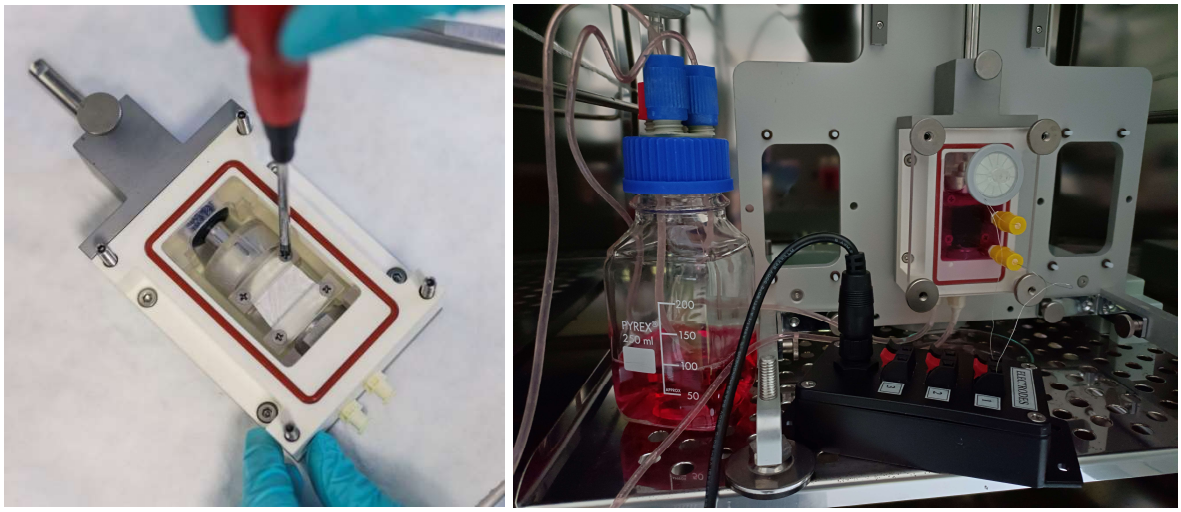

Figure 8.14 TC-3 bioreactor from Ebers: (left) a dynamic cultivation chamber with costum 3D printed holder and PU scaffold attached; (right) the chamber connected to the motion structure, the electrical and medium circuits of the bioreactor system. (Figure made by the author of this thesis).

After optimizing the process, it was still difficult to achieve consistent results, especially with embryonic stem cells. Stem cells naturally form clusters in which cells attach to other cells more strongly than to the surface of the scaffold. (Abdal Dayem et al., 2018; Mustafa et al., 2022) Thus, the cell clusters are easily released from the scaffold when the flow rate of the medium is slightly increased or when the scaffold is inadvertently bent during handling.

This problem was eventually overcome by using a mixed cell population. Figure 8.15 presents the results of dynamic cultivation of a sequential mixed population of fibroblasts and embryonic stem cells grown on an anisotropic PU scaffold coated with PPy, compared to a reference cells in TCDs under static conditions.

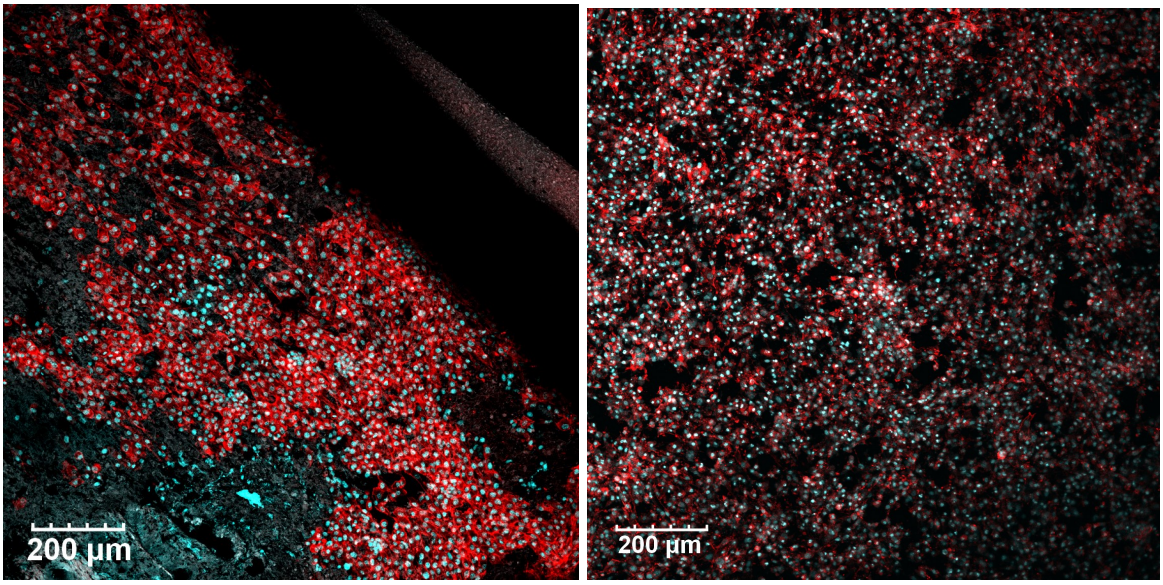

Figure 8.15 Sequential mixed cell population of NIH/3T3 fibroblasts and ES R1 embryonic stem cells grown on: (left) anisotropic PU scaffold coated with PPy under dynamic cultivation conditions of the Ebers TC-3 bioreactor; (right) reference TCD under static cultivation conditions. Magnification: 25×, red color – cytoskeletons, blue color – nuclei. (Figure made by the author of this thesis).

8.3.3 Image analysis answers "every" cell-evaluation related questions

The evaluation techniques used by the author of this thesis in laboratory practice to process the results of cytokompatibility testing of the presented substrates and scaffolds include:

Cell viability and proliferation evaluation

Commonly used assays providing quantitative data are based on the metabolic activity of cells or spectroscopic devices that count cells. The author of this work reviewed several available variants to quantify cells grown on PU scaffolds coated with PPy and albumin and gelatin.

In general, the most commonly used quantitative kit is the MTT assay. Dimethyl sulfoxide is a solvent used to dissolve formazan crystals into a homogeneous purple solution. However, this solvent dissolved all PU scaffolds and PPy coatings, adversely affecting the color of the solution whose absorbance would be subsequently measured.

An alternative approach to assessing cell viability involves measuring intracellular ATP levels. However, the results of the ATP assay were negatively affected by the presence of proteins used to coat the scaffold surface. This is because proteins interfere with the luciferase reaction by binding ATP or inhibiting enzyme activity, leading to an underestimation of cell viability.

Another quantitative kit is the neutral red uptake assay, which is a method for assessing cell viability based on the ability of viable cells to incorporate and bind neutral red. This method could not be used either due to its sensitivity to proteins, especially serum proteins.

Another method, which can be used for cell quantification, is UV-VIS spectrophotometry or flow cytometry. These methods require the cells to be first detached using trypsin to prepare a cell suspension that would then be measured. However, complications occurred in the detachment of cells from the surface of PU scaffolds, leading to unreliable data.

Cell morphology evaluation

Changes in cell beahviour are often projected in cell morphology. For its observation, microscopy is essential. Whether phase-contrast, or fluorescence microscopy is used, or for 3D structures scenning confocal, it is still a subjective evaluation influenced by inter-image variability and additionally burdened by the time-consuming manual evaluation.

Cell spreading evaluation

These assays evaluate how well cells attach to the substrate and whether they are able to spread, which are crucial for proper cellular function and integration with the surrounding tissue. However, the evaluation without automation of cell migration and wound healing is time-consuming, subjective, and inaccurate.

All of here addressed limitations of cytocompatibility testing evaluations, cay be addressed by image analysis. Cell image analysis offers a comprehensive solution to overcome the limitations encountered during conventional

cytocompatibility testing as well as enables quantification of subtle morphological responses beyond the capabilities of conventional assays. Several software programs providing this service exist, but the most versatile and free at the same time is the open-sourced **CellProfiler**. (Carpenter et al., 2006)

Unlike manual cell counting or subjective morphological evaluations, CellProfiler provides automated, high-throughput, and reproducible image analysis across a wide range of experimental conditions.

The author of this thesis used CellProfiler as an alternative to conventional cell viability assays, as shown in ArticleI. To make the quantification of cells on the PU scaffolds precise and reliable, the unified surface area of (22 × 22) mm^2 had to be prepared, seeded, and the total area (forty images of cell nuclei with 40× magnification for each observed sample) was manually acquired and then processed in CellProfiler.

Cell image analysis also enables reliable segmentation of individual cells and objective quantification of multiple parameters simultaneously, such as cell area, circularity, texture, orientation, fluorescence intensity, compactness, and much more. This cell image qualification was utilized in Article I and Appendix I.

In addition, the software can analyze time-lapse microscopy data, making it particularly powerful for quantifying cell migration, tracking, and wound healing assays. Its practical application is described in Zubková, S., 2024. *Využití elektrického pole k léčbě kožních poranění*. Bachelor thesis. Tomas Bata University in Zlín, Faculty of Technology.

CellProfiler allows the user to create customizable pipelines without requiring advanced programming skills, while still offering the flexibility needed for complex image-based experiments. One of its main advantages is that it is open-source, freely available, and supported by an active user community. However, challenges may arise during segmentation in low-quality or highly heterogeneous images, and optimization of pipelines can be time-consuming for beginners. Despite these, CellProfiler remains a valuable and robust tool for objective and quantitative cell analysis in biomaterials research.

CONTRIBUTION TO SCIENCE

As demonstrated in this dissertation, a broad range of polymers can be employed in tissue engineering, accompanied by numerous methods to produce, combine, and modify them. Even minor adjustments in the synthesis or processing of these polymers can substantially affect cellular behavior. Moreover, cultivation conditions exert a strong influence on cell physiology. Given the interaction of so many variables, the relationship between polymers and cells is both intricate and sensitive. The work presented here focuses on gaining a deeper understanding of this relationship, particularly in the context of developing electrosensitive tissues. The primary objective has been to identify how material design and cultivation conditions can be tuned to guide and support cells in forming functional, healthy tissue constructs.

At the beginning of the doctoral studies, the author already possessed a set of skills required for fundamental experimental work in laboratories of cell biology, gained through previous experience during bachelor's and master's theses. When the COVID-19 pandemic disrupted regular research workflows, further expertise in academic research management and project preparations was acquired and applied in practice right away (as the lead researcher on a project).

One of the most significant contributions of this dissertation lies in advancing knowledge of the synthesis and characterization of conductive polymers. The author not only prepared polypyrrole thin films with great electrical properties, which is important for the engineering of electrosensitive tissues, but also dug into the practical side of using them in tissue engineering. In particular, the author optimized their synthesis to show how easily they can be prepared and adjusted for successful cell seeding.

Especially new insights were gained with polyazulene, a generally less studied conductive polymer. Due to the lack of information on chemical synthesis protocols, she had to investigate polyazulene empirically. In order to obtain electrochemically prepared polyazulene, she traveled abroad to the University of Silesia in Katowice, Poland, where she became familiar with this method. This work ultimately led to the first study determining the cytocompatibility of polyazulene, which, to the author's knowledge, has not been addressed to date. This opens up exciting new possibilities for future research using polyazulene in tissue engineering.

Another key component of this research involved the development of bioactive fibrous scaffolds – mesh-like structures that provide surfaces for cell attachment and spatial organization during growth. These scaffolds were designed to offer multiple cell-instructive cues: 1) an elastic matrix mimicking the stretchable properties of native tissues, 2) uniaxially aligned fibers reflecting the anisotropic architecture of natural tissues, 3) a polypyrrole coating providing electrical conductivity, and 4) an albumin/gelatin coating emulating the composition of the natural extracellular environment.

Cytocompatibility experiments demonstrated, for instance, that alignment of fibers facilitated easier cell attachment and promoted directional growth along the fiber axis. This effect is particularly beneficial for constructing organized tissues such as myocardium, where cells naturally align in a similar fashion. Additionally, anisotropic scaffolds fabricated from polyvinylidene fluoride exhibited promising potential due to their combination of cytocompatibility and piezoelectric properties. These characteristics make them highly suitable for applications in cardiac and neural tissue engineering.

It is important to note that performing reliable experiments and evaluating cell behavior on these scaffolds posed several challenges. Difficulties such as static electricity, scaffold floating in the culture medium, and low surface wettability initially made it difficult for cells to attach and proliferate. Once these technical hurdles were resolved, the research progressed to investigations on how various types of dynamic stimulation (electrical, magnetic, and mechanical) influence cell behavior on the scaffolds. The rationale for applying such stimuli was to better mimic the dynamic environment experienced by cells in living tissues. The most complex and ambitious experiments involved combining multiple stimuli simultaneously, including hydrodynamic shear stress from media flow, tensile stress from scaffold stretching, and electrical stimulation applied to conductive surfaces. As documented in the dissertation, the implementation of this multifactorial system required extensive optimization due to numerous technical complications. Ultimately, successful cell culture was achieved in a multi-stimuli bioreactor using the multi cell-instructive scaffolds. A key finding of this work was that the creation of mixed cell populations helped embryonic stem cells to survive even under these demanding dynamic conditions.

To effectively analyze the extensive data generated and to overcome limitations in assessing cell viability on conductive thin films and scaffolds, advanced image analysis software was introduced into the cellular laboratory workflow. A comprehensive image analysis pipeline was developed and refined, enabling detailed evaluation of cell viability, morphology, and migration. Once optimized, this methodology proved to be a powerful and reliable tool, with strong potential for future routine use in studies of cell–material interactions.

In summary, this dissertation provides a cohesive account of how conductive polymers, smart scaffold designs, and dynamic cultivation conditions can be integrated to develop more life-like tissue constructs. The discoveries and methodologies presented here establish a solid foundation for continued research aimed at engineering functional tissue replacements. While the potential applications are broad, the findings are particularly promising for cardiac tissue repair and for advancing regenerative medicine more generally.

REFERENCES

Abdal Dayem, A., Lee, S., Y. Choi, H., Cho, S.-G., 2018. The Impact of Adhesion Molecules on the In Vitro Culture and Differentiation of Stem Cells. Biotechnol. J. 13, 1700575. https://doi.org/10.1002/biot.201700575

Adadi, N., Yadid, M., Gal, I., Asulin, M., Feiner, R., Edri, R., Dvir, T., 2020. Electrospun Fibrous PVDF-TrFe Scaffolds for Cardiac Tissue Engineering, Differentiation, and Maturation. Adv. Mater. Technol. 5, 1900820. https://doi.org/10.1002/admt.201900820

Adamow, A., Szukalski, A., Sznitko, L., Persano, L., Pisignano, D., Camposeo, A., Mysliwiec, J., 2020. Electrically controlled white laser emission through liquid crystal/polymer multiphases. Light Sci. Appl. 9, 19. https://doi.org/10.1038/s41377-020-0252-9

Alexande.jw, Wheeler, L., Rooney, R., Mcdonald, J., Macmilla.bg, 1973. Clinical Evaluation of Epigard, a New Synthetic Substitute for Homograft and Heterograft Skin. J. Trauma-Inj. Infect. Crit. Care 13, 374–383. https://doi.org/10.1097/00005373-197304000-00018

Ameloot, F., Mezzine, H., Khairallah, G., Hayek, G., Zaidi, M., Lhuillier, L., Talbi, M., Sot, M., Perone, J.M., 2019. Reconstruction of exenteration socket with Integra® dermal substitute and skin graft. J. Fr. Ophtalmol. 42, 746–752. https://doi.org/10.1016/j.jfo.2019.03.023

Amir, E., Amir, R.J., Campos, L.M., Hawker, C.J., 2011. Stimuli-Responsive Azulene-Based Conjugated Oligomers with Polyaniline-like Properties. J. Am. Chem. Soc. 133, 10046–10049. https://doi.org/10.1021/ja203267g

Anthony Atala Quotes. QuotesGram [WWW Document], n.d. . QuotesGram. URL https://quotesgram.com/img/anthony-atala-quotes/2987169/ (accessed 4.7.23).

Armes, S., 1987. Optimum Reaction Conditions for the Polymerization of Pyrrole by Iron(iii) Chloride in Aqueous-Solution. Synth. Met. 20, 365–371. https://doi.org/10.1016/0379-6779(87)90833-2

Arsyad, A., Saaid, F.I., Najihah, M.Z., Tan, W., 2023. FTIR studies on interactions among components in PVdF-HFP:PC:MPII electrolytes. IOP Conf. Ser. Earth Environ. Sci. 1151, 012060. https://doi.org/10.1088/1755-1315/1151/1/012060

Atala, A., Bauer, S.B., Soker, S., Yoo, J.J., Retik, A.B., 2006. Tissue-engineered autologous bladders for patients needing cystoplasty. The Lancet 367, 1241–1246. https://doi.org/10.1016/S0140-6736(06)68438-9

Ateh, D. d, Navsaria, H. a, Vadgama, P., 2006. Polypyrrole-based conducting polymers and interactions with biological tissues. J. R. Soc. Interface 3, 741–752. https://doi.org/10.1098/rsif.2006.0141

Badylak, S.F., Taylor, D., Uygun, K., 2011. Whole-Organ Tissue Engineering: Decellularization and Recellularization of Three-Dimensional Matrix Scaffolds, in: Yarmush, M.L., Duncan, J.S., Gray, M.L. (Eds.), Annual Review of Biomedical Engineering, Vol 13. Annual Reviews, Palo Alto, pp. 27–53. https://doi.org/10.1146/annurev-bioeng-071910-124743

Baji, A., Truong, V.K., Gangadoo, S., Yin, H., Chapman, J., Abtahi, M., Oopath, S.V., 2021. Durable Antibacterial and Antifungal Hierarchical Silver-Embedded Poly(vinylidene fluoride-co-hexafluoropropylene) Fabricated Using Electrospinning. ACS Appl. Polym. Mater. 3, 4256–4263. https://doi.org/10.1021/acsapm.1c00705

Baker, T.L., Goodwin, T.J., 1997. Three-dimensional culture of bovine chondrocytes in rotating-wall vessels. Vitro Cell. Dev. Biol. - Anim. 33, 358–365. https://doi.org/10.1007/s11626-997-0006-5

Bardajee, G.R., Hooshyar, Z., 2014. One-pot synthesis of biocompatible superparamagnetic iron oxide nanoparticles/hydrogel based on salep: Characterization and drug delivery. Carbohydr. Polym. 101, 741–751. https://doi.org/10.1016/j.carbpol.2013.10.028

Bassett, C.A.L., Pawluk, R.J., Becker, R.O., 1964. Effects of Electric Currents on Bone In Vivo. Nature 204, 652–654. https://doi.org/10.1038/204652a0

Ben Ayed, E., Ghorbel, N., Kallel, A., Putaux, J.-L., Boufi, S., 2022. Polyaniline-Grafted Chitin Nanocrystals as Conductive Reinforcing Nanofillers for Waterborne Polymer Dispersions. Biomacromolecules 23, 4167–4178. https://doi.org/10.1021/acs.biomac.2c00635

Berg, J., Eriksson, L., Claesson, P., Borve, K., 1994. 3-Component Langmuir-Blodgett-Films with a Controllable Degree of Polarity. Langmuir 10, 1225–1234. https://doi.org/10.1021/la00016a041

Bernhardt, A., Lode, A., Peters, F., Gelinsky, M., 2011. Optimization of culture conditions for osteogenically-induced mesenchymal stem cells in β-tricalcium phosphate ceramics with large interconnected channels. J. Tissue Eng. Regen. Med. 5, 444–453. https://doi.org/10.1002/term.331

Beygisangchin, M., Abdul Rashid, S., Shafie, S., Sadrolhosseini, A.R., Lim, H.N., 2021a. Preparations, Properties, and Applications of Polyaniline and Polyaniline Thin Films—A Review. Polymers 13, 2003. https://doi.org/10.3390/polym13122003

Beygisangchin, M., Abdul Rashid, S., Shafie, S., Sadrolhosseini, A.R., Lim, H.N., 2021b. Preparations, Properties, and Applications of Polyaniline and Polyaniline Thin Films—A Review. Polymers 13, 2003. https://doi.org/10.3390/polym13122003

Bian, L., Zhai, D.Y., Mauck, R.L., Burdick, J.A., 2011. Coculture of Human Mesenchymal Stem Cells and Articular Chondrocytes Reduces Hypertrophy and Enhances Functional Properties of Engineered Cartilage. Tissue Eng. Part A 17, 1137–1145. https://doi.org/10.1089/ten.tea.2010.0531

Bonartsev, A.P., Bonartseva, G.A., Reshetov, I.V., Kirpichnikov, M.P., Shaitan, K.V., 2019. Application of Polyhydroxyalkanoates in Medicine and the Biological Activity of Natural Poly(3-Hydroxybutyrate). Acta Naturae 11, 4–16. https://doi.org/10.32607/20758251-2019-11-2-4-16

Borah, R., Das, J.M., Upadhyay, J., 2022. Surface Functionalized Polyaniline Nanofibers:Chitosan Nanocomposite for Promoting Neuronal-like Differentiation of Primary Adipose Derived Mesenchymal Stem Cells and Urease Activity. ACS Appl. Bio Mater. 5, 3193–3211. https://doi.org/10.1021/acsabm.2c00171

Bose, S., Robertson, S.F., Bandyopadhyay, A., 2018. Surface modification of biomaterials and biomedical devices using additive manufacturing. Acta Biomater. 66, 6–22. https://doi.org/10.1016/j.actbio.2017.11.003

Boukamp, P., Petrussevska, R.T., Breitkreutz, D., Hornung, J., Markham, A., Fusenig, N.E., 1988. Normal keratinization in a spontaneously immortalized aneuploid human keratinocyte cell line. J. Cell Biol. 106, 761–771. https://doi.org/10.1083/jcb.106.3.761

Boyce, S.T., Lalley, A.L., 2018. Tissue engineering of skin and regenerative medicine for wound care. Burns Trauma 6, 4. https://doi.org/10.1186/s41038-017-0103-y

Bursac N., Parker K.K., Iravanian S., Tung L., 2002. Cardiomyocyte Cultures With Controlled Macroscopic Anisotropy. Circ. Res. 91, e45–e54. https://doi.org/10.1161/01.RES.0000047530.88338.EB

Cao, Y., Vacanti, J.P., Paige, K.T., Upton, J., Vacanti, C.A., 1997. Transplantation of chondrocytes utilizing a polymer-cell construct to produce tissue-engineered cartilage in the shape of a human ear. Plast. Reconstr. Surg. 100, 297–302; discussion 303-304. https://doi.org/10.1097/00006534-199708000-00001

Capáková, Z., Radaszkiewicz, K.A., Acharya, U., Truong, T.H., Pacherník, J., Bober, P., Kašpárková, V., Stejskal, J., Pfleger, J., Lehocký, M., Humpolíček, P., 2020. The biocompatibility of polyaniline and polypyrrole 21: Doping with organic phosphonates. Mater. Sci. Eng. C 113, 110986. https://doi.org/10.1016/j.msec.2020.110986

Carpenter, A.E., Jones, T.R., Lamprecht, M.R., Clarke, C., Kang, I.H., Friman, O., Guertin, D.A., Chang, J.H., Lindquist, R.A., Moffat, J., Golland, P., Sabatini, D.M., 2006. CellProfiler: image analysis software for identifying

and quantifying cell phenotypes. Genome Biol. 7, R100. https://doi.org/10.1186/gb-2006-7-10-r100

Carrel, A., 1912. ON THE PERMANENT LIFE OF TISSUES OUTSIDE OF THE ORGANISM. J. Exp. Med. 15, 516–528. https://doi.org/10.1084/jem.15.5.516

Çaykara, T., Sande, M.G., Azoia, N., Rodrigues, L.R., Silva, C.J., 2020. Exploring the potential of polyethylene terephthalate in the design of antibacterial surfaces. Med. Microbiol. Immunol. (Berl.) 209, 363–372. https://doi.org/10.1007/s00430-020-00660-8

Chauhan, N.P.S., Jangid, N.K., Kaur, N., Rathore, B.S., Gholipourmalekabadi, M., Mozafari, M., 2019. Medicines: Polymers for, Encyclopedia of Polymer Applications, Vols I-Iii. Crc Press-Taylor & Francis Group, Boca Raton. https://doi.org/10.1201/9781351019422-140000298

Chen, H.-C., Hu, Y.-C., 2006. Bioreactors for tissue engineering. Biotechnol. Lett. 28, 1415–1423. https://doi.org/10.1007/s10529-006-9111-x

Chen, X., Issi, J.-P., Devaux, J., Billaud, D., 1995. Chemically oxidized polypyrrole: Influence of the experimental conditions on its electrical conductivity and morphology. Polym. Eng. Sci. 35, 642–647. https://doi.org/10.1002/pen.760350803

Chen, Y., Wang, F., Dong, L., Li, Z., Chen, L., He, X., Gong, J., Zhang, J., Li, Q., 2019. Design and Optimization of Flexible Polypyrrole/Bacterial Cellulose Conductive Nanocomposites Using Response Surface Methodology. Polymers 11, 960. https://doi.org/10.3390/polym11060960

Cheng, K.-C., Sun, Y.-M., Hsu, S., 2023. Development of double network polyurethane–chitosan composite bioinks for soft neural tissue engineering. J. Mater. Chem. B. https://doi.org/10.1039/D3TB00120B

Citi, S., 2019. The mechanobiology of tight junctions. Biophys. Rev. 11, 783–793. https://doi.org/10.1007/s12551-019-00582-7

Cronin, T.D., Brauer, R.O., 1971. Augmentation Mammaplasty. Surg. Clin. North Am., Cosmetic Surgery 51, 441–452. https://doi.org/10.1016/S0039-6109(16)39388-4

Cui, Z., Ni, N.C., Wu, J., Du, G.-Q., He, S., Yau, T.M., Weisel, R.D., Sung, H.-W., Li, R.-K., 2018. Polypyrrole-chitosan conductive biomaterial synchronizes cardiomyocyte contraction and improves myocardial electrical impulse propagation. Theranostics 8, 2752–2764. https://doi.org/10.7150/thno.22599

Cvek, M., Zahoranova, A., Mrlik, M., Sramkova, P., Minarik, A., Sedlacik, M., 2020. Poly(2-oxazoline)-based magnetic hydrogels: Synthesis,

performance and cytotoxicity. Colloids Surf. B Biointerfaces 190, 110912. https://doi.org/10.1016/j.colsurfb.2020.110912

Deniz, P., Guler, S., Çelik, E., Hosseinian, P., Aydin, H.M., 2020. Use of cyclic strain bioreactor for the upregulation of key tenocyte gene expression on Poly(glycerol-sebacate) (PGS) sheets. Mater. Sci. Eng. C 106, 110293. https://doi.org/10.1016/j.msec.2019.110293

Di Nicola, V., 2019. Omentum a powerful biological source in regenerative surgery. Regen. Ther. 11, 182–191. https://doi.org/10.1016/j.reth.2019.07.008

di Pompeo, F.S., Paolini, G., Firmani, G., Sorotos, M., 2022. History of breast implants: Back to the future. JPRAS Open 32, 166–177. https://doi.org/10.1016/j.jpra.2022.02.004

Dickson, K., Lee, K.C., Abdulsalam, A., Amirize, E., Kankam, H.K.N., ter Horst, B., Gardiner, F., Bamford, A., Hejmadi, R.K., Moiemen, N., n.d. A Histological and Clinical Study of MatriDerm (R) Use in Burn Reconstruction. J. Burn Care Res. https://doi.org/10.1093/jbcr/irad024

Du, V., Luciani, N., Richard, S., Mary, G., Gay, C., Mazuel, F., Reffay, M., Menasché, P., Agbulut, O., Wilhelm, C., 2017. A 3D magnetic tissue stretcher for remote mechanical control of embryonic stem cell differentiation. Nat. Commun. 8, 400. https://doi.org/10.1038/s41467-017-00543-2

Du, X., Chen, Y., Dong, W., Han, B., Liu, M., Chen, Q., Zhou, J., 2016. A nanocomposite-based electrochemical sensor for non-enzymatic detection of hydrogen peroxide. Oncotarget 8, 13039–13047. https://doi.org/10.18632/oncotarget.14308

Duchet, J., Legras, R., Demoustier-Champagne, S., 1998. Chemical synthesis of polypyrrole: structure–properties relationship. Synth. Met. 98, 113–122. https://doi.org/10.1016/S0379-6779(98)00180-5

Fee, T., Downs, C., Eberhardt, A., Zhou, Y., Berry, J., 2016. Image-based quantification of fiber alignment within electrospun tissue engineering scaffolds is related to mechanical anisotropy. J. Biomed. Mater. Res. A 104, 1680–1686. https://doi.org/10.1002/jbm.a.35697

Ferraz, N., Strømme, M., Fellström, B., Pradhan, S., Nyholm, L., Mihranyan, A., 2012. In vitro and in vivo toxicity of rinsed and aged nanocellulose–polypyrrole composites. J. Biomed. Mater. Res. A 100A, 2128–2138. https://doi.org/10.1002/jbm.a.34070

Firda, P.B.D., Jeon, J.-W., 2022. Recovery of Electrochemical Properties of Polyaniline-Based Multilayer Films with Improved Electrochemical

Stability. ACS Appl. Polym. Mater. 4, 4850–4859. https://doi.org/10.1021/acsapm.2c00445

Firda, P.B.D., Malik, Y.T., Oh, J.K., Wujcik, E.K., Jeon, J.-W., 2021. Enhanced Chemical and Electrochemical Stability of Polyaniline-Based Layer-by-Layer Films. Polymers 13, 2992. https://doi.org/10.3390/polym13172992

Flora, B., Kumar, R., Mahdieh, R., Zarei, K., Chehrazi, S., Kaur, S.D., Sharma, A., Mohapatra, P., Sakshi, A., Singh, A., Kesari, K.K., Gupta, P.K., 2023. Recent Updates on Metal-Polymer Nanocomposites in 3D Bioprinting for Tissue Engineering Applications. Nanofabrication 8, 12–15. https://doi.org/10.37819/nanofab.008.291

Fu, J., Wang, Y.-K., Yang, M.T., Desai, R.A., Yu, X., Liu, Z., Chen, C.S., 2010. Mechanical regulation of cell function with geometrically modulated elastomeric substrates. Nat. Methods 7, 733–736. https://doi.org/10.1038/nmeth.1487

Fung, Y.C., 1981. Biomechanics. Springer, New York, NY. https://doi.org/10.1007/978-1-4757-1752-5

Furuya, M., Shimono, N., Okamoto, M., 2017. Fabrication of biocomposites composed of natural rubber latex and bone tissue derived from MC3T3-E1 mouse preosteoblastic cells. Nanocomposites 3, 76–83. https://doi.org/10.1080/20550324.2017.1352111

Gajendiran, M., Choi, J., Kim, S.-J., Kim, Keongsoo, Shin, H., Koo, H.-J., Kim, Kyobum, 2017. Conductive biomaterials for tissue engineering applications. J. Ind. Eng. Chem. 51, 12–26. https://doi.org/10.1016/j.jiec.2017.02.031

Gao, H., Ge, C., Hou, B., Xin, H., Gao, X., 2019. Incorporation of 1,3-Free-2,6-Connected Azulene Units into the Backbone of Conjugated Polymers: Improving Proton Responsiveness and Electrical Conductivity. ACS Macro Lett. 8, 1360–1364. https://doi.org/10.1021/acsmacrolett.9b00657

German, N., Ramanaviciene, A., Ramanavicius, A., 2019. Formation of Polyaniline and Polypyrrole Nanocomposites with Embedded Glucose Oxidase and Gold Nanoparticles. Polymers 11, 377. https://doi.org/10.3390/polym11020377

Gh, D., Kong, D., Gautrot, J., Vootla, S.K., 2017. Fabrication and Characterization of Conductive Conjugated Polymer-Coated Antheraea mylitta Silk Fibroin Fibers for Biomedical Applications. Macromol. Biosci. 17, 1600443. https://doi.org/10.1002/mabi.201600443

Gogoi, D., Choudhury, A.J., Chutia, J., Pal, A.R., Khan, M., Choudhury, M., Pathak, P., Das, G., Patil, D.S., 2014. Development of advanced antimicrobial and sterilized plasma polypropylene grafted muga

(antheraea assama) silk as suture biomaterial. Biopolymers 101, 355–365. https://doi.org/10.1002/bip.22369

Golgovici, F., Cârlan, M.-S., Popescu, A.-G., Anicai, L., 2020. Electrochemical Synthesis of Polypyrrole and Polypyrrole-Indomethacin Coatings on NiCr Alloys Involving Deep Eutectic Solvents. Metals 10, 1130. https://doi.org/10.3390/met10091130

Gorejová, R., Oriňaková, R., Orságová Králová, Z., Baláž, M., Kupková, M., Hrubovčáková, M., Haverová, L., Džupon, M., Oriňak, A., Kaľavský, F., Kovaľ, K., 2020. In Vitro Corrosion Behavior of Biodegradable Iron Foams with Polymeric Coating. Materials 13, 184. https://doi.org/10.3390/ma13010184

Gorgol, D., Mrlík, M., Mikulka, F., Víchová, Z., Mahelová, L., Ilčíková, M., Minařík, A., 2024. Smart Biopolymer Scaffolds Based on Hyaluronic Acid and Carbonyl Iron Microparticles: 3D Printing, Magneto-Responsive, and Cytotoxicity Study. ACS Appl. Bio Mater. 7, 7483–7493. https://doi.org/10.1021/acsabm.4c00567

Goss, R.J., Grimes, L.N., 1975. Epidermal downgrowths in regenerating rabbit ear holes. J. Morphol. 146, 533–542. https://doi.org/10.1002/jmor.1051460408

Goss, R.J., Grimes, L.N., 1972. Tissue Interactions in the Regeneration of Rabbit Ear Holes. Am. Zool. 12, 151–157.

Grądzka, E., Makowska, P., Winkler, K., 2018. Chemically formed conducting polyazulene: From micro- to nanostructures. Synth. Met. 246, 115–121. https://doi.org/10.1016/j.synthmet.2018.10.002

Graham, F.L., Smiley, J., Russell, W.C., Nairn, R., 1977. Characteristics of a Human Cell Line Transformed by DNA from Human Adenovirus Type 5. J. Gen. Virol. 36, 59–72. https://doi.org/10.1099/0022-1317-36-1-59

Grancarić, A.M., Jerković, I., Koncar, V., Cochrane, C., Kelly, F.M., Soulat, D., Legrand, X., 2018. Conductive polymers for smart textile applications. J. Ind. Text. 48, 612–642. https://doi.org/10.1177/1528083717699368

Greenwood, J.E., Wagstaff, M.J.D., Rooke, M., Caplash, Y., 2016. Reconstruction of Extensive Calvarial Exposure After Major Burn Injury in 2 Stages Using a Biodegradable Polyurethane Matrix. Eplasty 16, e17.

Guarino, V., Zuppolini, S., Borriello, A., Ambrosio, L., 2016. Electro-Active Polymers (EAPs): A Promising Route to Design Bio-Organic/Bioinspired Platforms with on Demand Functionalities. Polymers 8, 185. https://doi.org/10.3390/polym8050185

Guerra, N.B., Cassel, J.B., Henckes, N.A.C., dos Santos de Oliveira, F., Cirne-Lima, E.O., dos Santos, L.A.L., 2018. Chemical and in vitro

characterization of epoxidized natural rubber blends for biomedical applications. J. Polym. Res. 25, 172. https://doi.org/10.1007/s10965-018-1542-2

Guimard, N.K., Gomez, N., Schmidt, C.E., 2007. Conducting polymers in biomedical engineering. Prog. Polym. Sci., Polymers in Biomedical Applications 32, 876–921. https://doi.org/10.1016/j.progpolymsci.2007.05.012

Gupta, P., Ismadi, M.-Z., Verma, P.J., Fouras, A., Jadhav, S., Bellare, J., Hourigan, K., 2016. Optimization of agitation speed in spinner flask for microcarrier structural integrity and expansion of induced pluripotent stem cells. Cytotechnology 68, 45–59. https://doi.org/10.1007/s10616-014-9750-z

Hammond, T.G., Hammond, J.M., 2001. Optimized suspension culture: the rotating-wall vessel. Am. J. Physiol.-Ren. Physiol. 281, F12–F25. https://doi.org/10.1152/ajprenal.2001.281.1.F12

Han, P.-P., Yuan, Y.-J., 2009. Metabolic profiling as a tool for understanding defense response of Taxus Cuspidata cells to shear stress. Biotechnol. Prog. 25, 1244–1253. https://doi.org/10.1002/btpr.209

He, X., Li, L., Tang, M., Zeng, Y., Li, H., Yu, X., 2019. Biomimetic electrical stimulation induces rat bone marrow mesenchymal stem cells to differentiate into cardiomyocyte-like cells via TGF-beta 1 in vitro. Prog. Biophys. Mol. Biol., Biomembranes and Related Systems: From Molecular Structure to Cellular Function 148, 47–53. https://doi.org/10.1016/j.pbiomolbio.2017.09.023

Henle, W., Henle, G., 1980. Epidemiologic Aspects of Epstein-Barr Virus (ebv)-Associated Diseases*. Ann. N. Y. Acad. Sci. 354, 326–331. https://doi.org/10.1111/j.1749-6632.1980.tb27975.x

Hernández, D., Millard, R., Sivakumaran, P., Wong, R.C.B., Crombie, D.E., Hewitt, A.W., Liang, H., Hung, S.S.C., Pébay, A., Shepherd, R.K., Dusting, G.J., Lim, S.Y., 2016. Electrical Stimulation Promotes Cardiac Differentiation of Human Induced Pluripotent Stem Cells. Stem Cells Int. 2016, 1718041. https://doi.org/10.1155/2016/1718041

Hippler, M., Lemma, E.D., Bertels, S., Blasco, E., Barner-Kowollik, C., Wegener, M., Bastmeyer, M., 2019. 3D Scaffolds to Study Basic Cell Biology. Adv. Mater. 31, 1808110. https://doi.org/10.1002/adma.201808110

Hirata, A., Takano, Y., Kamimura, Y., Fujiwara, O., 2010. Effect of the averaging volume and algorithm on the in situ electric field for uniform electric- and magnetic-field exposures. Phys. Med. Biol. 55, N243. https://doi.org/10.1088/0031-9155/55/9/N03

Hookway, T.A., Matthys, O.B., Mendoza-Camacho, F.N., Rains, S., Sepulveda, J.E., Joy, D.A., McDevitt, T.C., 2019. Phenotypic Variation Between Stromal Cells Differentially Impacts Engineered Cardiac Tissue Function. Tissue Eng. Part A 25, 773–785. https://doi.org/10.1089/ten.tea.2018.0362

Hoque, M.E., 2017. Robust formulation for the design of tissue engineering scaffolds: A comprehensive study on structural anisotropy, viscoelasticity and degradation of 3D scaffolds fabricated with customized desktop robot based rapid prototyping (DRBRP) system. Mater. Sci. Eng. C 72, 433–443. https://doi.org/10.1016/j.msec.2016.11.019

Hou, B., Li, J., Zhou, Z., Tan, W.L., Yang, X., Zhang, J., McNeill, C.R., Ge, C., Wang, J., Gao, X., 2022. Incorporation of Electron-Rich Indacenodithiophene Units into the Backbone of 2,6-Azulene-Based Conjugated Polymers for Proton-Responsive Materials and p-Type Polymeric Semiconductors. ACS Mater. Lett. 4, 392–400. https://doi.org/10.1021/acsmaterialslett.1c00767

Huang, J., Lu, L., Zhang, J., Hu, X., Zhang, Y., Liang, W., Wu, S., Luo, Z., 2012. Electrical Stimulation to Conductive Scaffold Promotes Axonal Regeneration and Remyelination in a Rat Model of Large Nerve Defect. PLoS ONE 7, e39526. https://doi.org/10.1371/journal.pone.0039526

Humpolicek, P., Kasparkova, V., Pachernik, J., Stejskal, J., Bober, P., Capakova, Z., Radaszkiewicz, K.A., Junkar, I., Lehocky, M., 2018a. The biocompatibility of polyaniline and polypyrrole: A comparative study of their cytotoxicity, embryotoxicity and impurity profile. Mater. Sci. Eng. C-Mater. Biol. Appl. 91, 303–310. https://doi.org/10.1016/j.msec.2018.05.037

Humpolicek, P., Radaszkiewicz, K.A., Capakova, Z., Pachernik, J., Bober, P., Kasparkova, V., Rejmontova, P., Lehocky, M., Ponizil, P., Stejskal, J., 2018b. Polyaniline cryogels: Biocompatibility of novel conducting macroporous material. Sci. Rep. 8, 135. https://doi.org/10.1038/s41598-017-18290-1

Hursán, D., Ábel, M., Baán, K., Fako, E., Samu, G.F., Nguyën, H.C., López, N., Atanassov, P., Kónya, Z., Sápi, A., Janáky, C., 2022. CO2 Conversion on N-Doped Carbon Catalysts via Thermo- and Electrocatalysis: Role of C–NOx Moieties. ACS Catal. 12, 10127–10140. https://doi.org/10.1021/acscatal.2c01589

Iwasaki, K., Matsumoto, K., Hino, S., Yasunami, M., 1993. Electrochemical polymerization of alkyl-substituted azulenes. Synth. Met., Proceedings of the International Conference on Science and Technology of Synthetic Metals 55, 1062–1066. https://doi.org/10.1016/0379-6779(93)90200-G

Jaganathan, S.K., Prasath Mani, M., Ayyar, M., Rathanasamy, R., 2019. Biomimetic electrospun polyurethane matrix composites with tailor made properties for bone tissue engineering scaffolds. Polym. Test. 78, 105955. https://doi.org/10.1016/j.polymertesting.2019.105955

Jang, C.H., Lee, J.U., Kim, G.H., 2018. Effect of direct current electrical stimulation on the recovery of facial nerve crush injury. J. Ind. Eng. Chem. 64, 143–150. https://doi.org/10.1016/j.jiec.2018.03.011

Janvier, A.J., Canty-Laird, E., Henstock, J.R., 2020. A universal multi-platform 3D printed bioreactor chamber for tendon tissue engineering. J. Tissue Eng. 11, 2041731420942462. https://doi.org/10.1177/2041731420942462

Jasenská, D., Kašpárková, V., Radaszkiewicz, K.A., Capáková, Z., Pacherník, J., Trchová, M., Minařík, A., Vajďák, J., Bárta, T., Stejskal, J., Lehocký, M., Truong, T.H., Moučka, R., Humpolíček, P., 2021. Conducting composite films based on chitosan or sodium hyaluronate. Properties and cytocompatibility with human induced pluripotent stem cells. Carbohydr. Polym. 253, 117244. https://doi.org/10.1016/j.carbpol.2020.117244

Jay, V., 2000. This month in history - Alexis Carrel. J. R. Soc. Med. 93, 108–108. https://doi.org/10.1177/014107680009300227

Jeong, J.-W., Shin, G., Park, S.I., Yu, K.J., Xu, L., Rogers, J.A., 2015. Soft Materials in Neuroengineering for Hard Problems in Neuroscience. Neuron 86, 175–186. https://doi.org/10.1016/j.neuron.2014.12.035

Jin, C., Wu, Y., Zhang, H., Xu, B., Liu, W., Ji, C., Li, P., Chen, Z., Chen, B., Li, J., Wu, X., Jiang, P., Hu, Y., Xiao, Z., Zhao, Y., Dai, J., 2022. Spinal cord tissue engineering using human primary neural progenitor cells and astrocytes. Bioeng. Transl. Med. 8, e10448. https://doi.org/10.1002/btm2.10448

Joung, I.S., Iwamoto, M.N., Shiu, Y.-T., Quam, C.T., 2006. Cyclic strain modulates tubulogenesis of endothelial cells in a 3D tissue culture model. Microvasc. Res. 71, 1–11. https://doi.org/10.1016/j.mvr.2005.10.005

Kade, J.C., Bakirci, E., Tandon, B., Gorgol, D., Mrlik, M., Luxenhofer, R., Dalton, P.D., 2022. The Impact of Including Carbonyl Iron Particles on the Melt Electrowriting Process. Macromol. Mater. Eng. 307, 2200478. https://doi.org/10.1002/mame.202200478

Kadlečková, M., Skopalová, K., Ptošková, B., Wrzecionko, E., Daďová, E., Kocourková, K., Mráček, A., Musilová, L., Smolka, P., Humpolíček, P., Minařík, A., 2022. Hierarchically Structured Surfaces Prepared by Phase Separation: Tissue Mimicking Culture Substrate. Int. J. Mol. Sci. 23, 2541. https://doi.org/10.3390/ijms23052541

Kaewchingduang, R., Paradee, N., Sirivat, A., Niamlang, S., 2019. Effects of conductive polyazulene and plasticizer embedded in deproteinized natural rubber transdermal patch on electrically controlled naproxen release-permeation. Int. J. Pharm. 561, 296–304. https://doi.org/10.1016/j.ijpharm.2019.02.046

Kamble, H., Vadivelu, R., Barton, M., Shiddiky, M.J.A., Nguyen, N.-T., 2018. Pneumatically actuated cell-stretching array platform for engineering cell patterns in vitro. Lab. Chip 18, 765–774. https://doi.org/10.1039/C7LC01316G

Kašpárková, V., Humpolíček, P., Capáková, Z., Bober, P., Stejskal, J., Trchová, M., Rejmontová, P., Junkar, I., Lehocký, M., Mozetič, M., 2017. Cell-compatible conducting polyaniline films prepared in colloidal dispersion mode. Colloids Surf. B Biointerfaces 157, 309–316. https://doi.org/10.1016/j.colsurfb.2017.05.066

Kašpárková, V., Humpolíček, P., Stejskal, J., Kopecká, J., Kuceková, Z., Moučka, R., 2016. Conductivity, impurity profile, and cytotoxicity of solvent-extracted polyaniline. Polym. Adv. Technol. 27, 156–161. https://doi.org/10.1002/pat.3611

Keane, T.J., Swinehart, I.T., Badylak, S.F., 2015. Methods of tissue decellularization used for preparation of biologic scaffolds and in vivo relevance. Methods 84, 25–34. https://doi.org/10.1016/j.ymeth.2015.03.005

Keša, P., Paúrová, M., Babič, M., Heizer, T., Matouš, P., Turnovcová, K., Mareková, D., Šefc, L., Herynek, V., 2021. Photoacoustic Properties of Polypyrrole Nanoparticles. Nanomaterials 11, 2457. https://doi.org/10.3390/nano11092457

Kihara, N., Nakayama, H., Fukutomi, T., 1997. True Polyazulene: Soluble Precursor of So-Called "Polyazulene." Macromolecules 30, 6385–6387. https://doi.org/10.1021/ma970510m

Kim, H.M., 2001. Bioactive ceramics: Challenges and perspectives. J. Ceram. Soc. Jpn. 109, S49–S57. https://doi.org/10.2109/jcersj.109.1268_S49

Kim, S., Jang, L.K., Jang, M., Lee, S., Hardy, J.G., Lee, J.Y., 2018. Electrically Conductive Polydopamine–Polypyrrole as High Performance Biomaterials for Cell Stimulation in Vitro and Electrical Signal Recording in Vivo. ACS Appl. Mater. Interfaces 10, 33032–33042. https://doi.org/10.1021/acsami.8b11546

Kitsara, M., Revet, G., Vartanian-Grimaldi, J.-S., Simon, A., Minguy, M., Miche, A., Humblot, V., Dufour, T., Agbulut, O., 2022. Cyto- and bio-compatibility assessment of plasma-treated polyvinylidene fluoride scaffolds for cardiac tissue engineering. Front. Bioeng. Biotechnol. 10.

Kleinman, H.K., Martin, G.R., 2005. Matrigel: Basement membrane matrix with biological activity. Semin. Cancer Biol. 15, 378–386. https://doi.org/10.1016/j.semcancer.2005.05.004

Krawetz, R., Taiani, J.T., Liu, S., Meng, G., Li, X., Kallos, M.S., Rancourt, D.E., 2010. Large-Scale Expansion of Pluripotent Human Embryonic Stem Cells in Stirred-Suspension Bioreactors. Tissue Eng. Part C Methods 16, 573–582. https://doi.org/10.1089/ten.tec.2009.0228

Krukiewicz, K., Czerwińska-Główka, D., Turczyn, R.M., Blacha-Grzechnik, A., Vallejo-Giraldo, C., Erfurt, K., Chrobok, A., Faure-Vincent, J., Pouget, S., Djurado, D., Biggs, M.J.P., 2023. Flexible, Transparent, and Cytocompatible Nanostructured Indium Tin Oxide Thin Films for Bio-optoelectronic Applications. ACS Appl. Mater. Interfaces 15, 45701–45712. https://doi.org/10.1021/acsami.3c10861

Kucekova, Z., Humpolicek, P., Kasparkova, V., Perecko, T., Lehocký, M., Hauerlandová, I., Sáha, P., Stejskal, J., 2014. Colloidal polyaniline dispersions: Antibacterial activity, cytotoxicity and neutrophil oxidative burst. Colloids Surf. B Biointerfaces 116, 411–417. https://doi.org/10.1016/j.colsurfb.2014.01.027

Kulkarni, M., Junkar, I., Humpolíček, P., Capáková, Z., Radaszkiewicz, K.A., Mikušová, N., Pacherník, J., Lehocký, M., Iglič, A., Hanáčková, M., Mozetič, M., 2017. Interaction of nanostructured TiO2 biointerfaces with stem cells and biofilm-forming bacteria. Mater. Sci. Eng. C 77, 500–507. https://doi.org/10.1016/j.msec.2017.03.174

Latonen, R.-M., Meana Esteban, B., Kvarnström, C., Ivaska, A., 2009. Electrochemical polymerization and characterization of a poly(azulene)-TiO2 nanoparticle composite film. J. Appl. Electrochem. 39, 653–661. https://doi.org/10.1007/s10800-008-9705-1

Le, H.Q., Ghatak, S., Yeung, C.C., Tellkamp, F., Günschmann, C., Dieterich, C., Yeroslaviz, A., Habermann, B., Pombo, A., Niessen, C.M., Wickström, S.A., 2016. Mechanical regulation of transcription controls Polycomb-mediated gene silencing during lineage commitment. Nat. Cell Biol. 18, 864–875. https://doi.org/10.1038/ncb3387

Lee, C.H., Shin, H.J., Cho, I.H., Kang, Y.-M., Kim, I.A., Park, K.-D., Shin, J.-W., 2005. Nanofiber alignment and direction of mechanical strain affect the ECM production of human ACL fibroblast. Biomaterials 26, 1261–1270. https://doi.org/10.1016/j.biomaterials.2004.04.037

Lee, J.H., Yoon, Y.C., Kim, H.S., Lee, J., Kim, E., Findeklee, C., Katscher, U., 2022. In vivo electrical conductivity measurement of muscle, cartilage, and peripheral nerve around knee joint using MR-electrical properties

tomography. Sci. Rep. 12, 73. https://doi.org/10.1038/s41598-021-03928-y

Levenberg, S., Rouwkema, J., Macdonald, M., Garfein, E.S., Kohane, D.S., Darland, D.C., Marini, R., van Blitterswijk, C.A., Mulligan, R.C., D'Amore, P.A., Langer, R., 2005. Engineering vascularized skeletal muscle tissue. Nat. Biotechnol. 23, 879–884. https://doi.org/10.1038/nbt1109

Li, X., Shu, X., Shi, Y., Li, H., Pei, X., 2023. MOFs and bone: Application of MOFs in bone tissue engineering and bone diseases. Chin. Chem. Lett. 34, 107986. https://doi.org/10.1016/j.cclet.2022.107986

Li, Y., Liao, C., Tjong, S.C., 2019. Electrospun Polyvinylidene Fluoride-Based Fibrous Scaffolds with Piezoelectric Characteristics for Bone and Neural Tissue Engineering. Nanomaterials 9, 952. https://doi.org/10.3390/nano9070952

Lins, L.C., Wianny, F., Livi, S., Dehay, C., Duchet-Rumeau, J., Gérard, J.-F., 2017. Effect of polyvinylidene fluoride electrospun fiber orientation on neural stem cell differentiation. J. Biomed. Mater. Res. B Appl. Biomater. 105, 2376–2393. https://doi.org/10.1002/jbm.b.33778

Loh, Q.L., Choong, C., 2013. Three-Dimensional Scaffolds for Tissue Engineering Applications: Role of Porosity and Pore Size. Tissue Eng. Part B Rev. 19, 485–502. https://doi.org/10.1089/ten.teb.2012.0437

Ma, T., Xu, L., Chen, Y., Zhang, J., Han, X., Jiang, L., 2022. Full-thickness lower eyelid defect reconstruction using a pedicle rotation temporal flap and Acellular Human Dermis Graft (Alloderm). J. Plast. Reconstr. Aesthet. Surg. 75, 3414–3419. https://doi.org/10.1016/j.bjps.2022.04.082

MacNee, W., 2006. Pathology, pathogenesis, and pathophysiology. BMJ 332, 1202–1204. https://doi.org/10.1136/bmj.332.7551.1202

Mahmoodian, M., Pourabbas, B., Mohajerzadeh, S., 2015. Effect of anionic dopants on thickness, morphology and electrical properties of polypyrrole ultra-thin films prepared by in situ chemical polymerization. Thin Solid Films 583, 255–263. https://doi.org/10.1016/j.tsf.2015.03.043

Maity, S., Sarkar, A., 2017. 4 - Monitoring fibrous capsule formation, in: Narayan, R.J. (Ed.), Monitoring and Evaluation of Biomaterials and Their Performance In Vivo. Woodhead Publishing, pp. 69–80. https://doi.org/10.1016/B978-0-08-100603-0.00004-3

Man, K., Liu, J., Phan, K.M., Wang, K., Lee, J.Y., Sun, X., Story, M., Saha, D., Liao, J., Sadat, H., Yang, Y., 2022. Dimensionality-Dependent Mechanical Stretch Regulation of Cell Behavior. ACS Appl. Mater. Interfaces 14, 17081–17092. https://doi.org/10.1021/acsami.2c01266

Mandoli, C., Pagliari, F., Pagliari, S., Forte, G., Di Nardo, P., Licoccia, S., Traversa, E., 2010. Stem Cell Aligned Growth Induced by CeO2 Nanoparticles in PLGA Scaffolds with Improved Bioactivity for Regenerative Medicine. Adv. Funct. Mater. 20, 1617–1624. https://doi.org/10.1002/adfm.200902363

Mani, M.P., Jaganathan, S.K., Khudzari, A.Z.M., Prabhakaran, P., 2019. Development of advanced nanostructured polyurethane composites comprising hybrid fillers with enhanced properties for regenerative medicine. Polym. Test. 73, 12–20. https://doi.org/10.1016/j.polymertesting.2018.11.014

Maráková, N., Humpolíček, P., Kašpárková, V., Capáková, Z., Martinková, L., Bober, P., Trchová, M., Stejskal, J., 2017. Antimicrobial activity and cytotoxicity of cotton fabric coated with conducting polymers, polyaniline or polypyrrole, and with deposited silver nanoparticles. Appl. Surf. Sci. 396, 169–176. https://doi.org/10.1016/j.apsusc.2016.11.024

Marcus, A.A., 2020. Fourth retraction for Haruko Obokata, focus of STAP cell scandal, after Harvard investigation. Retraction Watch. URL https://retractionwatch.com/2020/02/13/fourth-retraction-for-haruko-obokata-focus-of-stap-cell-scandal-after-harvard-investigation/ (accessed 4.7.23).

Matějka, R., Koňařík, M., Štěpanovská, J., Lipenský, J., Chlupáč, J., Turek, D., Pražák, Š., Brož, A., Šimůnková, Z., Mrázová, I., Forostyak, S., Kneppo, P., Rosina, J., Bačáková, L., Pirk, J., 2020. Bioreactor Processed Stromal Cell Seeding and Cultivation on Decellularized Pericardium Patches for Cardiovascular Use. Appl. Sci. 10, 5473. https://doi.org/10.3390/app10165473

McCrary, M.W., Bousalis, D., Mobini, S., Song, Y.H., Schmidt, C.E., 2020. Decellularized tissues as platforms for in vitro modeling of healthy and diseased tissues. Acta Biomater. 111, 1–19. https://doi.org/10.1016/j.actbio.2020.05.031

Medeiros, C.C.G., Borghetti, R.L., Nicoletti, N., da Silva, V.D., Cherubini, K., Salum, F.G., de Figueiredo, M.A.Z., 2014. Polymethylmethacrylate dermal fillers: evaluation of the systemic toxicity in rats. Int. J. Oral Maxillofac. Surg. 43, 62–67. https://doi.org/10.1016/j.ijom.2013.06.009

Mezhuev, Ya.O., Artyukhov, A.A., Piskareva, A.I., Shtil'man, M.I., Gol'din, M.M., Korshak, Yu.V., Solov'eva, I.V., Evseev, A.K., 2015. Synthesis of aqueous polypyrrole dispersions stabilized with polyvinyl alcohol and preparation of hemocompatible films based on them. Russ. J. Appl. Chem. 88, 1026–1032. https://doi.org/10.1134/S107042721506021X

Mi, H.-Y., Jing, X., Napiwocki, B.N., Hagerty, B.S., Chen, G., Turng, L.-S., 2017. Biocompatible, degradable thermoplastic polyurethane based on polycaprolactone-block-polytetrahydrofuran-block-polycaprolactone copolymers for soft tissue engineering. J. Mater. Chem. B 5, 4137–4151. https://doi.org/10.1039/c7tb00419b

Mi, H.-Y., Jing, X., Yilmaz, G., Hagerty, B.S., Enriquez, E., Turng, L.-S., 2018. In situ synthesis of polyurethane scaffolds with tunable properties by controlled crosslinking of tri-block copolymer and polycaprolactone triol for tissue regeneration. Chem. Eng. J. 348, 786–798. https://doi.org/10.1016/j.cej.2018.04.198

Mohammadi Amirabad, L., Massumi, M., Shamsara, M., Shabani, I., Amari, A., Mossahebi Mohammadi, M., Hosseinzadeh, S., Vakilian, S., Steinbach, S.K., Khorramizadeh, M.R., Soleimani, M., Barzin, J., 2017. Enhanced Cardiac Differentiation of Human Cardiovascular Disease Patient-Specific Induced Pluripotent Stem Cells by Applying Unidirectional Electrical Pulses Using Aligned Electroactive Nanofibrous Scaffolds. ACS Appl. Mater. Interfaces 9, 6849–6864. https://doi.org/10.1021/acsami.6b15271

Mojena-Medina, D., Martínez-Hernández, M., de la Fuente, M., García-Isla, G., Posada, J., Jorcano, J.L., Acedo, P., 2020. Design, Implementation, and Validation of a Piezoelectric Device to Study the Effects of Dynamic Mechanical Stimulation on Cell Proliferation, Migration and Morphology. Sensors 20, 2155. https://doi.org/10.3390/s20072155

Mukasheva, F., Adilova, L., Dyussenbinov, A., Yernaimanova, B., Abilev, M., Akilbekova, D., 2024. Optimizing scaffold pore size for tissue engineering: insights across various tissue types. Front. Bioeng. Biotechnol. 12. https://doi.org/10.3389/fbioe.2024.1444986

Murai, M., Amir, E., Amir, R.J., Hawker, C.J., 2012. Azulene-based conjugated polymers: unique seven-membered ring connectivity leading to stimuli-responsiveness. Chem. Sci. 3, 2721–2725. https://doi.org/10.1039/C2SC20615C

Murphy, C.M., O'Brien, F.J., 2010. Understanding the effect of mean pore size on cell activity in collagen-glycosaminoglycan scaffolds. Cell Adhes. Migr. 4, 377–381. https://doi.org/10.4161/cam.4.3.11747

Mustafa, A.I., Ebrahim, A.A., Abel Halim, W.A.L., Fawzy, E., Abdou, A.F., 2022. Serum Soluble Intercellular Adhesion Molecule-1 (sICAM-1): A Novel Potential Biomarker in Severe Acne Vulgaris. Indian J. Dermatol. 67, 512. https://doi.org/10.4103/ijd.ijd_387_21

Navale, S.T., Mane, A.T., Ghanwat, A.A., Mulik, A.R., Patil, V.B., 2014. Camphor sulfonic acid (CSA) doped polypyrrole (PPy) films:

Measurement of microstructural and optoelectronic properties. Measurement 50, 363–369. https://doi.org/10.1016/j.measurement.2014.01.012

Nazari, H., Kehtari, M., Rad, I., Ashtari, B., Joghataei, M.T., 2020. Electrical stimulation induces differentiation of human cardiosphere-derived cells (hCDCs) to committed cardiomyocyte. Mol. Cell. Biochem. 470, 29–39. https://doi.org/10.1007/s11010-020-03742-6

Neoh, K.G., Kang, E.T., Tan, T.C., 1988. Chemical synthesis and characterization of electroactive and partially soluble polyazulene. Polym. Bull. 19. https://doi.org/10.1007/BF00263932

Nikkhah, M., Edalat, F., Manoucheri, S., Khademhosseini, A., 2012. Engineering microscale topographies to control the cell–substrate interface. Biomaterials 33, 5230–5246. https://doi.org/10.1016/j.biomaterials.2012.03.079

Niklason, L.E., Gao, J., Abbott, W.M., Hirschi, K.K., Houser, S., Marini, R., Langer, R., 1999. Functional Arteries Grown in Vitro. Science 284, 489–493. https://doi.org/10.1126/science.284.5413.489

Niklason, L.E., Langer, R.S., 1997. Advances in tissue engineering of blood vessels and other tissues. Transpl. Immunol. 5, 303–306. https://doi.org/10.1016/s0966-3274(97)80013-5

Nimmo, C.M., Owen, S.C., Shoichet, M.S., 2011. Diels−Alder Click Cross-Linked Hyaluronic Acid Hydrogels for Tissue Engineering. Biomacromolecules 12, 824–830. https://doi.org/10.1021/bm101446k

Ning, C., Zhou, Z., Tan, G., Zhu, Y., Mao, C., 2018. Electroactive polymers for tissue regeneration: Developments and perspectives. Prog. Polym. Sci. 81, 144–162. https://doi.org/10.1016/j.progpolymsci.2018.01.001

Nishimura, I., Hisanaga, R., Sato, T., Arano, T., Nomoto, S., Ikada, Y., Yoshinari, M., 2015. Effect of osteogenic differentiation medium on proliferation and differentiation of human mesenchymal stem cells in three-dimensional culture with radial flow bioreactor. Regen. Ther. 2, 24–31. https://doi.org/10.1016/j.reth.2015.09.001

Nokhbatolfoghahaei, H., Bohlouli, M., Paknejad, Z., Rad, M.R., Amirabad, L.M., Salehi-Nik, N., Khani, M.M., Shahriari, S., Nadjmi, N., Ebrahimpour, A., Khojasteh, A., 2020. Bioreactor cultivation condition for engineered bone tissue: Effect of various bioreactor designs on extra cellular matrix synthesis. J. Biomed. Mater. Res. A 108, 1662–1672. https://doi.org/10.1002/jbm.a.36932

Nur Hidayah, S., Dania Adila, A.R., Sharaniza, A.R., Muhammad Abid, A., Mohd Muzamir, M., 2024. Sequentially crosslinked collagen-based

hydrogel to form a semi-interpenetrating network for enhanced stability to hydrolytic degradation and electrochemical properties. Polym. Adv. Technol. 35, e6546. https://doi.org/10.1002/pat.6546

Olaru, M., Simionescu, N., Doroftei, F., David, G., 2023. Strategy Based on Michael Addition Reaction for the Development of Bioinspired Multilayered and Multiphasic 3D Constructs. Polymers 15, 1635. https://doi.org/10.3390/polym15071635

Oluwasanmi, J., Chvapil, M., 1976. Comparative-Study of 4 Materials in Local Burn Care in Rabbit Model. J. Trauma-Inj. Infect. Crit. Care 16, 348–353. https://doi.org/10.1097/00005373-197605000-00003

Oriňaková, R., Gorejová, R., Králová, Z.O., Petráková, M., Oriňak, A., 2021. Novel trends and recent progress on preparation methods of biodegradable metallic foams for biomedicine: a review. J. Mater. Sci. 56, 13925–13963. https://doi.org/10.1007/s10853-021-06163-y

Ostergard, D.R., 2012. Evidence-based Medicine for Polypropylene Mesh Use Compared With Native Tissue Vaginal Prolapse Repair. Urology 79, 12–14. https://doi.org/10.1016/j.urology.2011.07.1438

Österholm, A., Petr, A., Kvarnström, C., Ivaska, A., Dunsch, L., 2008. The Nature of the Charge Carriers in Polyazulene as Studied by in Situ Electron Spin Resonance−UV−Visible−Near-Infrared Spectroscopy. J. Phys. Chem. B 112, 14149–14157. https://doi.org/10.1021/jp805813s

Padmavathy, N., Vijayaraghavan, R., 2008. Enhanced bioactivity of ZnO nanoparticles—an antimicrobial study. Sci. Technol. Adv. Mater. 9, 035004. https://doi.org/10.1088/1468-6996/9/3/035004

Paduano, F., Marrelli, M., White, L.J., Shakesheff, K.M., Tatullo, M., 2016. Odontogenic Differentiation of Human Dental Pulp Stem Cells on Hydrogel Scaffolds Derived from Decellularized Bone Extracellular Matrix and Collagen Type I. Plos One 11, e0148225. https://doi.org/10.1371/journal.pone.0148225

Pajvani, U.B., Du, X., Combs, T.P., Berg, A.H., Rajala, M.W., Schulthess, T., Engel, J., Brownlee, M., Scherer, P.E., 2003. Structure-Function Studies of the Adipocyte-secreted Hormone Acrp30/Adiponectin: IMPLICATIONS FOR METABOLIC REGULATION AND BIOACTIVITY*. J. Biol. Chem. 278, 9073–9085. https://doi.org/10.1074/jbc.M207198200

Pandey, A., Iraqi, M., Toledo, E., Al-Kader Yassin, A., Podvalni, E., Naaz, S., Pandit, J.J., Martin, C.U., Le Saux, G., Porgador, A., Schvartzman, M., 2023. Elastic Microstructures: Combining Biochemical, Mechanical, and Topographical Cues for the Effective Activation and Proliferation of

Cytotoxic T Cells. ACS Appl. Mater. Interfaces 15, 31103–31113. https://doi.org/10.1021/acsami.3c01871

Pang, A.L., Arsad, A., Ahmadipour, M., 2021. Synthesis and factor affecting on the conductivity of polypyrrole: a short review. Polym. Adv. Technol. 32, 1428–1454. https://doi.org/10.1002/pat.5201

Patois, T., Lakard, B., Martin, N., Fievet, P., 2010. Effect of various parameters on the conductivity of free standing electrosynthesized polypyrrole films. Synth. Met. 160, 2180–2185. https://doi.org/10.1016/j.synthmet.2010.08.005

Peng, Z., Shu, B., Zhang, Y., Wang, M., 2019. Endothelial Response to Pathophysiological Stress. Arterioscler. Thromb. Vasc. Biol. 39, e233–e243. https://doi.org/10.1161/ATVBAHA.119.312580

Perry, D., Frame, J., 2020. The history and development of breast implants. Ann. R. Coll. Surg. Engl. 102, 478–482. https://doi.org/10.1308/rcsann.2020.0003

Petráková, M., Gorejová, R., Shepa, J., Macko, J., Kupková, M., Mičušík, M., Baláž, M., Hajdučková, V., Hudecová, P., Kožár, M., Šišková, B., Sáha, P., Oriňaková, R., 2024. Effect of Gentamicin Sulfate and Polymeric Polyethylene Glycol Coating on the Degradation and Cytotoxicity of Iron-Based Biomaterials. ACS Omega 9, 27113–27126. https://doi.org/10.1021/acsomega.4c01002

Pich, A., Lu, Y., Adler, H.-J.P., 2006. Polymeric particles with conjugated polymer: Layer on its surface as effective adsorbents of amino acids. Polymer 47, 6536–6543. https://doi.org/10.1016/j.polymer.2006.07.055

Pourkhodadad, S., Hosseinkazemi, H., Bonakdar, S., Nekounam, H., 2023. Biomimetic engineered approaches for neural tissue engineering: Spinal cord injury. J. Biomed. Mater. Res. B Appl. Biomater. 111, 701–716. https://doi.org/10.1002/jbm.b.35171

Pruitt, B.A., Jr, Levine, N.S., 1984. Characteristics and Uses of Biologic Dressings and Skin Substitutes. Arch. Surg. 119, 312–322. https://doi.org/10.1001/archsurg.1984.01390150050013

Puhl, D.L., Funnell, J.L., Fink, T.D., Swaminathan, A., Oudega, M., Zha, R.H., Gilbert, R.J., 2023. Electrospun fiber-mediated delivery of neurotrophin-3 mRNA for neural tissue engineering applications. Acta Biomater. 155, 370–385. https://doi.org/10.1016/j.actbio.2022.11.025

Qi, F., Wang, Y., Ma, T., Zhu, S., Zeng, W., Hu, X., Liu, Z., Huang, J., Luo, Z., 2013. Electrical regulation of olfactory ensheathing cells using conductive polypyrrole/chitosan polymers. Biomaterials 34, 1799–1809. https://doi.org/10.1016/j.biomaterials.2012.11.042

Rahimi, A., Mashak, A., 2013. Review on rubbers in medicine: natural, silicone and polyurethane rubbers. Plast. Rubber Compos. 42, 223–230. https://doi.org/10.1179/1743289811Y.0000000063

Raimondi, M.T., Moretti, M., Cioffi, M., Giordano, C., Boschetti, F., Laganà, K., Pietrabissa, R., 2006. The effect of hydrodynamic shear on 3D engineered chondrocyte systems subject to direct perfusion. Biorheology 43, 215–222. https://doi.org/10.1177/0006355X2006043003004006

Rasmussen, Seth C., 2011. Electrically Conducting Plastics: Revising the History of Conjugated Organic Polymers, in: Strom, E.T., Rasmussen, S. C. (Eds.), 100(plus) Years of Plastics, Leo Baekeland and Beyond. Amer Chemical Soc, Washington, pp. 147–163.

Ravichandran, R., Sundarrajan, S., Venugopal, J.R., Mukherjee, S., Ramakrishna, S., 2010. Applications of conducting polymers and their issues in biomedical engineering. J. R. Soc. Interface 7. https://doi.org/10.1098/rsif.2010.0120.focus

Razaq, A., Mihranyan, A., Welch, K., Nyholm, L., Strømme, M., 2009. Influence of the Type of Oxidant on Anion Exchange Properties of Fibrous Cladophora Cellulose/Polypyrrole Composites. J. Phys. Chem. B 113, 426–433. https://doi.org/10.1021/jp806517h

Rezaeeyazdi, M., Colombani, T., Memic, A., Bencherif, S.A., 2018. Injectable Hyaluronic Acid-co-Gelatin Cryogels for Tissue-Engineering Applications. Materials 11, 1374. https://doi.org/10.3390/ma11081374

Robert Langer | Polaris Partners, n.d. URL https://polarispartners.com/partner/robert-langer/ (accessed 4.7.23).

Rodriguez-Boulan, E., Kreitzer, G., Müsch, A., 2005. Organization of vesicular trafficking in epithelia. Nat. Rev. Mol. Cell Biol. 6, 233–247. https://doi.org/10.1038/nrm1593

Rosenfeld, D., Landau, S., Shandalov, Y., Raindel, N., Freiman, A., Shor, E., Blinder, Y., Vandenburgh, H.H., Mooney, D.J., Levenberg, S., 2016. Morphogenesis of 3D vascular networks is regulated by tensile forces. Proc. Natl. Acad. Sci. 113, 3215–3220. https://doi.org/10.1073/pnas.1522273113

Sagadevan, S., Schirhagl, R., Rahman, M.Z., Ismail, M.F.B., Lett, J.A., Fatimah, I., Kaus, N.H.M., Oh, W.-C., 2023. Recent advancements in polymer matrix nanocomposites for bone tissue engineering applications. J. Drug Deliv. Sci. Technol. 82, 104313. https://doi.org/10.1016/j.jddst.2023.104313

Sak-Bosnar, M., Budimir, M.V., Kovac, S., Kukulj, D., Duic, L., 1992. Chemical and electrochemical characterization of chemically synthesized

conducting polypyrrole. J. Polym. Sci. Part Polym. Chem. 30, 1609–1614. https://doi.org/10.1002/pola.1992.080300813

Sasso, C., Beneventi, D., Zeno, E., Chaussy, D., Petit-Conil, M., Belgacem, N., 2011. Polypyrrole and Polypyrrole/Wood-Derived Materials Conducting Composites: A Review. BIORESOURCES 6, 3585–3620.

Sawai, J., Yoshikawa, T., 2004. Quantitative evaluation of antifungal activity of metallic oxide powders (MgO, CaO and ZnO) by an indirect conductimetric assay. J. Appl. Microbiol. 96, 803–809. https://doi.org/10.1111/j.1365-2672.2004.02234.x

Scherer, W., Syverton, J., Gey, G., 1953. Studies on the Propagation Invitro of Poliomyelitis Viruses .4. Viral Multiplication in a Stable Strain of Human Malignant Epithelial Cells (strain Hela) Derived from an Epidermoid Carcinoma of the Cervix. J. Exp. Med. 97, 695-. https://doi.org/10.1084/jem.97.5.695

Schwendner, M., Ille, S., Kirschke, J.S., Bernhardt, D., Combs, S.E., Meyer, B., Krieg, S.M., 2023. Clinical evaluation of vertebral body replacement of carbon fiber–reinforced polyetheretherketone in patients with tumor manifestation of the thoracic and lumbar spine. Acta Neurochir. (Wien) 165, 897–904. https://doi.org/10.1007/s00701-023-05502-z

Shrestha, B.K., Shrestha, S., Baral, E.R., Lee, J.Y., Kim, B.-S., Park, C.H., Kim, C.S., 2019. π-Conjugated polyaniline-assisted flexible titania nanotubes with controlled surface morphology as regenerative medicine in nerve cell growth. Chem. Eng. J. 360, 701–713. https://doi.org/10.1016/j.cej.2018.12.027

Shu, C., Qin, C., Chen, L., Wang, Y., Shi, Z., Yu, J., Huang, J., Zhao, C., Huan, Z., Wu, C., Zhu, M., Zhu, Y., n.d. Metal-Organic Framework Functionalized Bioceramic Scaffolds with Antioxidative Activity for Enhanced Osteochondral Regeneration. Adv. Sci. n/a, 2206875. https://doi.org/10.1002/advs.202206875

Skopalova, K., Radaszkiewicz, K.A., Kasparkova, V., Stejskal, J., Bober, P., Junkar, I., Mozetic, M., Capakova, Z., Lehocky, M., Kasparova, M., Pachernik, J., Humpolicek, P., 2021. Modulation of Differentiation of Embryonic Stem Cells by Polypyrrole: The Impact on Neurogenesis. Int. J. Mol. Sci. 22, 501. https://doi.org/10.3390/ijms22020501

Slouf, M., Gajdosova, V., Dybal, J., Sticha, R., Fulin, P., Pokorny, D., Mateo, J., Panisello, J.J., Canales, V., Medel, F., Bistolfi, A., Bracco, P., 2023. European Database of Explanted UHMWPE Liners from Total Joint Replacements: Correlations among Polymer Modifications, Structure, Oxidation, Mechanical Properties and Lifetime In Vivo. Polymers 15, 568. https://doi.org/10.3390/polym15030568

Smith, J.A., Mele, E., 2021. Electrospinning and Additive Manufacturing: Adding Three-Dimensionality to Electrospun Scaffolds for Tissue Engineering. Front. Bioeng. Biotechnol. 9.

Tallawi, M., Rosellini, E., Barbani, N., Cascone, M.G., Rai, R., Saint-Pierre, G., Boccaccini, A.R., 2015. Strategies for the chemical and biological functionalization of scaffolds for cardiac tissue engineering: a review. J. R. Soc. Interface 12, 20150254. https://doi.org/10.1098/rsif.2015.0254

Tanasa, E., Zaharia, C., Hudita, A., Radu, I.-C., Costache, M., Galateanu, B., 2020. Impact of the magnetic field on 3T3-E1 preosteoblasts inside SMART silk fibroin-based scaffolds decorated with magnetic nanoparticles. Mater. Sci. Eng. C 110, 110714. https://doi.org/10.1016/j.msec.2020.110714

Tandon, N., Goh, B., Marsano, A., Chao, P.-H.G., Montouri-Sorrentino, C., Gimble, J., Vunjak-Novakovic, G., 2009. Alignment and elongation of human adipose-derived stem cells in response to direct-current electrical stimulation, in: 2009 Annual International Conference of the IEEE Engineering in Medicine and Biology Society. Presented at the 2009 Annual International Conference of the IEEE Engineering in Medicine and Biology Society, pp. 6517–6521. https://doi.org/10.1109/IEMBS.2009.5333142

Teo, B.K.K., Wong, S.T., Lim, C.K., Kung, T.Y.S., Yap, C.H., Ramagopal, Y., Romer, L.H., Yim, E.K.F., 2013. Nanotopography Modulates Mechanotransduction of Stem Cells and Induces Differentiation through Focal Adhesion Kinase. ACS Nano 7, 4785–4798. https://doi.org/10.1021/nn304966z

Thakur, V.K., Ding, G., Ma, J., Lee, P.S., Lu, X., 2012. Hybrid Materials and Polymer Electrolytes for Electrochromic Device Applications. Adv. Mater. 24, 4071–4096. https://doi.org/10.1002/adma.201200213

Thunberg, J., Kalogeropoulos, T., Kuzmenko, V., Hägg, D., Johannesson, S., Westman, G., Gatenholm, P., 2015. In situ synthesis of conductive polypyrrole on electrospun cellulose nanofibers: scaffold for neural tissue engineering. Cellulose 22, 1459–1467. https://doi.org/10.1007/s10570-015-0591-5

Todaro, G., Green, H., 1963. Quantitative Studies of Growth of Mouse Embryo Cells in Culture and Their Development into Established Lines. J. Cell Biol. 17, 299-. https://doi.org/10.1083/jcb.17.2.299

Tulloch, N.L., Muskheli, V., Razumova, M.V., Korte, F.S., Regnier, M., Hauch, K.D., Pabon, L., Reinecke, H., Murry, C.E., 2011. Growth of Engineered Human Myocardium With Mechanical Loading and Vascular Coculture.

Circ. Res. 109, 47–59. https://doi.org/10.1161/CIRCRESAHA.110.237206

Uda, M., Kawashima, H., Mayama, H., Hirai, T., Nakamura, Y., Fujii, S., 2021. Locomotion of a Nonaqueous Liquid Marble Induced by Near-Infrared-Light Irradiation. Langmuir 37, 4172–4182. https://doi.org/10.1021/acs.langmuir.1c00041

Unadkat, H.V., Hulsman, M., Cornelissen, K., Papenburg, B.J., Truckenmüller, R.K., Carpenter, A.E., Wessling, M., Post, G.F., Uetz, M., Reinders, M.J.T., Stamatialis, D., van Blitterswijk, C.A., de Boer, J., 2011. An algorithm-based topographical biomaterials library to instruct cell fate. Proc. Natl. Acad. Sci. 108, 16565–16570. https://doi.org/10.1073/pnas.1109861108

Upadhyay, J., Kumar, A., Gogoi, B., Buragohain, A.K., 2014. Biocompatibility and antioxidant activity of polypyrrole nanotubes. Synth. Met. 189, 119–125. https://doi.org/10.1016/j.synthmet.2014.01.004

Vacanti, C.A., 2006. The history of tissue engineering. J. Cell. Mol. Med. 10, 569–576. https://doi.org/10.1111/j.1582-4934.2006.tb00421.x

Vaitkuviene, A., Ratautaite, V., Mikoliunaite, L., Kaseta, V., Ramanauskaite, G., Biziuleviciene, G., Ramanaviciene, A., Ramanavicius, A., 2014. Some biocompatibility aspects of conducting polymer polypyrrole evaluated with bone marrow-derived stem cells. Colloids Surf. Physicochem. Eng. Asp., Selected papers from the 26th European Colloid and Interface Society conference (26th ECIS 2012) 442, 152–156. https://doi.org/10.1016/j.colsurfa.2013.06.030

Van Vlierberghe, S., Vanderleyden, E., Boterberg, V., Dubruel, P., 2011. Gelatin Functionalization of Biomaterial Surfaces: Strategies for Immobilization and Visualization. Polymers 3, 114–130. https://doi.org/10.3390/polym3010114

Velez-Suberbie, M.L., Tarrant, R.D.R., Tait, A.S., Spencer, D.I.R., Bracewell, D.G., 2013. Impact of aeration strategy on CHO cell performance during antibody production. Biotechnol. Prog. 29, 116–126. https://doi.org/10.1002/btpr.1647

Venkatesh, S., Vishista, K., 2018. Identification of the best chemical equivalent ratio to produce emeraldine salt exhibiting better pseudo capacitance. Electrochimica Acta 263, 76–84. https://doi.org/10.1016/j.electacta.2018.01.032

Vítková, L., Musilová, L., Achbergerová, E., Kolařík, R., Mrlík, M., Korpasová, K., Mahelová, L., Capáková, Z., Mráček, A., 2022. Formulation of Magneto-Responsive Hydrogels from Dually Cross-Linked Polysaccharides: Synthesis, Tuning and Evaluation of Rheological

Properties. Int. J. Mol. Sci. 23, 9633. https://doi.org/10.3390/ijms23179633

Vogler, E.A., 1998. Structure and reactivity of water at biomaterial surfaces. Adv. Colloid Interface Sci. 74, 69–117. https://doi.org/10.1016/S0001-8686(97)00040-7

Wang, F., Lai, Y.-H., Kocherginsky, N.M., Kosteski, Yu.Yu., 2003. The First Fully Characterized 1,3-Polyazulene: High Electrical Conductivity Resulting from Cation Radicals and Polycations Generated upon Protonation. Org. Lett. 5, 995–998. https://doi.org/10.1021/ol0274615

Wang, H., Klosterhalfen, B., Klinge, U., Muellen, A., Jockenhoevel, S., n.d. Influence of polypropylene mesh degradation on tissue inflammatory reaction. J. Biomed. Mater. Res. A. https://doi.org/10.1002/jbm.a.37494

Wang, J.-. S., Dunne, N., 2008. 10 - Bone cement fixation: acrylic cements, in: Revell, P.A. (Ed.), Joint Replacement Technology, Woodhead Publishing Series in Biomaterials. Woodhead Publishing, pp. 212–251. https://doi.org/10.1533/9781845694807.2.212

Wang, X.D., Gu, X.S., Yuan, C.W., Chen, S.J., Zhang, P.Y., Zhang, T.Y., Yao, J., Chen, F., Chen, G., 2004. Evaluation of biocompatibility of polypyrrole in vitro and in vivo. J. Biomed. Mater. Res. A 68A, 411–422. https://doi.org/10.1002/jbm.a.20065

Wong, D.W., Gan, W.L., Teo, Y.K., Lew, W.S., 2018. Interplay of cell death signaling pathways mediated by alternating magnetic field gradient. Cell Death Discov. 4, 1–9. https://doi.org/10.1038/s41420-018-0052-7

Wrzecionko, E., Minařík, A., Smolka, P., Minařík, M., Humpolíček, P., Rejmontová, P., Mráček, A., Minaříková, M., Gřundělová, L., 2017. Variations of Polymer Porous Surface Structures via the Time-Sequenced Dosing of Mixed Solvents. ACS Appl. Mater. Interfaces 9, 6472–6481. https://doi.org/10.1021/acsami.6b15774

Wu, C.-H., Liu, C.-Y., 2023. Optimization of compression molding for double-concave lenses. Int. J. Adv. Manuf. Technol. 125, 5089–5099. https://doi.org/10.1007/s00170-023-11052-6

Wu, D.T., Munguia-Lopez, J.G., Cho, Y.W., Ma, X., Song, V., Zhu, Z., Tran, S.D., 2021. Polymeric Scaffolds for Dental, Oral, and Craniofacial Regenerative Medicine. Molecules 26, 7043. https://doi.org/10.3390/molecules26227043

Wu, M., Zhong, C., Deng, Y., Zhang, Q., Zhang, X., Zhao, X., 2020. Resveratrol loaded glycyrrhizic acid-conjugated human serum albumin nanoparticles for tail vein injection II: pharmacokinetics, tissue

distribution and bioavailability. Drug Deliv. 27, 81–90. https://doi.org/10.1080/10717544.2019.1704944

Xia, Y., Wang, X., Xia, X., Xu, R., Zhang, S., Wu, J., Liang, Y., Gu, C., Tu, J., 2017. A Newly Designed Composite Gel Polymer Electrolyte Based on Poly(Vinylidene Fluoride-Hexafluoropropylene) (PVDF-HFP) for Enhanced Solid-State Lithium-Sulfur Batteries. Chem. – Eur. J. 23, 15203–15209. https://doi.org/10.1002/chem.201703464

Xia, Z., Zhang, H., Li, Q., Yi, C., Xing, Z., Qin, Z., Zhao, H., Jing, J., Zhao, C., Cai, K., 2024. The Biomimetic Electrical Stimulation System Inducing Osteogenic Differentiations of BMSCs. ACS Appl. Mater. Interfaces 16, 56730–56743. https://doi.org/10.1021/acsami.4c11890

Xu, T., Miszuk, J.M., Zhao, Y., Sun, H., Fong, H., 2015. Electrospun Polycaprolactone 3D Nanofibrous Scaffold with Interconnected and Hierarchically Structured Pores for Bone Tissue Engineering. Adv. Healthc. Mater. 4, 2238–2246. https://doi.org/10.1002/adhm.201500345

Yan, H., Wang, Y., Li, L., Zhou, X., Shi, X., Wei, Y., Zhang, P., 2020. A micropatterned conductive electrospun nanofiber mesh combined with electrical stimulation for synergistically enhancing differentiation of rat neural stem cells. J. Mater. Chem. B 8, 2673–2688. https://doi.org/10.1039/C9TB02864A

Yang, J., Zhang, J., Ding, C., Dong, D., Shang, P., 2018. Regulation of Osteoblast Differentiation and Iron Content in MC3T3-E1 Cells by Static Magnetic Field with Different Intensities. Biol. TRACE Elem. Res. 184, 214–225. https://doi.org/10.1007/s12011-017-1161-5

Yang, K., Jung, H., Lee, H.-R., Lee, J.S., Kim, S.R., Song, K.Y., Cheong, E., Bang, J., Im, S.G., Cho, S.-W., 2014. Multiscale, Hierarchically Patterned Topography for Directing Human Neural Stem Cells into Functional Neurons. ACS Nano 8, 7809–7822. https://doi.org/10.1021/nn501182f

Yin, Z., Chen, X., Chen, J.L., Shen, W.L., Hieu Nguyen, T.M., Gao, L., Ouyang, H.W., 2010. The regulation of tendon stem cell differentiation by the alignment of nanofibers. Biomaterials 31, 2163–2175. https://doi.org/10.1016/j.biomaterials.2009.11.083

Zhang, F., Su, K., Fang, Y., Sandhya, S., Wang, D.-A., 2015. A mixed co-culture of mesenchymal stem cells and transgenic chondrocytes in alginate hydrogel for cartilage tissue engineering. J. Tissue Eng. Regen. Med. 9, 77–84. https://doi.org/10.1002/term.1641

Zhang, L., Gu, F., Chan, J., Wang, A., Langer, R., Farokhzad, O., 2008. Nanoparticles in Medicine: Therapeutic Applications and Developments. Clin. Pharmacol. Ther. 83, 761–769. https://doi.org/10.1038/sj.clpt.6100400

Zhang, Y., Zhang, M.Q., 2002. Calcium phosphate/chitosan composite scaffolds for controlled in vitro antibiotic drug release. J. Biomed. Mater. Res. 62, 378–386. https://doi.org/10.1002/jbm.10312

Zhang, Z., Feng, S., Wei, Q., Wu, L., n.d. Preparation and surface modification of ultrahigh throughput tannic acid coblended polyethersulfone ultrafiltration membranes for hemodialysis. J. Appl. Polym. Sci. https://doi.org/10.1002/app.53640

Zheng, H., Tian, Y., Gao, Q., Yu, Y., Xia, X., Feng, Z., Dong, F., Wu, X., Sui, L., 2020. Hierarchical Micro-Nano Topography Promotes Cell Adhesion and Osteogenic Differentiation via Integrin α2-PI3K-AKT Signaling Axis. Front. Bioeng. Biotechnol. 8. https://doi.org/10.3389/fbioe.2020.00463

Zhuang, X., 2020. Azulene-Based Molecules, Polymers, and Frameworks for Optoelectronic and Energy Applications. Small Methods 4. https://doi.org/10.1002/smtd.202000628

Zuščíková, L., Greifová, H., Bažány, D., Lukáč, N., Jambor, T., 2024. Current approaches and techniques of 3D cell culture systems: a review. Arch. Ecotoxicol. 6, 22–27. https://doi.org/10.36547/ae.2024.6.1.22-27

LIST OF FIGURES

LIST OF TABLES

LIST OF ABBREVIATIONS AND SYMBOLS

AFM	Atomic force microscopy
APS	Ammonium persulfate
ATP	Adenosine triphosphate
CIPs	Carbonyl iron particles
DEX	Dextran
DMTMM	4-(4,6-dimethoxy-1,3,5-triazin-2-yl)-4-methylmorpholinium chloride
DNA	Deoxyribonucleic acid
ECM	Extracellular matrix
EDC	1-ethyl-3-(3-dimethylaminopropyl)carbodiimide hydrochloride
FAK	Focal adhesion kinase
FeCl3	Iron(III) chloride
FTIR	Fourier transform infrared
HA	Hyaluronic acid
hMSC	Human mesenchymal stem cell
ITO	Indium tin oxide
ITS	Insulin–transferrin–selenium
LIF	Leukemia inhibitory factor
MTT	3-(4,5-dimethylthiazol-2-yl)-2,5-diphenyltetrazolium bromide
NHS	N-hydroxysuccinimide
PANI	Polyaniline
PAz	Polyazulene
PPy	Polypyrrole
PU	Polyurethane
PUPPy	Pulyurethane/polypyrrole composite
PVDF	Polyvinylidene fluoride

PVDF-HFP	Polyvinylidene fluoride-co-hexafluoropropylene
SEM	Scanning electron microscopy
TCDs	Tissue culture dishes
TE	Tissue engineering
TruePAz	True Polyazulene
UV	Ultraviolet
Vis	Visible

Article I

Mahelová, L., Slobodian, P., Kocourková, K., Minařík, A., Moučka, R., Trchová, M., Martínková, M., Skopalová, K., Víchová, Z., Kašpárková, V., Humpolíček, P., 2024. *Method for in situ polypyrrole coating, and the example of its use for functionalization of polyurethane anisotropic electrospun mats.* Heliyon 10. https://doi.org/10.1016/j.heliyon.2024.e27883

Heliyon 10 (2024) e27883

Contents lists available at ScienceDirect

Heliyon

journal homepage: www.cell.com/heliyon

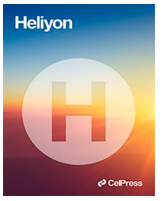

Research article

Method for *in situ* polypyrrole coating, and the example of its use for functionalization of polyurethane anisotropic electrospun mats

Leona Mahelová [a], Petr Slobodian [a,b], Karolína Kocourková [b], Antonín Minařík [a,b], Robert Moučka [a], Miroslava Trchová [c], Martina Martínková [a], Kateřina Skopalová [a], Zdenka Víchová [a], Věra Kašpárková [a,d], Petr Humpolíček [a,d,*]

[a] *Centre of Polymer Systems, University Institute, Tomas Bata University in Zlín, Trida T. Bati 5678, 76001, Zlin, Czech Republic*
[b] *Department of Physics and Materials Engineering, Faculty of Technology, Tomas Bata University in Zlin, Vavreckova 5669, 76001, Zlin, Czech Republic*
[c] *Central Laboratories, Laboratory of Molecular Spectroscopy, University of Chemistry and Technology Prague, Technicka 5, 166 28 Prague 6, Czech Republic*
[d] *Department of Fat, Surfactant and Cosmetics Technology, Faculty of Technology, Tomas Bata University in Zlin, Vavreckova 5669, 76001, Zlin, Czech Republic*

ARTICLE INFO

Keywords:
Coating
Conductivity
Image analysis
Anisotropy
Stem cells

ABSTRACT

The *in situ* coating of polymer substrate with polypyrrole, described herein with detailed know-how, represents a novel technique of surface functionalization. The choice of oxidizing agent and the polymerization time both affect the properties of the thin polypyrrole layer. The specific conductivity, free surface energy, thickness, topography, and FTIR spectra of polypyrrole layer were determined. The conductive coatings were further used to functionalize both isotropic and anisotropic electrospun polyurethane nanofibrous mats to show their applicability and study the bioactive effect of both the anisotropy and conductivity together. The morphology of composites was studied by means of atomic force microscopy and scanning electron microscopy. A complex cytocompatibility study was performed, including determining cytotoxicity by optical and fluorescence microscopy, the advanced qualification of cell morphology by cell-image analysis, and a study of stem cell behavior. The results clearly showed the significant impact of substrate modification on cells, especially on fibroblasts while the embryonic stem cells were less affected. This study shows not only the effective way to prepare a thin conducting layer based on polypyrrole but also demonstrates its importance for the fabrication of smart biomaterials.

1. Introduction

The successful application of polymers in tissue engineering is conditioned by an understanding of their interaction with cells, which is influenced by a number of material properties. The material's good **electrical conductivity** offers notable advantages in many tissues, especially electrosensitive ones (e.g., cardiac or neural tissue). Conductive scaffolds mimic the native conductivity of tissues, thereby promoting cell-substrate interactions, cell-cell communication, and cell signaling, leading to improved tissue integration and functionality. Also, conductive scaffolds can provide a platform for controlled electrical stimulation, which creates an

* Corresponding author. Tomas Bata University in Zlín, Trida T. Bati 5678, 76001, Zlin, Czech Republic.
E-mail address: humpolicek@utb.cz (P. Humpolíček).

https://doi.org/10.1016/j.heliyon.2024.e27883
Received 25 September 2023; Received in revised form 4 March 2024; Accepted 7 March 2024
Available online 13 March 2024

environment that guides cell behavior; for example, enhances cell growth and migration, expedites nerve regeneration, or promotes cardiomyogenesis [1–4]. In this context, electrically conductive polymers (CPs) are at the center of attention, mainly thanks to their intrinsically combined electron- and ion-based conductivity.

Among CPs, polypyrrole (PPy) is a promising representative due to its high conductivity and stability. The study by Wang et al. (2004) confirmed that PPy extracts do not induce acute or subacute toxicity, hemolysis, allergenicity, or mutagenesis *in vivo* [5]. On the other hand, Hsu et al. (2008) identified the limits of PPy cytocompatibility when PPy is in contact with various tissues [6]. *In vitro* studies then showed that there are differences between the cytotoxicity and embryotoxicity of PPy salt and PPy base [7] and that low molecular products present in PPy base can induce neurogenesis in embryonic stem cells [8]. In addition, an improvement in cell/PPy interactions can be obtained by adjusting many factors, such as the method of synthesis (chemical or electrochemical) and the various conditions of synthesis, the used oxidation agents and dopant ions, and even the rinsing procedure [9].

Regarding oxidation agents, iron(III) chloride ($FeCl_3$) [9–13], ammonium persulfate (APS) [13,14], sodium persulfate [15] hydrogen peroxide [16], cupric chloride [17], phosphomolybdic acid [18], and many others can be used for the PPy synthesis. In the here presented study, the former two oxidants in the list were employed and compared. The choice of oxidant has a considerable effect on the resulting cytocompatibility and other key properties, such as the electrical conductivity [19]. Previous studies utilized PPy in the form of powders [20–23], co-polymers [24–26], or colloidal dispersions [27–29], though, only a few studies are concerned with PPy *in situ* coating [30–32] and even less are put in the connection with its cytocompatibility [33].

The **surface properties** of a biomaterial play a critical role in cell/material interaction. According to Ravichandran et al. (2010), the major limitation on the cytocompatibility of PPy (and conductive polymers in general) is its hydrophobicity, which decreases the successful entrapment of proteins to the surface [34]. Nevertheless, this disadvantage can be overcome by doping with various anionic dopants [20] or by the coating of PPy with extracellular matrix components [35]. These allow the initial adhesion and growth of cells, which subsequently produce their own extracellular matrix and thus colonize the surfaces more easily.

For the best results with respect to cytocompatibility, the **topography** of biomaterials should be modified at both the micro-scale and nano-scale depending on the type of cultured cells [36]. The topographical treatment of materials is an economically effective way of improving the biological activity of any biomaterial surface. The principle is that a surface structure determines the availability of suitable binding sites for adhesive proteins, thereby affecting their surface distribution. As a result, biomaterials with topographic modifications acquire capabilities that were originally reserved only for growth factors [37]. This is related to the fact that most types of cells can sense the orientation, texture, and physical properties of biomaterials [38].

Moreover, a biomaterial's **iso/anisotropy** plays a crucial role. This is related to the fact that the extracellular matrix is often anisotropic *in vivo* [39]. Many studies have aimed to simulate the *in vivo* anisotropic structure of the myocardium through a series of topographical features, because cardiomyocytes establish their native *in vivo* phenotype – aligned actin fibers, parallel sarcomeric arrangements, and nuclear elongation [40] and the contractile properties of cardiac tissues are directly related to cellular orientation and elongation. In fact, not only cardiomyocytes but the majority of cell types cultured on grooved profiles elongate and align themselves along the major axis of the topographic anisotropic surface features, such as grooves [41]. In response to the anisotropic topography, uniaxially oriented nanofibers have also been reported to induce morphological changes in many cell types, including cytoskeletal rearrangements, nuclear elongation, and even axon extrusion from neuronal stem cells [42,43].

Iso/anisotropy can thus be considered another cell-instructive material property, especially when discussing stem cell behavior. However, CPs, e.g. PPy, cannot form solid materials themselves and thus their topography and anisotropy cannot be controlled. The preparation of composites, therefore, seems to be the most effective solution to this problem. Previously, cryogels of various polymers with either PPy or polyaniline were prepared [44,45] but the adjustability of their anisotropy was limited. A more effective approach is to prepare a composite combining an anisotropic substrate with the surface functionalization with CPs.

In the present study, electrospun polyurethane (PU) mats were combined with PPy to prepare composites (**PUPPy**) with controllable anisotropy, topography, and conductivity. This study contributes to the current knowledge of substrate coating with PPy and its impact on cytocompatibility.

As the main novelty, we present a method that makes the process of coating a substrate with PPy as simple, fast and versatile as possible, so it is applicable to any substrate; such as the nanofibrous nonwoven mats reported here. Previously reported PPy coating methods are certainly functional, but require the involvement of electricity in the process [46], or specific solvents [47] or stabilizers [48], furthermore they may be limited by the long polymerization time [33] and, last but not least, the low temperature during the reaction process [47–50]. In comparison to these, here presented PPy coating is synthesized chemically *in situ* in aqueous solution at room temperature in seconds without the use of any stabilizers or modifiers, resulting in a uniform thin layer with high conductivity. Therefore, the method allows for the use of PPy coating in a common practice or big manufacturing facility. A drawback of this method may be its speed. Since the reaction occurs quickly, we emphasize the importance of controlling the polymerization time of PPy, as exceeding the time has a negative effect on the topography and leads to the disruption of the PPy coating.

Another strength of our study is the quantitative and qualitative cell-image analysis, which graphically illustrates the impact of the anisotropic topography of the nanofibrous substrate, the electrical conductivity of the PPy coatings, and their combinations on cell morphology. On the basis of previously described knowledge, we hypothesized that coating an anisotropic substrate with conducting PPy will lead to the preparation of a cell-instructive composite. The study presents a complex cytocompatibility experiment employing electrospun nonwoven nanofiber PU mats both in their pristine and modified forms. Three types of modifications were tested:

1. An uniaxial orientation of fibers in the PU mats to achieve anisotropy;
2. Coating the oriented PU mats with PPy to enhance electro-conductivity;
3. Coating the PUPPy composite with gelatin and albumin to increase cytocompatibility.

The effects of these modifications on the behavior of a mouse fibroblast cell line and a mouse embryonic stem cell line were observed.

2. Materials and methods

2.1. Electrospinning, purification, and orientation of nanofibrous nonwoven PU mats

Desmopan 385 S (Covestro AG, Germany) was dissolved in a 3:1 solvent mixture of dimethylformamide (Brenntag, Poland) and methylisobutylketon (Penta Chemicals, Czech Republic) to a concentration of 12.5 %. The final solution had a viscosity of 1.3 Pa s and a conductivity of 31.5 mS/cm due to the addition of sodium chloride (Penta Chemicals, Czech Republic). Then, the solution was loaded into syringes connected to 32 jets of the electrospinning device Nanospider (Elmarco, Czech Republic). The solution was extruded into a high-voltage electric field (75 kV). A planar collector with a backing film drawn at a speed of 0.1 m/min was located 19 cm from the jets. The final product had 4 deposited layers with a basis weight of 9.01 g/m^2.

To remove impurities and unbound residues, such as solvents and salts, from the manufacture, the electrospun PU mats measuring (15 × 15) cm^2 were immersed in 500 mL of ultrapure water and shaken for 7 d, while the water was changed every 48 h, and then dried for 1 h at 50 °C.

Next, these isotropic PU mats with randomly oriented fibres were taped to the microscope cover glass. To obtain anisotropic PU mats with aligned fibres, the PU mats were manually stretched 1 cm over a heat source at 150 °C and attached in the stretched state with tape to the microscope cover glass without any delay. In both cases, overlaps were cut off to obtain a uniform area of (22 × 22) mm^2.

2.2. Synthesis of PPy coatings

PPy *in situ* synthesis was used to coat the surfaces of various substrates. First, cell culture dishes were coated with PPy and the properties of PPy coatings such as topography, thickness, specific conductivity, surface free energy, and basic cytocompatibility were analyzed on these coated dishes. Secondly, indium tin oxide (ITO) glass was used as a support suitable for FTIR spectroscopy analysis of deposited PPy thin layers. Finally, the electrospun PU fibrous mats were coated with PPy to create PUPPy composites. The structure and biocompatibility of the latter materials were then studied in detail.

The PPy *in situ* polymerization was conducted using pyrrole (Sigma-Aldrich, USA) as a monomer and APS (Sigma-Aldrich, USA) or $FeCl_3$ (IPL, Czech Republic) as an oxidation agent. Solutions of the monomer (0.2 M) and the oxidation agent (0.25 M) in ultrapure water were prepared and allowed to stand for about 1 h at room temperature conditioned at 20 °C before being pipetted into cell culture dishes (empty or containing ITO glass supports or PU mats) in a ratio of 1:1. The polymerization reaction was carried out for 15 s (t_1), 30 s (t_2), or 60 s (t_3) at room temperature conditioned at 20 °C. To terminate the PPy coating formation, the excess reaction mixture was discarded and the surfaces covered with PPy coatings were immediately and thoroughly rinsed with 0.2 M hydrochloric acid (Penta Chemicals, Czech Republic), which had two roles here: It washed out the residual unreacted substances and at the same time doped the PPy coatings. Then, the resulting substrates with PPy coatings were rinsed with methanol (Penta Chemicals, Czech Republic) and allowed to dry overnight at room temperature conditioned at 20 °C.

The variation in polymerization time is presented here to demonstrate its significant influence on the topography of the final PPy coatings. Besides that, all subsequent syntheses and analyses were performed on samples prepared with the same polymerization time: (t_1) = 15 s, which was chosen as the most appropriate because it resulted in the most uniform surface. Furthermore, PUPPy composites were formed by oxidizing PPy with $FeCl_3$ only, which was selected for its superior cytocompatibility.

2.3. Characterization of physicochemical properties

Atomic force microscopy (AFM): The surface topographies of PPy coatings synthesized on cell culture dishes using various oxidizing agents and reaction times were measured by means of a Dimension ICON atomic force microscope (Bruker Corporation, USA). Measurements were performed at a scan rate of 0.5 Hz with a resolution of (512 × 512) pixels in tapping mode in an air atmosphere at room temperature (22 °C, 50 % RH). A silicone-nitride probe with a resonant frequency of 70 ± 25 kHz and a spring constant of 0.4 N/m (ScanAsyst-Air, Bruker) was used.

The morphology of PUPPy composites was studied using an NTEGRA Prima (NT-MDT) atomic force microscope in tapping mode in air in an atmosphere at room temperature (22 °C, 50 % RH). An NSG01 (TipsNano) silicon probe of force constant 1.45–15.1 N/m was used. The sample area was scanned at a rate of 0.4 Hz in (512 × 512) pixel format.

Thickness measurements of PPy coatings on cell culture dishes surfaces were scanned using AFM. A silicone rubber mask was attached to the cell culture dishes before and during the PPy coating process. After polymerization was terminated, the silicone mask was removed to prepare clean edges for the thin PPy layers. AFM characterization was performed using a Dimension ICON in ScanAsyst mode using ScanAsyst-Air silicon nitride probe with a spring constant of 0.4 N/m (Bruker Corporation, USA). The measurements were performed under laboratory conditions (temperature and atmosphere). The scanning rate was 0.5 Hz.

Images were processed using Gwyddion – Free SPM data analysis software, version 2.55 (D. Nečas, P. Klapetek, Czech Metrology Institute, Czech Republic). The images were edited using Data Levelling and Background Subtraction – functions Plane level and Polynomial Background. Profile sections were made in the middle of the measured area. The parameters R_a (the arithmetic average surface roughness value) and R_z (average peak-to-valley depth profile parameter) were obtained from 3 profile sections.

Specific conductivity: The electric conductivity of PPy coatings deposited on cell celture dishes was determined at room temperature by the four-point van der Pauw method. A Keithley 6517B electrometer, a Keithley 2410 source meter, and a Keithley 7002 switch (USA) were used.

Surface free energy: Measurements of contact angles on PPy coatings in cell celture dishes were carried out by a Theta Optical Tensiometer (Biolin Scientific, Finland). For all PPy coatings, demineralized water, ethylene glycol, and diiodomethane (Sigma-Aldrich, USA) were used as test liquids. The sessile static droplets with a volume of 10 μL were used and contact angles were recorded after (10 ± 2) s at room temperature. The measurement was repeated ten times for each sample. The surface free energy was determined using the "acid-base" method.

FTIR spectroscopy: The spectra of thin PPy coatings deposited on ITO support were obtained using a Thermo Scientific Nicolet iN10 Infrared Microscope with a Thermo Scentific Omnic Picta user interface equipped with a liquid nitrogen cooled MCT-A detector (mercury cadmium telluride) in reflection micro-spectroscopic mode. The spectra were measured in the spectral range 4000–650 cm^{-1} with the resolution 4 cm^{-1}, 64 scans and Happ-Genzel apodization. The aperture of the microscope was set to (150 × 150) μm^2.

Scanning electron microscopy (SEM): Surface images of PUPPy composites were obtained by a Phenom Pro SEM, (Phenom-world BV). For SEM observation, the PUPPy composites were cut into pieces (4 × 4) mm^2, fixed on stubs by conductive tape, and coated with gold and palladium. Samples were observed at an acceleration voltage of 10 kV in backscattered electron mode with a magnification of 4000 × . Images were processed in ImageJ software, version 1.53k (W. Rasband, National Institutes of Health, United States).

2.4. Preparation for and conditions of biological testing

Sterilization: The sterilization of all PPy coatings and PUPPy composites was accomplished by UV radiation for 30 min of each side.

Coating with bio-substances: To enhance the cytocompatibility of PPy coatings and PUPPy composites, solutions of bovine serum albumin (Sigma-Aldrich, USA) (40 mg/mL) and bovine gelatin (Sigma-Aldrich, USA) (0.1 %) in ultrapure water were applied to their surface. Three types of protein coatings were created on PPy coatings on cell culture dishes: 1) 1 mL of albumin solution only (Alb), 2) 1 mL of gelatin solution only (Gel), or 3) 0.5 mL of albumin solution and 0.5 mL of gelatin solution together (Alb/Gel). The last one was also used for coating PUPPy composites. The proteins from the solutions were allowed to adhere to the surfaces for 20 min. Then, the solutions with residual proteins were aspirated and surfaces were allowed to dry at room temperature for at least another 20 min.

Used cell lines: To describe the cytocompatiblity of the composites comprehensively, two cell lines were utilized. First, the mouse fibroblast cell line NIH/3T3 (ECACC 93061524, England) was applied. As a basis for the culture medium for fibroblats, Dulbecco's modified eagle's medium (DMEM) (BioSera, France) and sodium hydrogen carbonate (Penta, Czech Republic) were used. Then, calf serum (BioSera, France) (to the amount of 10 % of the total volume of the medium) and the antibiotics Penicillin/Streptomycin (BioSera, France) at a concentration of 100 μg/mL (to the amount of 1 % of the total volume of the medium with the serum together) were added to the DMEM. The second utilized cell line was the R1 mouse embryonic stem cell line [51]. For the cultivation for embryonic stem cells in an undifferentiated state, a culture medium based on DMEM (Gibco™, USA) was used. To the DMEM, the following supplements were added: fetal calf serum (BioSera, France) (to the amount of 16.5 % of the total volume of the medium), the antibiotics Penicillin/Streptomycin (BioSera, France) at a concentration of 100 μg/mL (to the amount of 1 % of the total volume of the medium with the serum together), 100 mM of non-essential amino acids (Gibco™, USA), 0.05 mM β-mercaptoethanol (Sigma-Aldrich, USA), and leukemia inhibitory factor (Chemicon, USA) at a concentration of 5 ng/mL.

Cell cultivation: Cells were cultivated in a biological incubator HERAcell 150i (Thermo Scientific, USA) with a controlled atmosphere of 5 % CO_2, temperature 37 °C, and constant relative humidity. Fibroblasts or embryonic stem cells at a concentration of 1 × 10^5 cells/mL of complete culture medium were seeded onto the surface of the PU mats, PUPPy composites, and references. As references, cell culture dishes were used for fibroblasts; however, for embryonic stem cells, cell culture dishes were gelatinized with 0.1 % porcine gelatin (Sigma-Aldrich, USA) in water. When cells had adhered to the surface (after 2 h), the aliquot part of the medium was added to achieve a volume of 2 mL. The samples with cells were then put in the incubator for 4 d with medium restitution every 2 d.

2.5. Evaluation of biological testing

Optical microscopy: In addition to regular visual checks of the cells, a phase contrast optical microscope (Olympus IX51, Japan) supplemented with a digital camera (Olympus E−450, Japan) was employed to obtain cell proliferation results from coated and seeded cell culture dishes. An optical microscope generally enables the quick and easy observation of living cells; however, the possibility of using it here was limited by the opacity of PU. Therefore, the PU mats and PUPPy composites were analyzed by fluorescence microscopy.

Fluorescence microscopy: Fluorescence microscopy was used for the further determination of cell morphology. Cells grown on the surfaces were rinsed with phosphate-buffered saline (BioSera, France), fixed with 2 mL of 4 % formaldehyde (Penta Chemicals, Czech Republic) in ultrapure water, and then permeabilized by 2 mL of 0.5 % Triton X 100 (Sigma-Aldrich, USA) in phosphate-buffered saline. Finally, the cells were stained with two fluorescent dyes: 1) ActinRed 555 or ActinGreen 488 (Life Technologies, USA) (1 drop/mL), which binds to the proteins in cytoskeletons, and 2) Hoechst 33258 (Sigma-Aldrich, USA) (20 μL/mL), which penetrates the nuclei where it binds to the DNA. The stained cells were observed by an Olympus IX 81 phase-contrast inverted fluorescence microscope (Olympus, Japan) with a Leica DFC480 camera (Leica Microsystems, Japan).

Quantification using CellProfiler software: Since all PUPPy composites had a unified surface area of (22 × 22) mm^2, it was

possible to perform a proper quantification of grown cells. As references, pre-cut bottoms of cell culture dishes with the same (22 × 22) mm^2 surface area were used. After 2 d of mouse fibroblast cultivation, the cells were fixed, stained, and photographed using the fluorescence microscope. Forty images of cell nuclei with 40 × magnification were manually acquired from the surface of each observed sample for further quatification. Five images of cytoskeletons and five images of cell nuclei with 100 × magnification were acquired from the surface of each observed sample for further morphology qualification. Image analysis was then performed using the open-access CellProfiler software 4.0.7 [52]. For the identification of stained nuclei and cytosceletons, the images were converted to grayscale, and any white regions caused by structural inequalities were excluded.

3. Results and discussion

3.1. Synthesis and characterization of PPy coatings

As commonly known and understood, the chemical synthesis is facile and relativelly quick procedure for producing CPs. The rate of chemical reaction can be, however, modified by several variables, such as the type and concentration of the oxidation agent, presence of dopants, change of temperature and reaction time [53]. The last factor is crucial, especially in the process of PPy coating synthesis. To create a uniform PPy layer, stopping the polymerization reaction at the right time is essential. Otherwise, PPy aglomerates start to grow as time progresses and break free from the surface, and eventually a poorly adhering powder is created instead of a thin PPy coating.

Topography: The PPy coatings prepared with different oxidation agents and reaction times on cell culture dishes were investigated by AFM. The obtained AFM visualization (Fig. 1) shows PPy particles within the thin coating layer that grow in size as the chemical reaction progresses. Coatings prepared at longer reaction times are difficult to observe by AFM, because the movement of detached particles causes defects in the pictures. This phenomenon was significantly worse in PPy coatings prepared using APS. The reason lies in the considerably higher reaction rate of the polymerization initiated by APS.

The fact that the topography of PPy coatings depends on the reaction time is also supported by the roughness analysis, as shown in Table 1. The R_z parameter, which represents the height difference between the highest and the lowest points of the surface, increases gradually with the reaction time length. This dependence is valid for both PPy^{APS} and PPy^{FeCl3}. The average surface roughness parameter R_a is also the lowest for both PPy coatings prepared in the shortest time (t_1) of 15 s. Also when comparing the measured values, the surface roughness of PPy^{APS} is significantly higher than that of PPy^{FeCl3}, which corresponds to the discussion of the AFM images in Fig. 1.

Based on these results, it is clear that the most uniform coating is obtained by the shortest reaction time. Since this setting has the greatest potential for further studies, the following experiments and measurements were performed on PPy coatings synthesized with the reaction time $(t_1) = 15$ s only. These PPy coatings on cell culture dishes were further studied to better understand their physiological properties and to distinguish between the effects of two various oxidizing agents.

Thickness: The PPy coatings were prepared with different oxidation agents on cell culture dishes with an attached silicon mask used to create clean edges observable by AFM. As can be seen in Fig. 2, AFM profilometry indicated the PPy^{APS} and PPy^{FeCl3} coatings to have different thicknesses. The former, PPy^{APS} coating, has the thickness of approximately 50 nm, while the later, PPy^{FeCl3} coating, is about 30 nm thick.

Specific conductivity: Conductivity measurements on PPy coatings deposited on cell culture dishes prepared with various oxidation agents (reaction time (t_1) 15 s) were performed by the four-point van der Pauw method, which is a commonly used technique for measuring the resistivity and conductivity of thin film or sheet-like samples [54–56]. Results of this measurement are strongly

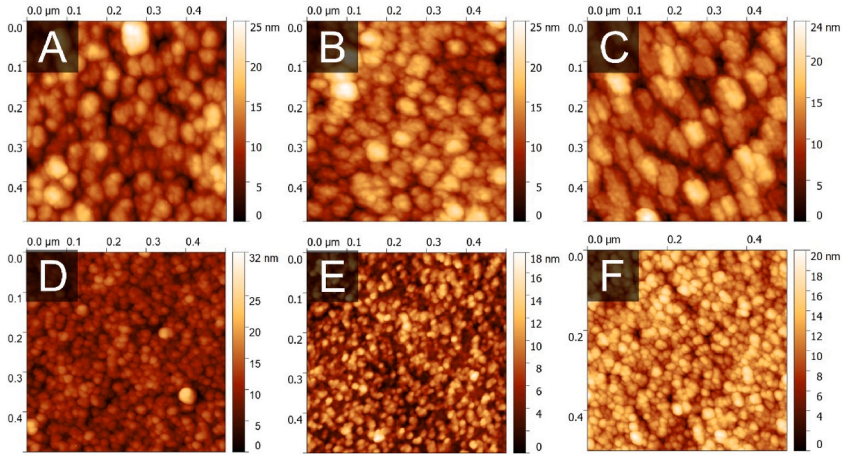

Fig. 1. AFM of PPy coatings on cell culture dishes (0.5 × 0.5) μm^2. PPy^{APS} (up A to C), PPy^{FeCl3} (down D to F). Reaction times: (t_1) 15 s (left column), (t_2) 30 s (middle column), (t_3) 60 s (right column).

Table 1
Roughness analysis of PPy^{APS} and PPy^{FeCl3} coatings prepared in (t_1) 15 s, (t_2) 30 s, and (t_3) 60 s. The errors represent standard deviations.

	(t_1) 15 s		(t_2) 30 s		(t_3) 60 s	
	R_a [nm]	R_z [nm]	R_a [nm]	R_z [nm]	R_a [nm]	R_z [nm]
PPy^{APS}	2.26 ±0.04	12.8 ±1.4	2.6 ±0.3	14.0 ±1.7	2.52 ±0.17	16.5 ±0.4
PPy^{FeCl3}	1.79 ±0.13	9.4 ±0.7	1.92 ±0.11	10.9 ±0.6	1.87 ±0.04	11.7 ±0.3

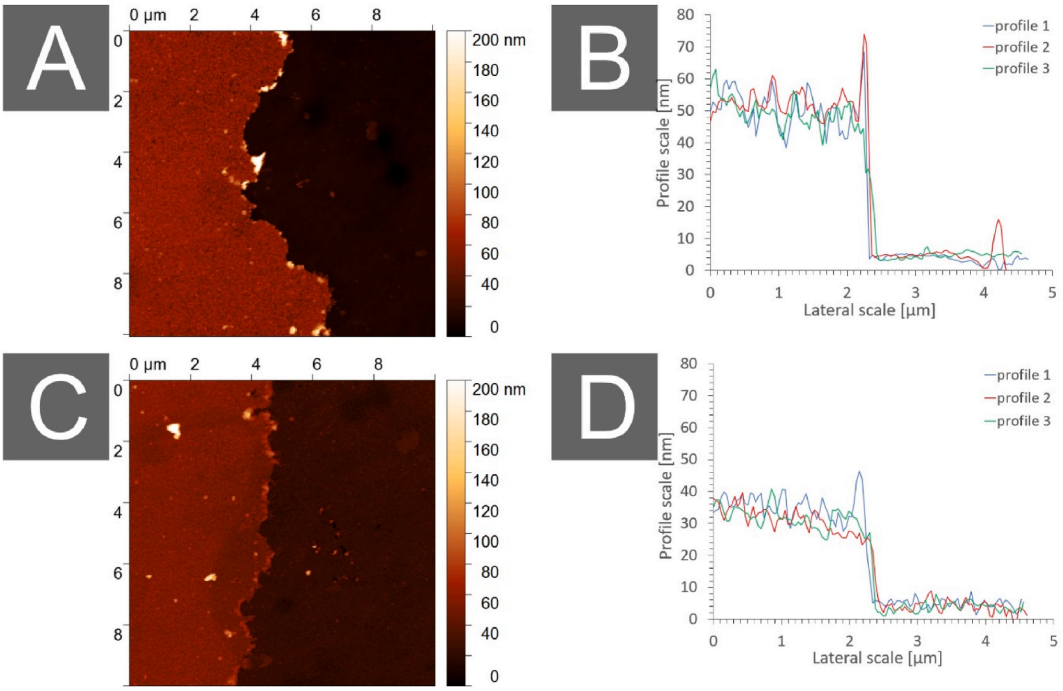

Fig. 2. AFM profilometry of the edges of PPy coatings on cell culture dishes (10 × 10) µm². PPy^{APS} (A,B), PPy^{FeCl3} (C,D). Reaction time: (t_1) 15 s.

dependent on the coating thickness, so it was necessary to calculate the actual measured thicknesses from Fig. 2 to obtain comparable data and that highlighted some differences. According to the results, PPy^{APS} demonstrated higher specific conductivity, concretely 85.03 ± 0.05 S/cm, in comparison to PPy^{FeCl3}, which had a specific conductivity of 67.22 ± 0.01 S/cm.

In general, the conductivity of PPy strongly depends on many factors (discussed in the introduction), mainly the synthesis method, conditions, and especially doping. Therefore, thin PPy layers prepared through chemical synthesis of monomer and oxidant exhibit conductivity in a wide range from zero or very low conductivity (~10^{-10} S/cm) to nearly 2 × 10^3 S/cm [47,53,54,57–59].

Surface free energy: The contact angles measured on PPy coatings on cell culture dishes prepared with various oxidation agents for the reaction time (t_1) 15 s are shown in Table 2. On both PPy^{APS} and PPy^{FeCl3}, water contact angles were slightly above the Berg limit of $\sigma = 65°$ [60,61]; thus, both may be considered mildly hydrophobic. The results further indicate very close values for the total surface energy (γ^{TOT}) of all samples: 43.9 ± 2.0 mJ/m² for PPy^{FeCl3}, and 44.5 ± 0.9 mJ/m² for PPy^{APS}. However, the dispersive Lifshitz-van der Waals component (γ^{LW}) and the polar acid-base component (γ^{AB}) showed variations of around 6 mJ/m². In both cases, the electron-acceptor parameter (γ^{+}) was almost negligible. On the other hand, the electron-donor parameter (γ^{-}) was twice as high for PPy^{FeCl3} – in numerical values, 16.0 ± 2.5 mJ/m².

Table 2
Contact angles and surface free energy of PPy^{APS} and PPy^{FeCl3} coatings on cell culture dishes prepared in (t_1) 15 s. The errors represent standard deviations.

	Contact angles σ = [deg]			Surface energy components γ = [mJ/m²]				
	water	ethylene glycol	diiodo-methane	γ^{TOT}	γ^{LW}	γ^{AB}	γ^{+}	γ^{-}
PPy^{APS}	70±8	30.3±1.7	44.1±0.7	44.5±0.9	37.5±0.4	7.0±0.8	1.6±0.8	8±4
PPy^{FeCl3}	67±3	41±3	32.0±1.4	44±2	43.4±0.4	0.5±1.7	0.00±0.06	16±3

FTIR spectra: FTIR spectroscopy was performed to confirm the successful polymerization of PPy. Since cell culture dishes are made of polystyrene which is unsuitable for FTIR spectroscopy, ITO glass was used as a substrate for the PPy coating. As shown in Fig. 3, the FTIR spectra of PPy obtained in reflection mode on an ITO substrate prepared *in situ* using APS or $FeCl_3$ oxidant for the reaction time (t_1) 15 s are weak, but practically identical to the spectrum of granular PPy dispersed in KBr used as a reference. They exhibit bands situated at 1543 cm^{-1} (C–C stretching vibrations in the pyrrole ring), at 1454 cm^{-1} (C–N stretching vibrations in the ring), the broad band with a maximum at about 1305 cm^{-1} (C–H or C–N in-plane deformation modes), and a maximum at 1166 cm^{-1} (breathing vibrations of the pyrrole rings). The band at 1042 cm^{-1} corresponds to C–H and N–H in-plane deformation vibrations, while the peaks with maxima at about 894 and 786 cm^{-1} correspond to the C–H out-of-plane deformation vibrations of the ring [62].

3.2. Cytocompatibility optimization of PPy coatings

Although many studies report PPy to be a cytocompatible material [5,63], this study shows its limitations. The cell response to polymer surface may be negatively affected by its hydrophobicity [34] and low values of the electron-donor component of free surface energy [64]. These features of PPy coatings may be controlled through different factors, such as the used oxidizing agents and dopants, the conditions of synthesis, and post-synthesis fate. In this study, the resulting water contact angles for both PPy^{APS} and PPy^{FeCl3} (Table 2) were decreased almost down to the Berg limit of $\sigma = 65°$ [60,61]. As shown in Fig. 4 B and F, NIH/3T3 mouse fibroblasts tended to die on these PPy surfaces. Slightly better cytocompatibility was observed on PPy^{FeCl3} which has somewhat higher electron-donor component (Table 2); however, the results were still not sufficient for successful cell adhesion and proliferation.

According to Satriano et al. (2003), the presence of serum proteins reduces the impact of the electron-donor component and the cell response is rather dependent on the total value of the surface free energy [64]. Furthermore, Azioune et al. (2002) report that electrochemically synthesized PPy films (with values of surface free energy components close to ours) demonstrate hydrophobic interactions with human serum albumin and that such PPy films strongly adsorb proteins [20].

Therefore, the PPy coatings prepared on cell culture dishes with the reaction time (t_1) 15 s were further biofunctionalized by the adhesion of selected bio-substances Alb and Gel as these change the biological activity of the treated surface [35,65]. As the results in Fig. 4 show, the presence of Alb or Gel on the PPy-coating increased its cytocompatibility; however, the combination of both Alb/Gel together led to the most significant cytocompatibility improvement. These positive results, which were likely achieved due to functional carboxyl and amino groups of proteins and peptides, comply with studies by Wu et al. (2020) [66] and Van Vlierberghe et al. (2011) [67], which confirmed the biocompatibility and cell-interactive properties of albumin and gelatin.

3.3. Anisotropy of PUPPy composites

Further in this study, **PPy^{FeCl3}** and **Alb/Gel** were used to coat electrospun PU fibrous mats to prepare cytocompatible PUPPy composites with controlled conductivity and topography at the same time. Modification and control of topography can improve material bioactivity as it imitates natural cellular environment. In the case of nanofibrous scaffolds, the uniaxial orientation of fibers can be advantageous since the extracellular matrix of soft tissues are mostly anisotropic, except for, for example, the basal lamina. Nevertheless, attention should also be paid to mechanical anisotropy, which increases with fiber alignment [68].

The orientation of fibers in native electrospun PU mats is random, which makes the substrate isotropic. To obtain the uniaxial orientation of fibers, the PU mats were stretched by hand over a 150 °C heat source. After cooling in the stretched state, the PU mats retain their fibre orientation even after the stretching force is removed. The SEM and AFM images of the PUPPy composites presented in Fig. 1 show the effectiveness of this modification. As can be seen, the isotropic PUPPy composites (Fig. 5 A, C, E) consist of randomly oriented fibers. Topographic measurements of their cross-sections showed that irregularities of up to 3 μm in size were formed on the

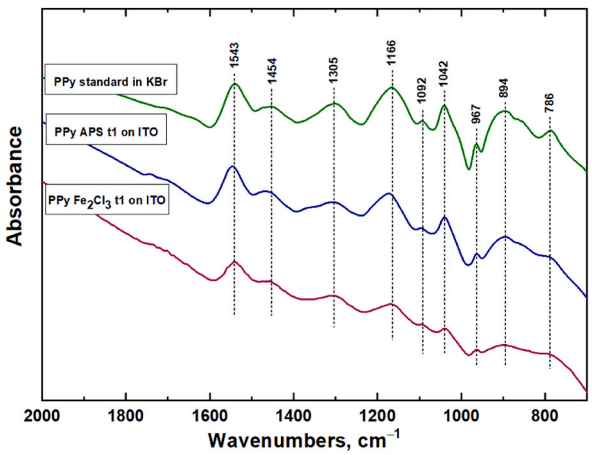

Fig. 3. FTIR spectra of PPy obtained in reflection mode on ITO support prepared *in situ* using APS or $FeCl_3$ oxidant for the reaction times (t_1) 15 s. The spectrum of granular PPy dispersed in KBr is included for comparison.

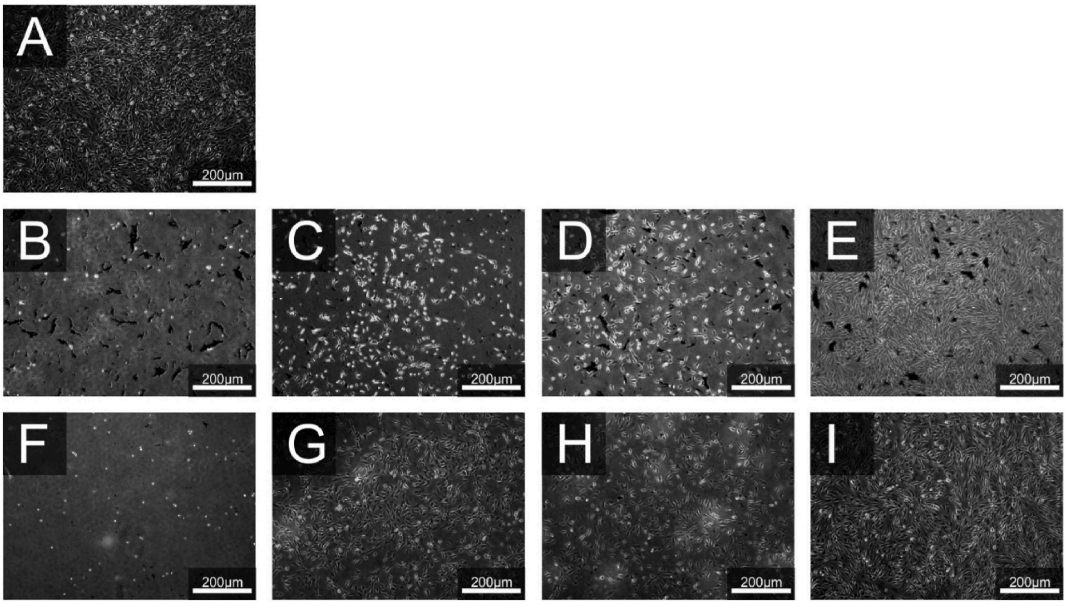

Fig. 4. Optical microscopy images of NIH/3T3 mouse fibroblasts cultivated on PPy-based coatings on cell culture dishes: (**A**) Reference, (**B**) PPy^{APS}, (**C**) PPy^{APS} with Alb, (**D**) PPy^{APS} with Gel, (**E**) PPy^{APS} with Alb/Gel, (**F**) PPy^{FeCl3}, (**G**) PPy^{FeCl3} with Alb, (**H**) PPy^{FeCl3} with Gel, (**I**) PPy^{FeCl3} with Alb/Gel. Reference cells were cultivated in cell culture dishes. All the images were captured after 72 h of cell culture at magnification 40 × .

surface, while the fiber diameter was approximately 0.5 μm. In contrast, fibers in the anisotropic PUPPy composites (Fig. 5 B, D, F) appear to be highly oriented, the heights of topographic features remaining similar. The surface roughness analysis also showed no significant differences between isotropic and anisotropic PUPPy. The roughness parameters of isotropic PUPPy were R_a = (0.38 ± 0.02) nm and R_z = (2.16 ± 0.09) nm, while anisotropic PUPPY had R_a = (0.31 ± 0.03) nm and R_z = (2.4 ± 0.3) nm. In general, although some fibers were torn after the manual stretching, the majority of the fibers lie in one direction. Therefore, this quick and easy way of aligning fibers may be considered successful.

3.4. Cytocompatibility of PUPPy composites

The impact of iso/anisotropic properties and conductivity on the morphology of NIH/3T3 mouse fibroblasts and R1 mouse embryonic stem cells was observed by means of fluorescence microscopy.

Fig. 6 shows how PPy coatings (with Alb/Gel) and fiber alignment affect the mouse fibroblast NIH/3T3 cell line. The effect of fiber orientation on the cytoskeleton is significant. Cells grown on isotropic PU mats (Fig. 6 B) primarily show a stellate-like morphology, similar to the shapes of fibroblasts cultivated as the reference in cell culture dishes (Fig. 6 A). In contrast, cells grown on anisotropic PU mats (Fig. 6 C) adopt distinctly prolonged shapes in the exact direction of the orientation of fibers. Further, many of these cells also possess elongated nuclei compared to the rounded cell nuclei on isotropic PU mats.

These results confirm the claim made by Yin et al. (2010) that cells respond to fiber orientation with cytoskeletal changes and the elongation of nuclei [43]. The explanation probably lies in contact guidance and cell-matrix interactions, whose amounts and distributions are influenced by the nanofiber alignment, which plays an important role in regulating cell functions, including proliferation and migration (distribution).

With respect to the conductive surface coating, it also significantly influences cell morphology, as can be seen, for example, in the case of isotropic PUPPy composites (Fig. 6 D). Cell cytoskeletons preferably assume rounded and lenticular shapes with a random direction because of the randomly oriented fibers in the substrate; the nuclei of these cells are classically rounded. The observed rounding of the fibroblast cytoskeletons may have been due to altered focal adhesion dynamics or cytoskeletal remodeling in response to the conductive coating of PPy. However, it should be noted that other factors, such as the change in the physical and mechanical properties of the PU substrate after coating with PPy and Alb/Gel, may also have an influence. The composition and distribution of the proteins bound to the substrate surface can affect the morphology of various cell lines [69]. The cultivation of fibroblasts on anisotropic PUPPy composites (Fig. 6 E) leads apparently to more spindle-shaped cytoskeletons; however, the surface coating prevents nuclei elongation; nevertheless, the orientation of cells is still according to the fiber orientation. In addition, it can be observed a reduction in protrusion formation in fibroblasts seeded on PUPPy composites. This may indicate a modulation of cell motility towards a more targeted and controlled behavior that is essential for processes in tissue regeneration and wound healing.

To determine the impact of the prepared PU mats and PUPPy composites on NIH/3T3 mouse fibroblast proliferation, a comparative quantitative assay was conducted. An analysis of 200 images was performed using CellProfiler software [52]. The results are shown in Fig. 7. As can be seen in the graph, the cells proliferated least on the isotropic PU mat (0.22), while on the anisotropic PU mat (0.87),

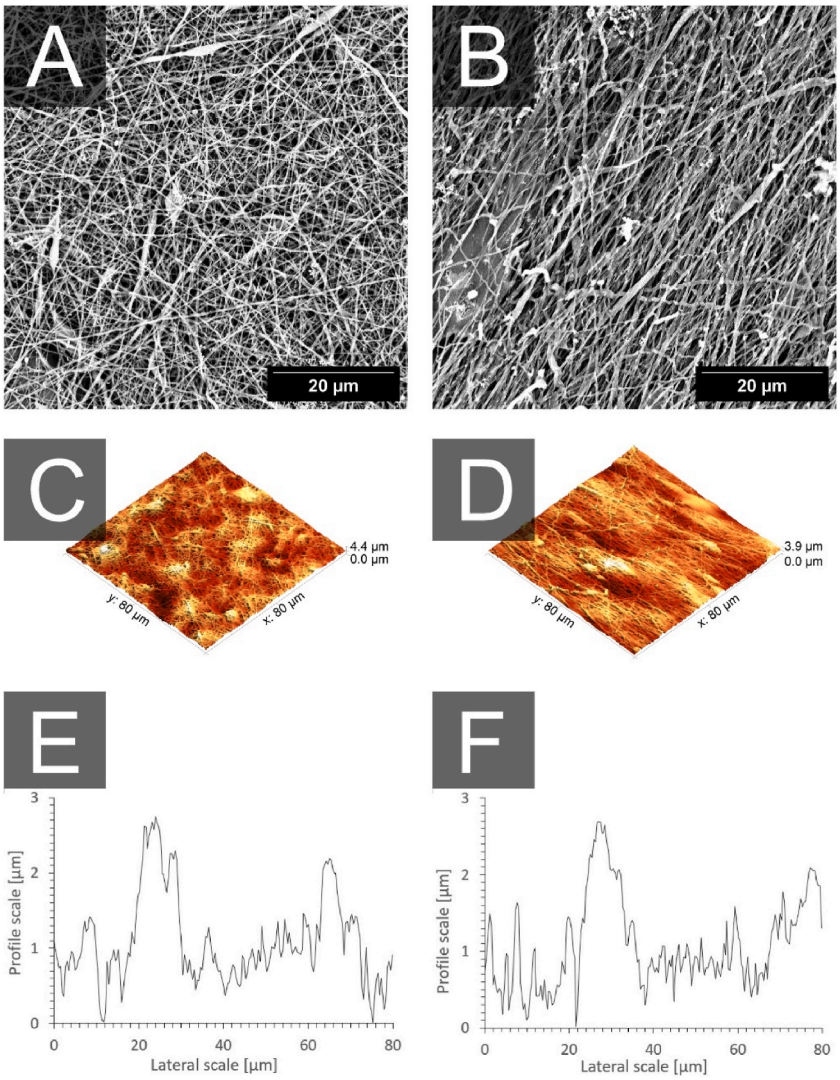

Fig. 5. Surface characterization of PUPPy composites: (**A, C, E**) Isotropic form with randomly oriented fibers; (**B, D, F**) Anisotropic form with uniaxially oriented fibers; (**A, B**) SEM images; (**C, D**) AFM images; (**E, F**) Profile sections.

the relative cell viability was comparable to the reference (1.00). It thus seems that the alignment of fibers itself has a significant impact on fibroblast well-being. On the other hand, the PPy^{FeCl3} coating with Alb/Gel used to create PUPPy composites removed this dependence, as cell viability was the same on both isotropic and anisotropic PUPPy composites (0.62). From this it can be concluded that the conductive PPy coating provides a uniform semi-favorable surface for fibroblast proliferation irrespective of the substrate underneath. This ensures a controlled and homogeneous cell spreading and attachment and thus the formation of a more stable cell network, similarly to the article by Tringides and Mooney (2024), where the formation of a uniform cell network was achieved with increased conductivity of their hydrogel scaffolds [70]. The results were verified using a one-way ANOVA with post-hoc Tukey's test, which showed whether the means of the measured values were statistically significantly different at the levels of significance $p \leq 0.05$ (*), $p \leq 0.01$ (**), or $p \leq 0.001$ (***).

In addition to the quantitative assay, a qualitative analysis of 50 images of NIH/3T3 mouse fibroblasts was also carried out using CellProfiler software [52]. Results in the form of four graphs are shown in Fig. 8, together with an explanatory scheme of crucial cell characteristics. First, each observed object (a cell or a nucleus) was translated into the best-fitting ellipse with the same second moments and statistical properties as the original area. The morphology of the cells, especially their elongation (Fig. 8 B), was then depicted by the length of the major and minor axes of the best-fitting ellipse and their comparison. The resulting median values of the measured cells clearly show that the fibroblasts grown on the anisotropic PU mat possessed the most prolonged shapes - the greatest lengths (major axes) and the thinnest widths (minor axes). In contrast, a comparatively rounded cell morphology was induced by PPy coatings, as may be observed for both the isotropic and anisotropic PUPPy composites.

The orientation of cells (Fig. 8 C) is displayed as an angle, written as θ in the explanatory scheme, between the x-axis and the major

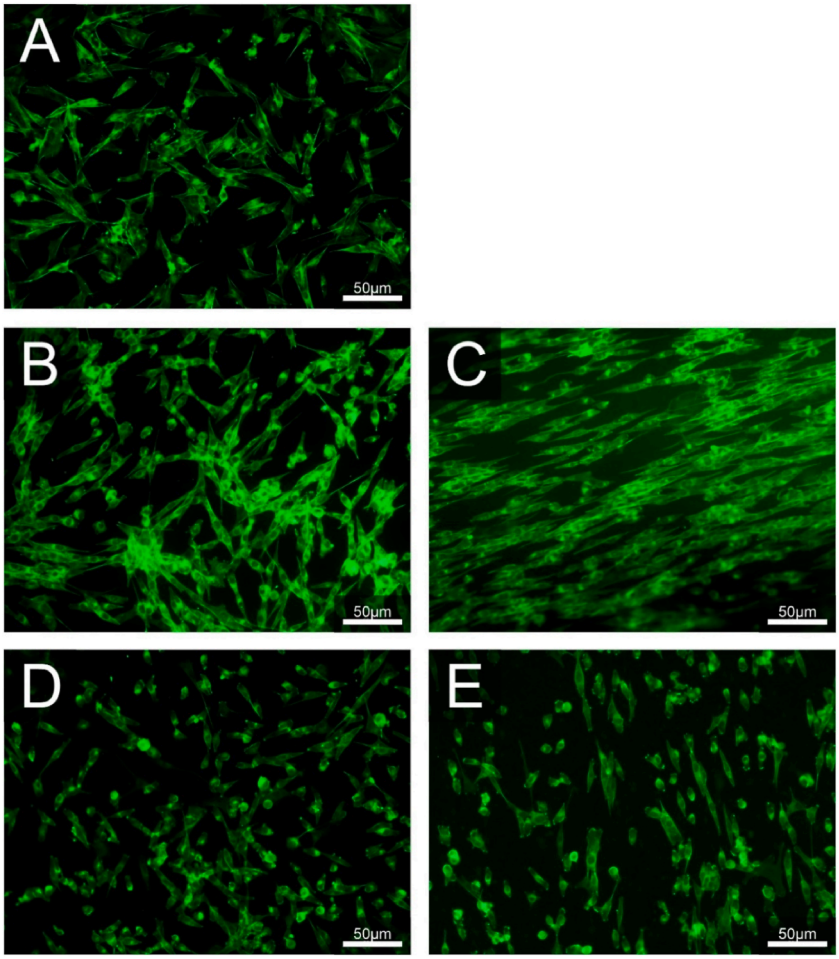

Fig. 6. Fluorescence microscopy images of NIH/3T3 mouse fibroblasts cultivated on: (**A**) Reference; (**B**) isotropic PU mat; (**C**) anisotropic PU mat; (**D**) isotropic PUPPy composite with Alb/Gel; (**E**) anisotropic PUPPy composite with Alb/Gel. Reference cells were cultivated in cell culture dishes. Green color: ActinGreen – actin. Magnification: 100 × . (For interpretation of the references to color in this figure legend, the reader is referred to the Web version of this article.)

axis of the best-fitting ellipse. For example, reference fibroblasts cultivated in cell culture dishes show random orientations, meaning randomly various angles from $-\pi/2$ to $+\pi/2$, which lead to a median close to 0 with a wide deviation. Very similar values were also obtained for cells grown on all other substrates except one – the anisotropic PU mat. Here, most cells were oriented uniaxially along the fiber direction, resulting in a given orientation and a very small standard deviation.

The morphology of cell nuclei (Fig. 8 E) was also analyzed. In the graph, the nucleus shape is described by an eccentricity defined as the ratio of the distance between the foci, written as F_1 and F_2 in the explanatory scheme, of the best-fitting ellipse and its major axis length. Values can vary from 0 (an ideal circle) to 1 (a line segment). As can be seen, the observed cells have relatively elongated nuclei, as is usual for fibroblasts – however, some more than others. Anisotropic PU mats established nuclei with higher eccentricity (0.73) than other observed substrates (around 0.63). These results suggest a correlation in the elongation of cell cytoskeleton and nuclus. The analysis of nuclei orientation (Fig. 8 F) was consistent with the orientation of cells (Fig. 8 C). This implies that the PPy coating prevented both the elongation and uniaxial orientation of fibroblasts and their nuclei.

All these outputs of the qualitative analysis of fibroblasts are in accordance with the morphological differences observed by fluorescence microscopy described in Fig. 6. The results were verified using one-way or two-way ANOVA tests with post-hoc Tukey's test, which showed whether the means of the measured values were statistically significantly different at the levels of significance $p \leq 0.05$ (*), $p \leq 0.01$ (**), or $p \leq 0.001$ (***).

Images of mouse embryonic stem cells cultivated on PU mats and PUPPy composites are shown in Fig. 9. No significant differences in cell behavior were found on any of the tested samples. Cells did not differ in proliferation, managed to survive in an undifferentiated state (in the presence of a medium containing leukemia inhibitory factor), and did not tend to grow apart on the surface at all; contrarywise, they clustered. Embryonic stem cells typically form dense clusters of various sizes and shapes when cultured in cell culture dishes (Fig. 9 A). The same behaviour of embryonic stem cells was observed on all tested substrates (Fig. 9 B – E). Clusters of

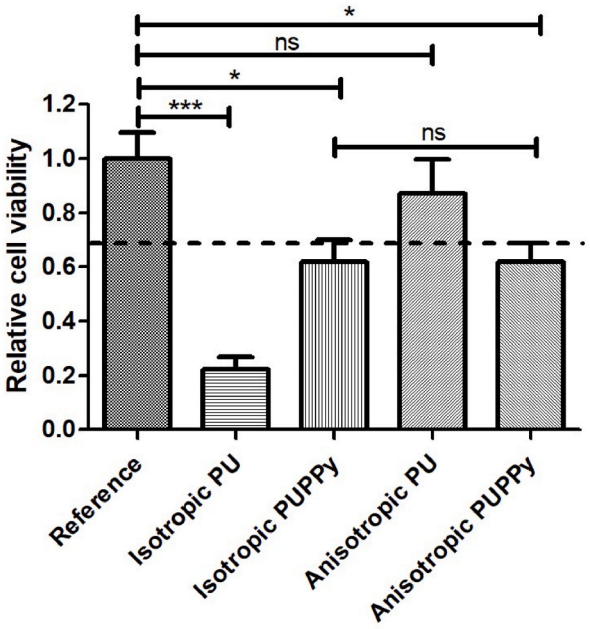

Fig. 7. Results of image analyses performed by CellProfiler software referring to the cytocompatibility of iso/anisotropic PU mats and PUPPy composites with the NIH/3T3 mouse fibroblast cell line. Reference cells were cultivated in cell culture dishes. Error bars show standard error of mean. One-way ANOVA with post-hoc Tukey's test: ns = $p > 0.05$, * = $p \leq 0.05$, *** = $p \leq 0.001$.

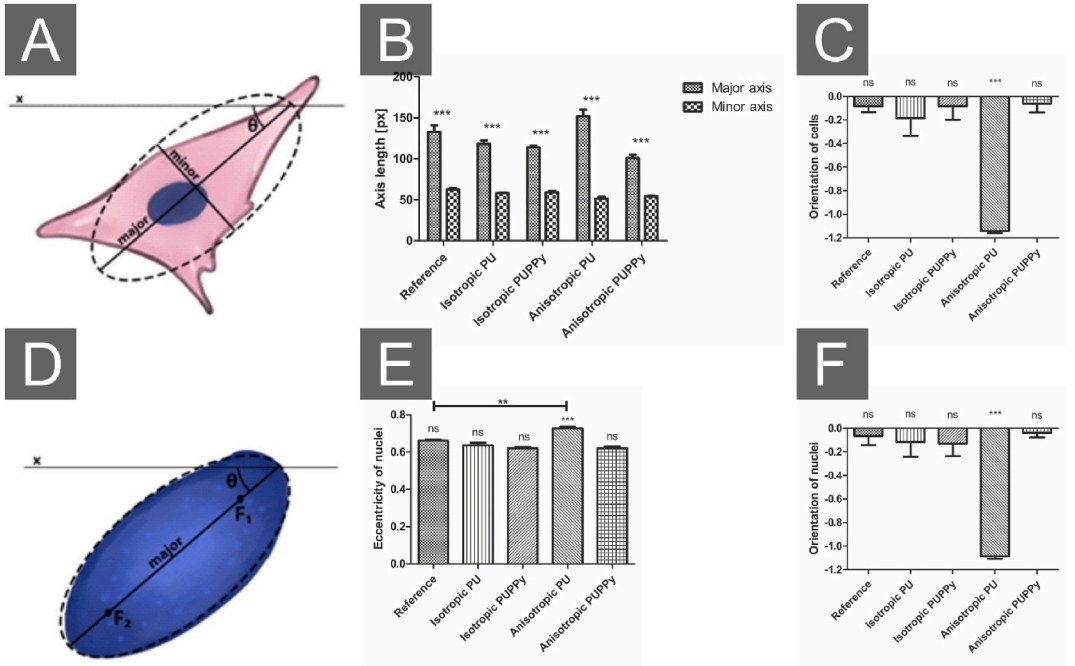

Fig. 8. Results of image analyses performed by CellProfiler software referring to NIH/3T3 mouse fibroblasts cultivated on iso/anisotropic PU mats and PUPPy composites. Explanatory schemes of calculated characteristics related to: (A) cells, (D) nuclei. Graphs: (B) morphology of cells, (C) orientation of cells, (E) eccentricity of nuclei, and (F) orientation of nuclei. Reference cells were cultivated in cell culture dishes. Error bars show standard error of mean. Two-way ANOVA for (B) and one-way ANOVA for (C, E, F) with post-hoc Tukey's test: ns = $p > 0.05$, ** = $p \leq 0.01$, *** = $p \leq 0.001$.

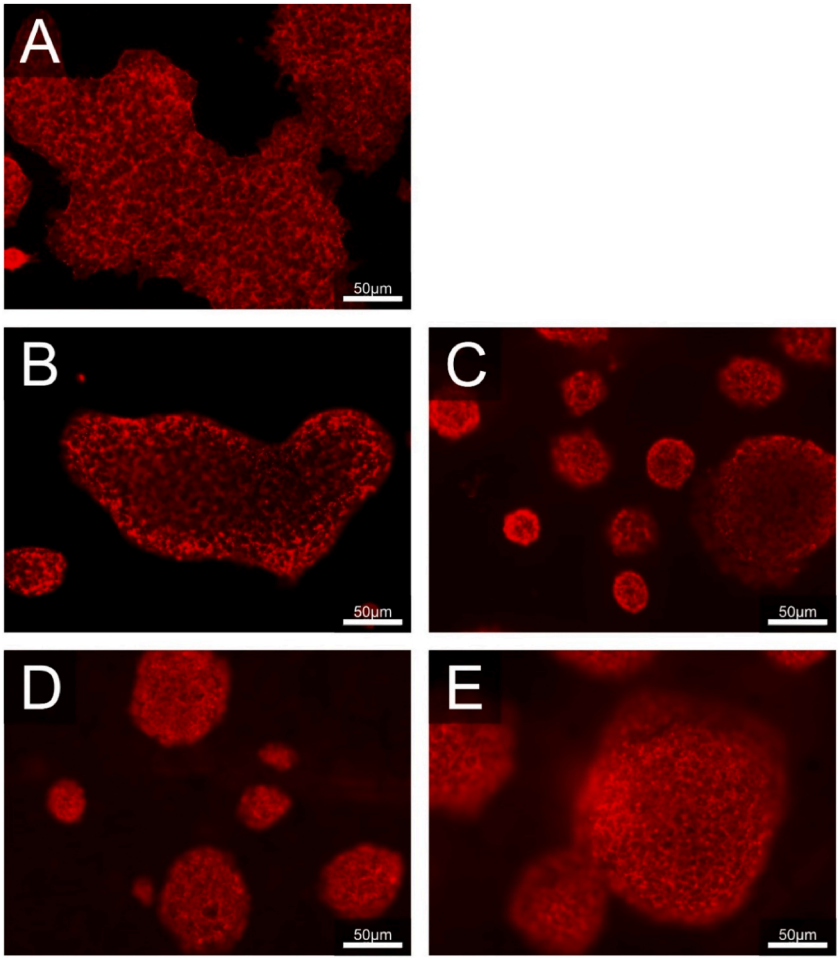

Fig. 9. Fluorescence microscopy images of R1 mouse embryonic stem cells cultivated on: (**A**) Reference; (**B**) isotropic PU mat with Alb/Gel; (**C**) anisotropic PU mat with Alb/Gel; (**D**) isotropic PUPPy composite with Alb/Gel; (**E**) anisotropic PUPPy composite with Alb/Gel. Reference cells were cultivated in cell culture dishes. Red color: ActinRed – actin. Magnification: 100 × . (For interpretation of the references to color in this figure legend, the reader is referred to the Web version of this article.)

different shapes and sizes were observed on each of them, regardless of the presence or absence of anisotropy or the PPy coating. In general, neither the fiber orientation nor the conductive PPy coating had a visible impact on the morphology of embryonic stem cells. The inert response of undifferentiated stem cells indicates that the coating can be applied without inducing unwanted differentiation or altering the basic properties of stem cells and suggests that the used coatings do not interfere with the fundamental stem cell characteristics, thus preserving their stemness.

4. Conclusions

This work presents a simple and fast *in situ* PPy coating technique applicable to different types of substrates. Here presented chemical synthesis of the coatings conducted at room temperature in an aqueous solution takes only a few seconds and does not require stabilizers or other modifiers. The findings demonstrate that the earlier the polymerization procedure is terminated, the more uniform PPy layer is produced. Furthermore, PPy coatings produced in 15 s retain good conductivity. Variations in PPy coatings were observed depending on the oxidizing agent utilized (APS vs $FeCl_3$). The coatings varied in conductivity, roughness, and thickness. On the other hand, both PPy^{APS} and PPy^{FeCl3} coatings showed limitations in their cytocompatibility, which was affected by their surface free energies. This limitation is however eliminated by techniques commonly used in cell cultures, coating with Alb/Gel.

Anisotropy, another factor influencing material/cell interactions, was introduced to PPy coating by its deposition on electrospun nonwoven nanofiber PU mats with manually uniaxially oriented fibers. The fiber alignment showed a significant effect on the morphology of mouse fibroblasts. Proven by cell image analyses, not only cytoskeletons but also cell nuclei demonstrated elongated shapes with uniform orientation strictly along the fibers. The PPy coating with Alb/Gel on the anisotropic PU mat suppresses fiber alignment's impact on fibroblast morphology while ensuring a uniform surface, crucial for tissue regeneration and wound healing

processes. Neither the coating nor fiber alignment visibly affects mouse embryonic stem cell behavior, preserving their fundamental properties without inducing unwanted differentiation.

The results of this study highlight the importance of the reaction time in the *in situ* synthesis of PPy coatings. Furthermore, it also deepens the current understanding of the impacts of polymer surface properties on cell behavior and hence contributes to the optimization of scaffold design with respect to achieving the growth of specific cells/tissues.

CRediT authorship contribution statement

Leona Mahelová: Writing – review & editing, Writing – original draft, Visualization, Software, Methodology, Investigation, Formal analysis, Data curation, Conceptualization. **Petr Slobodian:** Resources, Investigation. **Karolína Kocourková:** Investigation. **Antonín Minařík:** Investigation. **Robert Moučka:** Investigation. **Miroslava Trchová:** Investigation. **Martina Martínková:** Methodology. **Kateřina Skopalová:** Methodology. **Zdenka Víchová:** Methodology, Funding acquisition. **Věra Kašpárková:** Writing – review & editing, Validation, Supervision, Methodology. **Petr Humpolíček:** Writing – review & editing, Writing – original draft, Visualization, Validation, Supervision, Resources, Project administration, Methodology, Funding acquisition, Formal analysis, Data curation, Conceptualization.

Declaration of competing interest

The authors declare that they have no known competing financial interests or personal relationships that could have appeared to influence the work reported in this paper.

Acknowledgments

The authors acknowledge the support by the Czech Science Foundation (23-07425S). The project of Ministry of Education, Youth and Sports of the Czech Republic – DKRVO (RP/CPS/2022/001 and RP/CPS/2022/007) and Internal Grant Agency of Tomas Bata University in Zlín, Czech Republic (IGA/CPS/2024/007) are also acknowledged. The authors thank Ing. Daniela Minaříková, Ph.D. for her contribution to the preliminary study of polypyrrole thin films.

References

[1] M. Gajendiran, et al., Conductive biomaterials for tissue engineering applications, J. Ind. Eng. Chem. 51 (2017) 12–26, https://doi.org/10.1016/j.jiec.2017.02.031. Jul.
[2] G. Shi, M. Rouabhia, Z. Wang, L.H. Dao, Z. Zhang, A novel electrically conductive and biodegradable composite made of polypyrrole nanoparticles and polylactide, Biomaterials 25 (13) (2004) 2477–2488, https://doi.org/10.1016/j.biomaterials.2003.09.032. Jun.
[3] J. Huang, et al., Electrical stimulation to conductive scaffold promotes axonal regeneration and remyelination in a rat model of large nerve defect, PLoS One 7 (6) (2012) e39526, https://doi.org/10.1371/journal.pone.0039526. Jun.
[4] L. Mohammadi Amirabad, et al., Enhanced cardiac differentiation of human cardiovascular disease patient-specific induced pluripotent stem cells by applying unidirectional electrical pulses using aligned electroactive nanofibrous scaffolds, ACS Appl. Mater. Interfaces 9 (8) (2017) 6849–6864, https://doi.org/10.1021/acsami.6b15271. Mar.
[5] X. Wang, et al., Evaluation of biocompatibility of polypyrrole in vitro and in vivo, J. Biomed. Mater. Res. 68A (3) (2004) 411–422, https://doi.org/10.1002/jbm.a.20065.
[6] D. d Ateh, H. a Navsaria, P. Vadgama, Polypyrrole-based conducting polymers and interactions with biological tissues, J. R. Soc. Interface 3 (11) (2006) 741–752, https://doi.org/10.1098/rsif.2006.0141. Dec.
[7] P. Humpolicek, et al., The biocompatibility of polyaniline and polypyrrole: a comparative study of their cytotoxicity, embryotoxicity and impurity profile, Mater. Sci. Eng., C 91 (2018) 303–310, https://doi.org/10.1016/j.msec.2018.05.037. Oct.
[8] K. Skopalova, et al., Modulation of differentiation of embryonic stem cells by polypyrrole: the impact on neurogenesis, Int. J. Mol. Sci. 22 (2) (2021) 501, https://doi.org/10.3390/ijms22020501. Jan.
[9] N. Ferraz, M. Strømme, B. Fellström, S. Pradhan, L. Nyholm, A. Mihranyan, In vitro and in vivo toxicity of rinsed and aged nanocellulose–polypyrrole composites, J. Biomed. Mater. Res. 100A (8) (2012) 2128–2138, https://doi.org/10.1002/jbm.a.34070.
[10] S.P. Armes, Optimum reaction conditions for the polymerization of pyrrole by iron(III) chloride in aqueous solution, Synth. Met. 20 (3) (1987) 365–371, https://doi.org/10.1016/0379-6779(87)90833-2. Jun.
[11] J. Duchet, R. Legras, S. Demoustier-Champagne, Chemical synthesis of polypyrrole: structure–properties relationship, Synth. Met. 98 (2) (1998) 113–122, https://doi.org/10.1016/S0379-6779(98)00180-5. Dec.
[12] J. Upadhyay, A. Kumar, B. Gogoi, A.K. Buragohain, Biocompatibility and antioxidant activity of polypyrrole nanotubes, Synth. Met. 189 (2014) 119–125, https://doi.org/10.1016/j.synthmet.2014.01.004. Mar.
[13] P. Keša, et al., Photoacoustic properties of polypyrrole nanoparticles, Nanomaterials 11 (9) (2021), https://doi.org/10.3390/nano11092457. Art. no. 9, Sep.
[14] Ya O. Mezhuev, et al., Synthesis of aqueous polypyrrole dispersions stabilized with polyvinyl alcohol and preparation of hemocompatible films based on them, Russ. J. Appl. Chem. 88 (6) (2015) 1026–1032, https://doi.org/10.1134/S107042721506021X.
[15] A. Pich, Y. Lu, H.-J.P. Adler, Polymeric particles with conjugated polymer: layer on its surface as effective adsorbents of amino acids, Polymer 47 (19) (Sep. 2006) 6536–6543, https://doi.org/10.1016/j.polymer.2006.07.055.
[16] A. Vaitkuviene, et al., Some biocompatibility aspects of conducting polymer polypyrrole evaluated with bone marrow-derived stem cells, Colloids Surf. A Physicochem. Eng. Asp. 442 (2014) 152–156, https://doi.org/10.1016/j.colsurfa.2013.06.030. Feb.
[17] M. Sak-Bosnar, M.V. Budimir, S. Kovac, D. Kukulj, L. Duic, Chemical and electrochemical characterization of chemically synthesized conducting polypyrrole, J. Polym. Sci. Polym. Chem. 30 (8) (1992) 1609–1614, https://doi.org/10.1002/pola.1992.080300813.
[18] A. Razaq, A. Mihranyan, K. Welch, L. Nyholm, M. Strømme, Influence of the type of oxidant on anion exchange properties of fibrous cladophora cellulose/polypyrrole composites, J. Phys. Chem. B 113 (2) (2009) 426–433, https://doi.org/10.1021/jp806517h. Jan.
[19] X. Chen, J.-P. Issi, J. Devaux, D. Billaud, Chemically oxidized polypyrrole: influence of the experimental conditions on its electrical conductivity and morphology, Polym. Eng. Sci. 35 (8) (1995) 642–647, https://doi.org/10.1002/pen.760350803.
[20] A. Azioune, M.M. Chehimi, B. Miksa, T. Basinska, S. Slomkowski, Hydrophobic Protein−Polypyrrole interactions: the role of van der Waals and lewis Acid−Base forces as determined by contact angle measurements, Langmuir 18 (4) (2002) 1150–1156, https://doi.org/10.1021/la010444o. Feb.

[21] A. Azioune, K. Pech, B. Saoudi, M.M. Chehimi, G.P. McCarthy, S.P. Armes, Adsorption of human serum albumin onto polypyrrole powder and polypyrrole-silica nanocomposites, Synth. Met. 102 (1) (1999) 1419–1420, https://doi.org/10.1016/S0379-6779(98)00982-5. Jun.

[22] E.A. Sanches, et al., Nanostructured polypyrrole powder: a structural and morphological characterization, J. Nanomater. 2015 (2015) e129678, https://doi.org/10.1155/2015/129678. Sep.

[23] K.A. Noh, D.-W. Kim, C.-S. Jin, K.-H. Shin, J.H. Kim, J.M. Ko, Synthesis and pseudo-capacitance of chemically-prepared polypyrrole powder, J. Power Sources 124 (2) (2003) 593–595, https://doi.org/10.1016/S0378-7753(03)00813-9. Nov.

[24] B. Ustamehmetoğlu, N. Kizilcan, A.S. Saraç, A. Akar, Soluble polypyrrole copolymers, J. Appl. Polym. Sci. 82 (5) (2001) 1098–1106, https://doi.org/10.1002/app.1944.

[25] C. Biran, L. Toppare, T. Tinçer, Y. Yağci, V. Harabagiu, Mechanical properties of conducting H-type polysiloxane–polypyrrole graft copolymers and polytetrahydrofuran–polypyrrole block copolymers, J. Appl. Polym. Sci. 86 (7) (2002) 1663–1666, https://doi.org/10.1002/app.11031.

[26] O. Gunaydin, L. Toppare, Y. Yagci, V. Harabagiu, M. Pintela, B.C. Simionescu, Synthesis of conducting polysiloxane — polypyrrole graft copolymers, Polym. Bull. 47 (6) (2002) 501–508, https://doi.org/10.1007/s002890200014. Feb.

[27] M. Omastová, et al., Towards conducting inks: polypyrrole–silver colloids, Electrochim. Acta 122 (2014) 296–302, https://doi.org/10.1016/j.electacta.2013.11.037. Mar.

[28] A. Zelenev, W. Sonnenberg, E. Matijević, Preparation, characterization, and adhesion of monodispersed polypyrrole particles, Colloid Polym. Sci. 276 (9) (1998) 838–841, https://doi.org/10.1007/s003960050318. Oct.

[29] S. Káčerová, et al., Biocompatibility of colloidal polypyrrole, Colloids Surf. B Biointerfaces 232 (2023) 113605, https://doi.org/10.1016/j.colsurfb.2023.113605. Dec.

[30] S. Maity, Optimization of processing parameters of in-situ polymerization of pyrrole on woollen textile to improve its thermal conductivity, Prog. Org. Coating 107 (2017) 48–53, https://doi.org/10.1016/j.porgcoat.2017.03.010. Jun.

[31] Q. Zhu, et al., Epoxy coating with in-situ synthesis of polypyrrole functionalized graphene oxide for enhanced anticorrosive performance, Prog. Org. Coating 140 (2020) 105488, https://doi.org/10.1016/j.porgcoat.2019.105488. Mar.

[32] Y. Zhao, et al., A novel flexible sensor for respiratory monitoring based on in situ polymerization of polypyrrole and polyurethane coating, RSC Adv. 7 (78) (2017) 49576–49585, https://doi.org/10.1039/C7RA08331A. Oct.

[33] N. Maráková, et al., Antimicrobial activity and cytotoxicity of cotton fabric coated with conducting polymers, polyaniline or polypyrrole, and with deposited silver nanoparticles, Appl. Surf. Sci. 396 (2017) 169–176, https://doi.org/10.1016/j.apsusc.2016.11.024. Feb.

[34] R. Ravichandran, S. Sundarrajan, J.R. Venugopal, S. Mukherjee, S. Ramakrishna, Applications of conducting polymers and their issues in biomedical engineering, J. R. Soc. Interface 7 (suppl_5) (2010), https://doi.org/10.1098/rsif.2010.0120.focus. Oct.

[35] B. Garner, A.J. Hodgson, G.G. Wallace, P.A. Underwood, Human endothelial cell attachment to and growth on polypyrrole-heparin is vitronectin dependent, J. Mater. Sci. Mater. Med. 10 (1) (1999) 19–27, https://doi.org/10.1023/A:1008835925998. Jan.

[36] P. Slepička, N. Slepičková Kasálková, L. Bačáková, Z. Kolská, V. Švorčík, Enhancement of polymer cytocompatibility by nanostructuring of polymer surface, J. Nanomater. 2012 (2012) e527403, https://doi.org/10.1155/2012/527403. Jul.

[37] C.J. Wilson, R.E. Clegg, D.I. Leavesley, M.J. Pearcy, Mediation of biomaterial–cell interactions by adsorbed proteins: a review, Tissue Eng. 11 (1–2) (2005) 1–18, https://doi.org/10.1089/ten.2005.11.1. Jan.

[38] G.R. Mitchell, A. Tojeira, Role of anisotropy in tissue engineering, Procedia Eng. 59 (2013) 117–125, https://doi.org/10.1016/j.proeng.2013.05.100.

[39] M.E. Hoque, Robust formulation for the design of tissue engineering scaffolds: a comprehensive study on structural anisotropy, viscoelasticity and degradation of 3D scaffolds fabricated with customized desktop robot based rapid prototyping (DRBRP) system, Mater. Sci. Eng. C 72 (Mar. 2017) 433–443, https://doi.org/10.1016/j.msec.2016.11.019.

[40] N. Bursac, K.K. Parker, S. Iravanian, L. Tung, Cardiomyocyte cultures with controlled macroscopic anisotropy, Circ. Res. 91 (12) (2002) e45–e54, https://doi.org/10.1161/01.RES.0000047530.88338.EB. Dec.

[41] M. Nikkhah, F. Edalat, S. Manoucheri, A. Khademhosseini, Engineering microscale topographies to control the cell–substrate interface, Biomaterials 33 (21) (2012) 5230–5246, https://doi.org/10.1016/j.biomaterials.2012.03.079. Jul.

[42] F. Yang, R. Murugan, S. Wang, S. Ramakrishna, Electrospinning of nano/micro scale poly(l-lactic acid) aligned fibers and their potential in neural tissue engineering, Biomaterials 26 (15) (2005) 2603–2610, https://doi.org/10.1016/j.biomaterials.2004.06.051. May.

[43] Z. Yin, et al., The regulation of tendon stem cell differentiation by the alignment of nanofibers, Biomaterials 31 (8) (2010) 2163–2175, https://doi.org/10.1016/j.biomaterials.2009.11.083. Mar.

[44] P. Humpolicek, et al., Polyaniline cryogels: biocompatibility of novel conducting macroporous material, Sci. Rep. 8 (2018) 135, https://doi.org/10.1038/s41598-017-18290-1. Jan.

[45] K.A. Milakin, et al., Biocompatible and antibacterial gelatin-based polypyrrole cryogels, Polymer 197 (2020) 122491, https://doi.org/10.1016/j.polymer.2020.122491. May.

[46] F. Golgovici, M.-S. Cărlan, A.-G. Popescu, L. Anicai, Electrochemical synthesis of polypyrrole and polypyrrole-indomethacin coatings on NiCr alloys involving deep eutectic solvents, Metals 10 (9) (2020), https://doi.org/10.3390/met10091130. Art. no. 9, Sep.

[47] J. Thunberg, et al., In situ synthesis of conductive polypyrrole on electrospun cellulose nanofibers: scaffold for neural tissue engineering, Cellulose 22 (3) (2015) 1459–1467, https://doi.org/10.1007/s10570-015-0591-5. Jun.

[48] A. Wu, H. Kolla, S.K. Manohar, Chemical synthesis of highly conducting polypyrrole nanofiber film, Macromolecules 38 (19) (2005) 7873–7875, https://doi.org/10.1021/ma051299e. Sep.

[49] S. Sahoo, G. Karthikeyan, G. Ch Nayak, C.K. Das, Electrochemical characterization of in situ polypyrrole coated graphene nanocomposites, Synth. Met. 161 (15) (2011) 1713–1719, https://doi.org/10.1016/j.synthmet.2011.06.011. Aug.

[50] N. Vellguth, M. Shamsuyeva, S. Kroll, F. Renz, H.-J. Endres, Electrical conductivity in biocomposites via polypyrrole coating, J. Mater. Sci. Mater. Electron. 30 (3) (2019) 2373–2381, https://doi.org/10.1007/s10854-018-0510-2. Feb.

[51] A. Nagy, J. Rossant, R. Nagy, W. Abramow-Newerly, J.C. Roder, Derivation of completely cell culture-derived mice from early-passage embryonic stem cells, Proc. Natl. Acad. Sci. USA 90 (18) (1993) 8424–8428, https://doi.org/10.1073/pnas.90.18.8424. Sep.

[52] A.E. Carpenter, et al., CellProfiler: image analysis software for identifying and quantifying cell phenotypes, Genome Biol. 7 (10) (2006) R100, https://doi.org/10.1186/gb-2006-7-10-r100.

[53] A.L. Pang, A. Arsad, M. Ahmadipour, Synthesis and factor affecting on the conductivity of polypyrrole: a short review, Polym. Adv. Technol. 32 (4) (2021) 1428–1454, https://doi.org/10.1002/pat.5201. Apr.

[54] N.K. Guimard, N. Gomez, C.E. Schmidt, Conducting polymers in biomedical engineering, Prog. Polym. Sci. 32 (8) (2007) 876–921, https://doi.org/10.1016/j.progpolymsci.2007.05.012. Aug.

[55] T. Patois, B. Lakard, N. Martin, P. Fievet, Effect of various parameters on the conductivity of free standing electrosynthesized polypyrrole films, Synth. Met. 160 (19) (2010) 2180–2185, https://doi.org/10.1016/j.synthmet.2010.08.005. Oct.

[56] V. Kašpárková, et al., Cell-compatible conducting polyaniline films prepared in colloidal dispersion mode, Colloids Surf. B Biointerfaces 157 (2017) 309–316, https://doi.org/10.1016/j.colsurfb.2017.05.066. Sep.

[57] M. Mahmoodian, B. Pourabbas, S. Mohajerzadeh, Effect of anionic dopants on thickness, morphology and electrical properties of polypyrrole ultra-thin films prepared by in situ chemical polymerization, Thin Solid Films 583 (2015) 255–263, https://doi.org/10.1016/j.tsf.2015.03.043. May.

[58] C. Sasso, D. Beneventi, E. Zeno, D. Chaussy, M. Petit-Conil, N. Belgacem, Polypyrrole and polypyrrole/wood-derived materials conducting composites: a review, Bioresources 6 (3) (2011) 3585–3620.

[59] S.T. Navale, A.T. Mane, A.A. Ghanwat, A.R. Mulik, V.B. Patil, Camphor sulfonic acid (CSA) doped polypyrrole (PPy) films: measurement of microstructural and optoelectronic properties, Measurement 50 (2014) 363–369, https://doi.org/10.1016/j.measurement.2014.01.012. Apr.

[60] J. Berg, L. Eriksson, P. Claesson, K. Borve, 3-Component Langmuir-Blodgett-Films with a controllable degree of polarity, Langmuir 10 (4) (1994) 1225–1234, https://doi.org/10.1021/la00016a041. Apr.
[61] E.A. Vogler, Structure and reactivity of water at biomaterial surfaces, Adv. Colloid Interface Sci. 74 (1) (1998) 69–117, https://doi.org/10.1016/S0001-8686(97)00040-7. Feb.
[62] J. Stejskal, M. Trchová, Conducting polypyrrole nanotubes: a review, Chem. Pap. 72 (7) (2018) 1563–1595, https://doi.org/10.1007/s11696-018-0394-x. Jul.
[63] M.R. Abidian, J.M. Corey, D.R. Kipke, D.C. Martin, Conducting-polymer nanotubes improve electrical properties, mechanical adhesion, neural attachment, and neurite outgrowth of neural electrodes, Small 6 (3) (2010) 421–429, https://doi.org/10.1002/smll.200901868.
[64] C. Satriano, S. Carnazza, S. Guglielmino, G. Marletta, Surface free energy and cell attachment onto ion-beam irradiated polymer surfaces, Nucl. Instrum. Methods Phys. Res. Sect. B Beam Interact. Mater. Atoms 208 (2003) 287–293, https://doi.org/10.1016/S0168-583X(03)00647-5. Aug.
[65] M. Tallawi, et al., Strategies for the chemical and biological functionalization of scaffolds for cardiac tissue engineering: a review, J. R. Soc. Interface 12 (108) (2015) 20150254, https://doi.org/10.1098/rsif.2015.0254. Jul.
[66] M. Wu, C. Zhong, Y. Deng, Q. Zhang, X. Zhang, X. Zhao, Resveratrol loaded glycyrrhizic acid-conjugated human serum albumin nanoparticles for tail vein injection II: pharmacokinetics, tissue distribution and bioavailability, Drug Deliv. 27 (1) (Jan. 2020) 81–90, https://doi.org/10.1080/10717544.2019.1704944.
[67] S. Van Vlierberghe, E. Vanderleyden, V. Boterberg, P. Dubruel, Gelatin functionalization of biomaterial surfaces: strategies for immobilization and visualization, Polymers 3 (1) (2011), https://doi.org/10.3390/polym3010114. Art. no. 1, Mar.
[68] T. Fee, C. Downs, A. Eberhardt, Y. Zhou, J. Berry, Image-based quantification of fiber alignment within electrospun tissue engineering scaffolds is related to mechanical anisotropy, J. Biomed. Mater. Res. 104 (7) (2016) 1680–1686, https://doi.org/10.1002/jbm.a.35697.
[69] C.-H. Lin, X. Tang, P. Chen, S.-C. Luo, Unraveling the adhesion behavior of different cell lines on biomimetic PEDOT interfaces: the role of surface morphology and antifouling properties, ACS Appl. Bio Mater. (2023), https://doi.org/10.1021/acsabm.3c00833. Nov.
[70] C.M. Tringides, D.J. Mooney, Conductive hydrogel scaffolds for the 3D localization and orientation of fibroblasts, Macromol. Biosci. 24 (1) (2024) 2300044, https://doi.org/10.1002/mabi.202300044.

LIST OF PUBLICATIONS

Articles published in journals indexed on Web of Science:

Vítková, L., Musilová, L., Achbergerová, E., Kolařík, R., Mrlík, M., Korpasová, K., **Mahelová, L.**, Capáková, Z., Mráček, A., 2022. *Formulation of Magneto-Responsive Hydrogels from Dually Cross-Linked Polysaccharides: Synthesis, Tuning and Evaluation of Rheological Properties.* Int. J. Mol. Sci. 23, 9633. https://doi.org/10.3390/ijms23179633 IF: 5.6

Mahelová, L., Slobodian, P., Kocourková, K., Minařík, A., Moučka, R., Trchová, M., Martínková, M., Skopalová, K., Víchová, Z., Kašpárková, V., Humpolíček, P., 2024. *Method for in situ polypyrrole coating, and the example of its use for functionalization of polyurethane anisotropic electrospun mats.* Heliyon 10. https://doi.org/10.1016/j.heliyon.2024.e27883 IF: 3.6

Gorgol, D., Mrlík, M., Mikulka, F., Víchová, Z., **Mahelová, L.**, Ilčíková, M., Minařík, A., 2024. *Smart Biopolymer Scaffolds Based on Hyaluronic Acid and Carbonyl Iron Microparticles: 3D Printing, Magneto-Responsive, and Cytotoxicity Study.* ACS Appl. Bio Mater. 7, 7483–7493. https://doi.org/10.1021/acsabm.4c00567 IF: 4.7

Articles submitted to the editors of international journals with an impact factor:

Mahelová, L., Trchová, M., Kotowicz, S., Škoda, D., Kocourková, K., Víchová, Z., Vícha, J., Kašpárková, V., Humpolíček, P., 2025. *Is polyazulene cytocompatible? It depends.* Currently under review.

Three other co-authored articles are currently being prepared for submission.

Meeting abstracts from conferences indexed on Web of Science:

Mahelová, L., Slobodian, P., Humpolíček, P., 2023. *Aligned Polyurethane Nanofibers Coated with Polypyrrole: Anisotropy and Conductivity as Cell-Instructive Cues.* TISSUE Eng. PART A 29, 1166–1166.

CIRRICULUM VITAE

Ing. **Leona MAHELOVÁ**

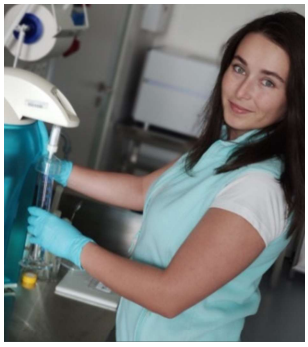

Personal information

(+420) 724 690 873
leonamahelova@gmail.com
Address: Družstevní 4516, 760 05 Zlín

Date of birth: July 26, 1995
Place of birth: Třebíč, the Czech Republic

Education

2020 – 2025	**Doctoral studies** Tomas Bata University in Zlín, Centre of polymer systems Biomaterials and Biocomposites Thesis: *Use of polymers for tissue engineering*
2018 – 2020	**Master's studies** Tomas Bata University in Zlín, Faculty of Technology Polymer Engineering Specialization: Medical and Pharmaceutical Materials Thesis: *Impact of surface properties of polymers on the Cytocompatibility*
2015 – 2018	**Bachelor's studies** Tomas Bata University in Zlín, Faculty of Technology Polymer Materials and Technologies Specialization: *Medical and Pharmaceutical Materials* *Thesis: Biomimetika*

Honours

2020	Award of the Rector of Tomas Bata University given for excellent academic results in the master's degree program and excellent master's thesis
2018	Award of the Dean of the Faculty of Technology given for excellent academic results in the bachelor's degree program
2018	Award of the Director of the Centre of Polymer Systems given for excellent bachelor's thesis

Conferences

2022	TERMIS-EU (Tissue Engineering and Regenerative Medicine International Society – European Union) Krakow, Poland Poster: *Aligned Polyurethane Nanofibers Coated with Polypyrrole: Anisotropy and Conductivity as Cell-Instructive Cues.*
2022	ECIS (European Colloid and Interface Society) Chania, Crete, Greece Poster: *Cytocompatibility of Polypyrrole Thin Layers Synthesized In Situ with Polyurethane Electrospun Mats.*

Trainings and internships

2024	Erasmus+ at the University of Silesia in Katowice, Poland
2022	Certificated course on the basics of scientific work at the Czech Academy of Sciences
2016 – 2020	Research internships at the Centre of Polymer Systems, Tomas Bata University in Zlín
2011 – 2013	Reserch internship at the Department of Population Biology Institute of Vertebrate Biology, Czech Academy of Science

Projects

03/2025 – current	TQ15000176 Natural Cosmetics: Innovated Cosmetic Products with Advanced Carriers of Active Ingredients Team member
10/2024 – current	GAČR 13-07425S Anisotropic and Electro-Conducting Biomaterials Team member
01/2024 – 08/2024	IGA/CPS/2024/007 Preparation of Smart Biomaterials for Tissue Engineering Team member

01/2023 – 12/2023	IGA/CPS/2023/001 Development of Advanced Biomaterials and Their Future Applications Team member
02/2021 – 02/2023	JUNG-2020-001 Smart Biomaterials Based on Conducting Polymers **Lead researcher**
01/2022 – 12/2022	IGA/CPS/2022/001 Preparation of Advanced Biomaterials and Their Use Team member
01/2021 – 12/2021	IGA/CPS/2021/001 Biocompatibility of Materials Team member
10/2020 – 12/2021	GAČR 19-16861S Interactions of Biomaterials with Stem Cells under Simulated *In Vivo* Conditions Team member
09/2020 – 12/2020	IGA/CPS/2020/001 Biocompatibility and Antimicrobial Activity of Materials Team member

Teaching and supervision

2020 – 2025 Training of students in cell biology laboratories and supervision of 8 bachelor's and master's theses. Defended are:

Šandová, K. *Effect of electric field on cell behaviour.* Zlín, 2024. Bachelor thesis. Tomas Bata University in Zlín, Faculty of Technology, Department of Fat, Surfactant and Cosmetics Technology.

Zubková, S. *Využití elektrického pole k léčbě kožních poranění.* Zlín, 2024. Bachelor thesis. Tomas Bata University in Zlín, Faculty of Technology, Department of Fat, Surfactant and Cosmetics Technology.

Stuchlíková, S. *Polyazulen a jeho biologické vlastnosti.* Zlín, 2023. Master thesis. Tomas Bata University in Zlín, Faculty of Technology, Department of Fat, Surfactant and Cosmetics Technology.